Versatile Biaryls and Fused Aromatics through Oxidative Coupling of Hydroquinones with (Hetero)Arenes

Takaaki Aijima,[a] Rina Ueda,[b] Takanori Nakane,[c,e] Fumiaki Makino,[d,e,f] Yusuke Ohnishi,[c] Keiichiro Nakajima,[a] Shinichiro Kamino,[b] Genji Kurisu,[c,e] Keiichi Namba,[d,e] Hiroki Nakata,[g] Kaiki Mogi,[g] Hironao Sajiki,[g] Shuji Akai[a] and Yoshinari Sawama*[a,h]

a. Graduate School of Pharmaceutical Sciences, Osaka University, 1-6, Yamadaoka, Suita, Osaka 565-0871, Japan; E-mail: sawama@phs.osaka-u.ac.jp
b. School of Pharmacy, Aichi Gakuin University, 1-100 Kusumoto-cho, Chikusa-ku, Nagoya 464-8650, Japan.
c. Institute for Protein Research, Osaka University, 3-2 Yamadaoka, Suita, Osaka 565-0871, Japan
d. Graduate School of Frontier Biosciences, Osaka University, 1-3 Yamadaoka, Suita, Osaka 565-0871, Japan.
e. JEOL YOKOGUSHI Research Alliance Laboratories, Osaka University, 1-3 Yama-daoka, Suita, Osaka 565-0871, Japan.
f. JEOL Ltd, 3-2-1 Musashino, Akishima, Tokyo 196-8558, Japan.
g. A Laboratory of Organic Chemistry, Gifu Pharmaceutical University, 1-25-4-Daigaku-nishi, Gifu 501-1196, Japan.
h. Deuterium Science Research Unit, Center for the Promotion of Interdisciplinary Education and Research, Kyoto University, Yoshida, Sakyo-ku, Kyoto 606-8501, Japan.

Abstract: Hydroquinones bearing an electron-withdrawing group at the C2-position effectively underwent oxidative coupling with indoles or arenes in the presence of 2,3-dichloro-5,6-dicyano *p*-benzoquinone (DDQ) and $FeCl_3$ to give the corresponding biaryls. Indole-based products were further converted into tetracyclic aromatics using DDQ and $FeCl_3$. Thiophene derivatives were also applicable to give the tetracyclic aromatics, possessing luminescent properties.

Introduction

Biaryls (compounds with benzene-benzene, benzene-indole, etc. units) and multi-fused aromatic heterocycles are the basic backbones of biologically active substances, natural products, and functional materials such as organic light-emitting diodes (OLEDs) (Figure 1).[1–4] For example, fluvastatin[1] (a HMG-CoA reductase inhibitor that is used to treat hypercholesterolemia) and azilsartan[2] (an angiotensin II receptor blocker used to treat hypertension) have a biaryl moiety in their structure. Azonazine,[3] isolated from a fungus in the Hawaiian marine sediments, has a tetracyclic fused dihydrobenzofuran-indoline moiety. Benzofuran-indole-fused tetracycle **A**[4] is

expected to be a raw material for OLEDs. Therefore, it is important to develop efficient and systematic synthetic methods to construct these highly functionalized aromatic derivatives.

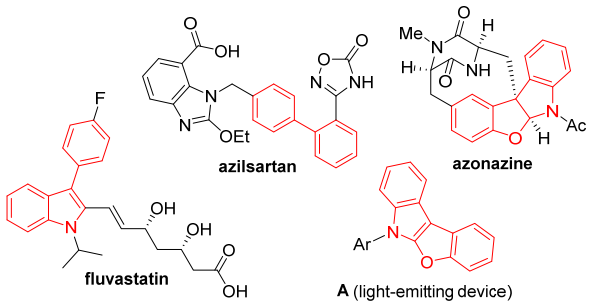

Figure 1. Structures of some useful compounds bearing biaryl and multi-fused aromatic backbones.

Hydroquinone can be easily modified by the Friedel–Crafts type reaction to the corresponding C2-functionalized hydroquinone (e.g., electron-withdrawing group substituted at the C2 position; **1**, Scheme 1C).[5] Moreover, benzoquinones (**2**), which are the oxidized forms of hydroquinones, can undergo nucleophilic addition on their *a*,*b*-unsaturated carbonyl moieties to give the corresponding benzene-fused products in a stepwise manner from hydroquinone.[6] On the other hand, tandem reactions are valuable as environmentally friend methods, as they do not require isolation and purification of reaction intermediates, thereby reducing the amount of wastes generated during the isolation of these intermediates.[7] Particularly, one-pot oxidative functionalizations of hydroquinones can be a powerful and straightforward tool to synthesize versatile aromatic products. Masson[8] and Jørgensen[9] have reported the asymmetric and oxidative one-pot reactions of hydroquinones with enamines and aliphatic aldehydes to construct dihydrobenzofuran derivatives (Scheme 1A). Furthermore, Zhong et al. have recently developed the one-pot synthesis of tetracyclic aromatics from 2-methoxycarbonyl hydroquinone (**1a**) and indoles, without the isolation of any reaction intermediates, in the presence of copper and cobalt co-catalysts under atmospheric molecular oxygen (Scheme 1B).[10] This transformation is realized by well-designed co-catalytic system, and thus considerably environmentally benign method to obtain cyclic compounds. However, to the best of our knowledge, there are no reports on the oxidative one-pot synthesis of biaryls from hydroquinones, bearing some electron-withdrawing groups (2-methoxycarbonyl, 2-acetyl and 2-foymyl).

Herein, we report a novel oxidative coupling reaction of hydroquinones **1** with indole and electron-rich benzene derivatives to construct highly functionalized biaryls **3** and **4** in

the presence of 2,3-dichloro-5,6-dicyano-*p*-benzoquinone (DDQ) and $FeCl_3$ as an oxidant and Lewis acid, respectively (Scheme 1C). Benzene-indole type biaryls **3** underwent further oxidative cyclization to benzofuran-indole-fused tetracyclic aromatics **5** in a stepwise manner. Benzofuran-thiophene derivative-fused tetracycles **6** and **7** could be directly constructed from benzoquinone (**2**) in a one-pot manner. Additionally, tetracyclic products **5**–**7** exhibited luminescence.

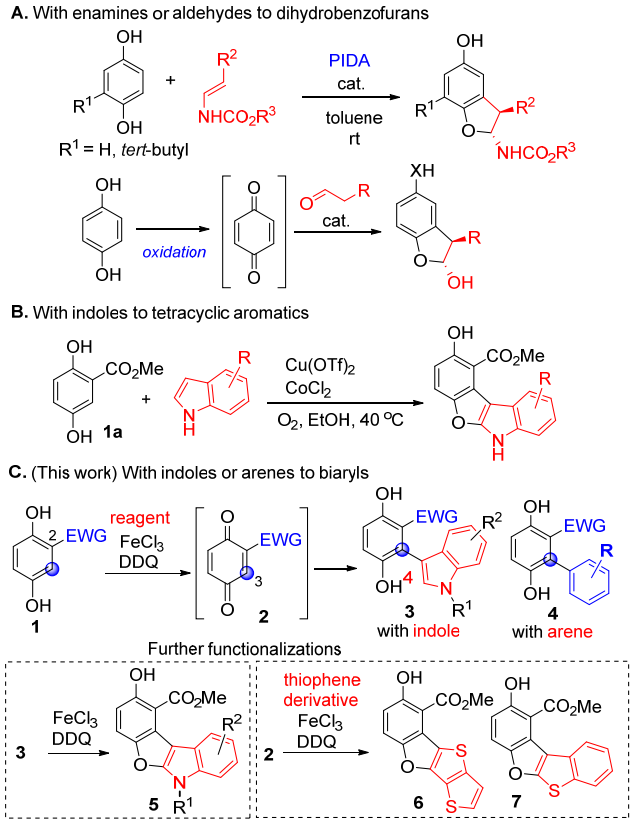

Scheme 1. Oxidative couplings of hydroquinones.

Results and discussion

First, the oxidative coupling of **1a** with indole was investigated (eq. 1). The oxidation of **1a** with DDQ produced the corresponding 2-methoxycarbonyl benzoquinone intermediate **2a**, which underwent the $FeCl_3$-catalyzed site-selective nucleophilic addition of indole at the C3 position of **2a** to give the desired biaryl product **3a** in 97% yield. This site-selectivity was attributed to the increased electrophilicity at the C3 position of **2a** owing to the electron-withdrawing ester group substituted at the C2 position. Phenyliodine (III) diacetate (PIDA) also acted as an effective oxidant to give **3a** in 95% yield. The effects of other Lewis acids and oxidants are described in Table S1.

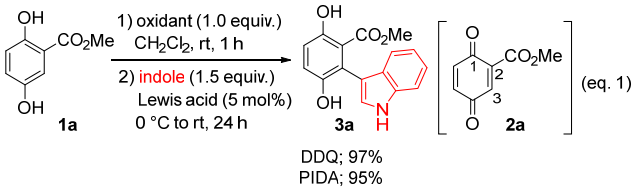

Next, the substrate scope of the indole nucleophiles and hydroquinones was investigated in the presence of DDQ (or PIDA)[11] and $FeCl_3$, (Scheme 2). When using *N*-methyl-, *N*-tosyl-, *N*-benzyl-, 5-methoxy-, 5-fluoro-, and 5-bromo indoles as nucleophiles with **1a**, the corresponding biaryl products **3b**–**3g** were obtained in good to excellent yields. 2-Methoxycarbonyl indole was also applicable to this reaction, affording biaryl **3k** that could be transformed into indole-fused 2-chromanone **8** as an important skeleton bearing bioactivity[12,13] by intramolecular cyclization between a hydroxy group and ester moiety under basic conditions. Furthermore, 2-acetyl- and 2-formyl hydroquinones **1b** and **1c** underwent oxidative coupling with indole to give the corresponding biaryls **3h** and **3i**, respectively. On the other hand, hydroquinone **1d** was not converted to biaryl **3j** because of the poor electrophilicity at the C3 position. Notably, electron-rich benzene derivatives could also be used instead of indole in the present oxidative coupling of **1a**. Anisole, 2-hydroxynaphthalene, 1,3,5-trimethoxybenzene, 1-bromo-3,5-dimethoxybenzene, and 1,4-dimethoxybenzene acted as nucleophiles to afford biaryls **4a**–**4e** in moderate to good yields.

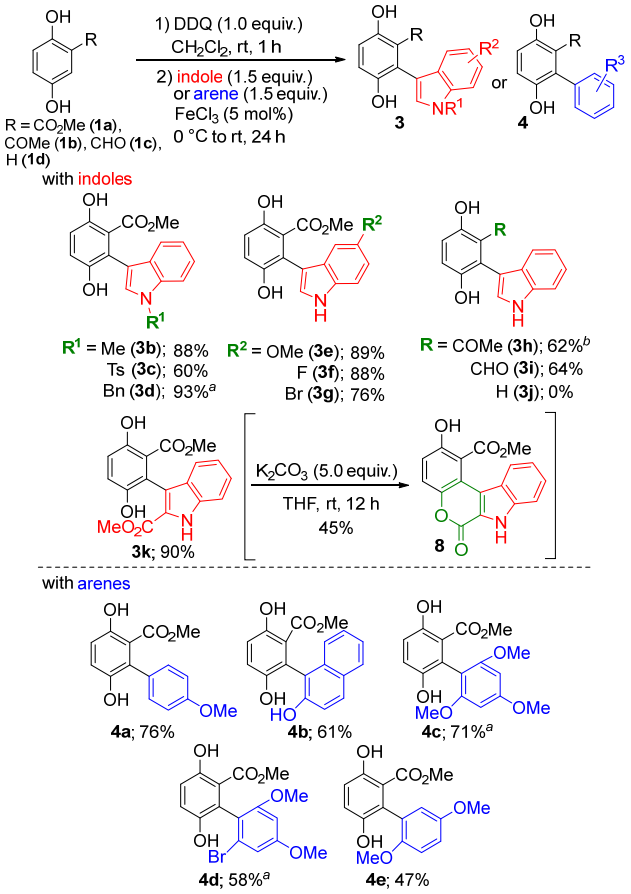

Scheme 2. Investigation of substrate scope. [a]PIDA (1.0 equiv.) was used instead of DDQ. [b]THF was used instead of CH_2Cl_2.

Indole-based biaryl **3a** was successfully converted to tetracyclic aromatic product **5a** in 91% yield in the presence of DDQ and catalytic $FeCl_3$ (Scheme 3A; direct path). This transformation can proceed via the oxidation of **3a** to benzoquinone **9**, followed by the $FeCl_3$-catalyzed cyclization of **9** to **5a** (stepwise path). The transformation of **9** to **5a** can be facilitated by the coordination of $FeCl_3$ as a Lewis acid to the two carbonyl moieties at the C1 position and the ester moiety at the C2 position of **9** (Scheme 3B). Reaction intermediate **B** was formed subsequently by the donation of the lone pair of electrons on the N atom of indole. The subsequent intramolecular nucleophilic attack of the carbonyl oxygen at the C4 position of **B** to the iminium moiety produced **C**. Finally, aromatization of **C** gave **5a**. Compounds **3d**, **3e**, and **3g** were also applicable as substrates in this reaction, affording the corresponding tetracyclic aromatic products **5b**–**5d** in good yields (Scheme 3C). Using the present oxidative coupling methods, versatile biaryls and tetracyclic aromatics could be constructed. Although **5a**–**5d** could be directly constructed by Zhong's

method in Scheme 1-B[10], our methodology has the benefit to apply the coupling reaction using thiophene derivatives instead of indoles, shown in next section.

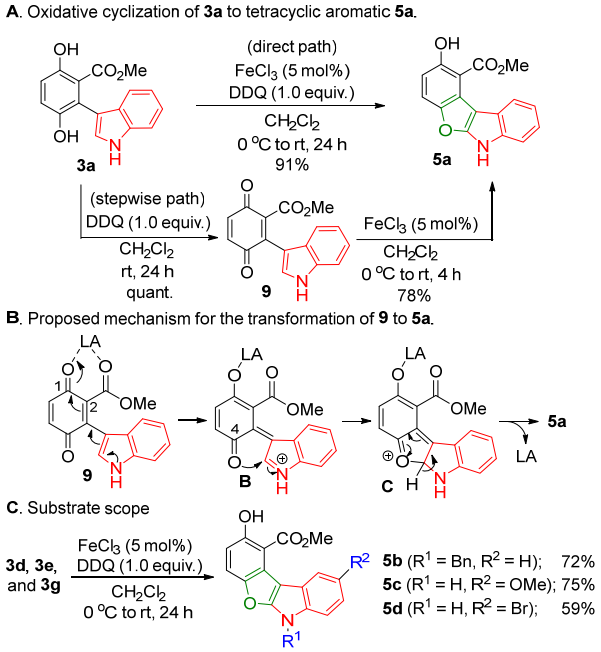

Scheme 3. Transformation of **3** to tetracyclic arene **5**. LA denotes Lewis acid.

The developed method was next applied for coupling using thiophene derivatives. The oxidative coupling of **1a** with thieno[3,2-*b*]thiophene in the presence of 1.0 equiv. of DDQ and catalytic $FeCl_3$ directly gave tetracyclic product **6**[14] in 19% yield, without the generation of biaryl **9**, unlike the case using indole (Scheme 4A). When the DDQ increased to 2.2 equiv., a complex mixture was obtained (Scheme 4B). Meanwhile, the reaction using benzoquinone **2a** as a substrate furnished **6** in 43% yield. The addition of K_2CO_3 suppressed the cyclization to give 3-thienothiophene-substituted benzoquinone **10** in 43% yield. This is because K_2CO_3 lowered the Lewis acidity of $FeCl_3$. The cyclization of **10** was catalyzed by $FeCl_3$ to afford **6** in 40% yield. Furthermore, the use of benzothiophene gave another type of tetracyclic aromatic product, **7**,[15] in 67% yield. Although low to moderate yields were obtained, novel tetracyclic aromatics bearing a thiophene skeleton could be synthesized using the developed oxidative coupling reactions.

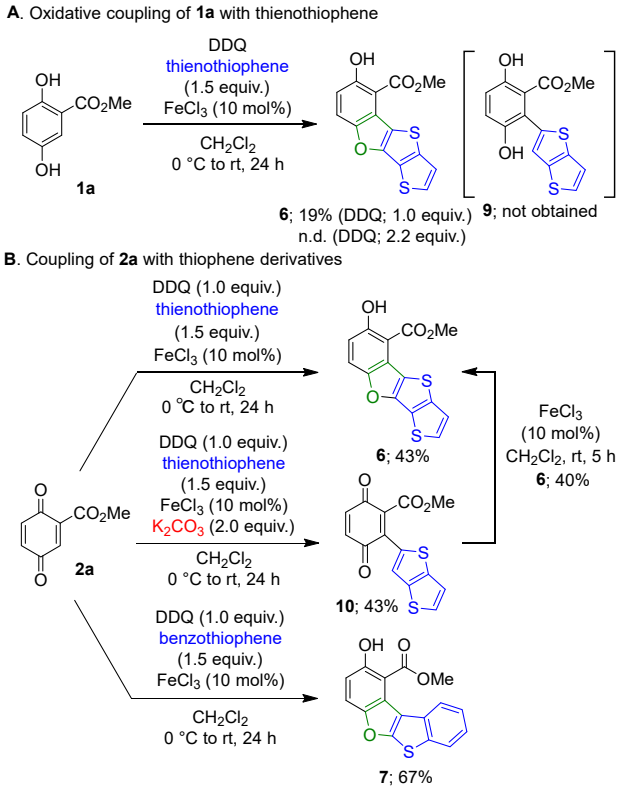

Scheme 4. Oxidative coupling with thiophene derivatives. n.d denotes 'not detected.'

Because Zhong, et al. have reported that a solution of **5** (2×10^{-5} M in toluene) shows blue-light emission at a wavelength of *ca*. 426 nm,[10] we also turned our attention to the photophysical properties of newly prepared compounds **6** and **7** (Figure. 2). Therefore, we investigated the photophysical properties of **5a**, **6** and **7** in the solution ($CHCl_3$ and toluene) and solid states. Figure 2A shows the fluorescence spectra in $CHCl_3$ as a representative (the fluorescence spectra in toluene are shown in Fig. S3). The fluorescence maximum decreased in the order **5a** (λ_{fl} = 441 nm) > **6** (λ_{fl} = 420 nm) > and **7** ($\lambda_{\phi l}$ = 410 nm). The relative fluorescence quantum yields of **5a**, **6**, and **7** in $CHCl_3$ were 47%, 26%, and 6%, respectively (see absorption spectra of **5a**, **6**, and **7** in CH_2Cl_2 in Figure S4). Among the three compounds, the longest fluorescence maximum wavelength was observed for **6** in the solid state. Compound **6** exhibited green fluorescence, with a fluorescence maximum at 520 nm (Figure 2B). The photophysical data of these compounds are summarized in Figure 2C. The results indicate that the incorporation of thienothiophene units into benzofuran extends the π-conjugation, endowing unique optical properties in the solid state.

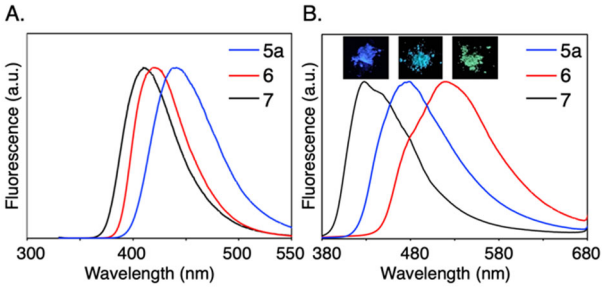

C.

	λ_{fl} [nm]			Φ_{fl} [%]		
	Solution			Solution[a]		
Entry	$CHCl_3$	Toluene	Solid	$CHCl_3$	Toluene	Solid
5a	441	425	479	47	53	12
6	420	416	521	26	31	8
7	410	404	428	6	6	9

Figure 2. (A) Normalized fluorescence spectra of **5a**, **6**, and **7** in $CHCl_3$. (B) Solid-state fluorescence spectra of **5a**, **6**, and **7**. Insets show the photographs of **5a**, **6,** and **7** under 365-nm irradiation. (C) Photophysical data of **5a**, **6,** and **7** in solution and solid state. [a]The relative fluorescence quantum yield (Φ_{fl}) was measured upon excitation at 366 nm using quinine sulfate (Φ_{fl} = 55% in 0.1 M H_2SO_4) as a reference material.

Conclusions

We have developed the oxidative coupling of hydroquinones bearing an electron-withdrawing group at the C2 position with (hetero)aromatics to afford biaryl products as pharmaceutically useful backbones. Furthermore, tetracyclic aromatics derived from indole and thiophene derivatives were constructed. The developed synthetic methodology can be a powerful tool for the flexible design of various polycyclic aromatics that have applications as functional luminescent materials.

Conflicts of interest

The authors declare no competing financial interest.

Acknowledgements

This study was partially supported by JST SPRING Grant Number JPMJSP2138 (for T.A.), MEXT KAKENHI Grant Number 20H05738 (for Y.S.). JSPS (MEXT grant in aid-for transformative research areas (B) Deuterium Science) KAKENHI Grant Number 20H05738 (for Y.S.), Life Science and Drug Discovery (Basis for Supporting Innovative Drug Discovery and Life Science Research (BINDS)) from AMED under Grant Number 23ama121054 (for Y.S.), Research Support Project for Life Science and Drug Discovery (Basis for Supporting Innovative Drug Discovery and Life Science Research (BINDS)) from AMED under Grant Number JP22ama121003 and JP22ama121001, and JEOL YOKOGUSHI Research Alliance Laboratories of Osaka University (to K.N. and G.K.).

Author Contributions

T.A., K.N., H.N., K.M., H.S. and S.A. contributed to organic synthesis. R.U. and S.K analyzed the luminescent property. T.N., F.M., Y.O., G.K. and K.N. performed MicroED analysis. Y.S. directed the project. T.A. and Y.S. wrote the manuscript.

Notes and references

1 E. Russo, E. Donato di Paola, P. Gareri, A. Siniscalchi, A. Labate, L. Gallelli, R. Citraro and G. De Sarro, *Pharmacol. Res.*, **2013**, *70*, 1.

2 Y. Xiao, T. Jin, X. Geng and X. Zhu, *Eur. J. Pharm. Sci.*, **2022**, *176*, 106241.

3 Q.-X. Wu, M. S. Crews, M. Draskovic, J. Sohn, T. A. Johnson, K. Tenney, F. A. Valeriote, X.-J. Yao, L. F. Bjeldanes and P. Crews, *Org. Lett.*, **2010**, *12*, 4458–4461.

4 R. K. Konidena, K. H. Lee and J. Y. Lee, *J. Mater. Chem. C.*, **2019**, *7*, 13912–13919.

5 (a) P. M. Hundnall, *Ullmann's Encyclopedia of Industrial Chemistry 2002*, Wiley-VCH, pp.473–480; (b) H. Naeimi, A. Amini and M. Moradian, *Org. Chem. Front.*, **2014**, *1*, 415; (c) J. Song, H. Zhao, Y. Liu, H. Han, Z. Li, W. Chu and Z. Sun, *New. J. Chem.*, **2017**, *41*, 372.

6 (a) M. Aslam, S. Mohandoss, P. Subramanian, S. You, W.-G. Yang, S. H. Kim and Y. R. Lee, *Org. Lett.*, **2021**, *23*, 1383–1387; (b) Z.-Y. Lu, W.-Q. Lan, F.-Y. Liu, J.-Y. Wang, X.-M. Zhang and L.-H. Liao, *Tetrahedron Lett.*, **2021**, *76*, 153233; (c) L. Zhang, J. Hu, R. Xu, S. Pan, X. Zeng and G. Zhong, *Adv. Synth. Catal.*, **2019**, *361*, 5449–5457; (d) K. J. Kaurich and P. A. Deck, *Tetrahedron*, **2018**, *74*, 2191–2196; (e) T. Varlet, C. Gelis, P. Retailleau, G. Bernadat, L. Neuville and G. Masson, *Angew. Chem. Int. Ed.*, **2020**, *59*, 8491–8496.

7 (a) J. M. Honnanayakanavar, O. Obulesu and S. Suresh, *Org. Biomol. Chem.*, **2022**, *20*, 2993; (b) S. Indu and K. P. Kaliappan, *RSC Adv.*, **2018**, *8*, 21292.

8 C. Gelis, M. Bekkaye, C. Lebèe, F. Blanchard and G. Masson, *Org. Lett.*, **2016**, *18*, 3422–3425.

9 K. L. Jensen, P. T. Franke, L. T. Nielsen, K. Daasbjerg and K. A. Jørgensen, *Angew. Chem. Int. Ed.*, **2010**, *49*, 129–133.

10 M. A. Bashir, Y. Zhang, H. Yu, B. Wang, W. Zhao and F. Zhong, *Green Chem.*, **2021**, *23*, 5031–5036.

11 For the reactions where the yields were low using DDQ as an oxidant, PIDA was used.

12 For the synthetic method, see: (a) C.-X. Gu, W.-W. Chen, B. Xu and M.-H. Xu, *Tetrahedron*, **2019**, *75*, 1605–1611; (b) P. Nealmongkol, K. Tangdenpaisal, S. Sitthimonchai, S. Ruchirawat and N. Thasana, *Tetrahedron*, **2013**, *69*, 9277–9283; (c) V. A. Vaillard, J. F. Guastavino, M. E. Budèn, J. I. Bardagí, S. M. Barolo and R. A. Rossi, *J. Org. Chem.*, **2012**, *77*, 1507–1519.

13 For the biological activities, see: C. Neagoie, E. Vedrenne, F. Buron, J.-Y. Mèrour, S. Rosca, S. Bourg, O. Lozach, L. Meijer, B. Baldeyrou, A. Lansiaux and S. Routier, *Eur. J. Med. Chem.*, **2012**, *49*, 379–396.

14 The substitution position of thienothiophene to form **6** was determined from its nanocrystals by MicroED (see SI), because a single crystal of **6** large enough for our in-house X-ray diffractometer could not be obtained. The microcrystals of **6** were bent and plate-like, and the data quality was limited by streaking of the diffraction spots and twinning. Nonetheless, the resulting map showed the structure of **6** unambiguously. (Crystallographic coordinates of the compound **6** are deposited to CCDC (ID 2294744) and COD (3000464). MicroED raw diffraction images are available at XRDa (ID 162).) The assignment by MicroED was also supported by chemical modification of thienothiophene to di-deuterated thienothiophene and the following similar reaction as shown in Scheme 5 (see SI). Nucleophilicity of the C2 position on a thiophene is known to be higher than that of the C3 position. Probably, the nucleophilic properties of thienothiophene and thiophene are similar.

15 The structure was determined by NOE experiments (SI). Nucleophilicity of the C3 position on benzothiophene is known to be high, similar to the case of indole.

Electronic Supplementary Information

Versatile Biaryls and Fused Aromatics through Oxidative Coupling of Hydroquinones with (Hetero)Arenes

Takaaki Aijima,[a] Rina Ueda,[b] Takanori Nakane,[c,e] Fumiaki Makino,[d,e,f] Yusuke Ohnishi,[c] Keiichiro Nakajima,[a] Shinichiro Kamino,[b] Genji Kurisu,[c,e] Keiichi Namba,[d,e] Hiroki Nakata,[g] Kaiki Mogi,[g] Hironao Sajiki,[g] Shuji Akai[a] and Yoshinari Sawama[*a,f]

[a]Graduate School of Pharmaceutical Sciences, Osaka University, 1-6, Yamadaoka, Suita, Osaka 565-0871, Japan.

[b] School of Pharmacy, Aichi Gakuin University, 1-100 Kusumoto-cho, Chikusa-ku, Nagoya 464-8650, Japan.

[c] Institute for Protein Research, Osaka University, 3-2 Yamadaoka, Suita, Osaka 565-0871, Japan.

[d] Graduate School of Frontier Biosciences, Osaka University, 1-3 Yamadaoka, Suita, Osaka 565-0871, Japan.

[e] JEOL YOKOGUSHI Research Alliance Laboratories, Osaka University, 1-3 Yamadaoka, Suita, Osaka 565-0871, Japan.

[r] JEOL Ltd, 3-2-1 Musashino, Akishima, Tokyo 196-8558, Japan.

[g] A Laboratory of Organic Chemistry, Gifu Pharmaceutical University, 1-25-4-Daigaku-nishi, Gifu 501-1196, Japan.

[h] Deuterium Science Research Unit, Center for the Promotion of Interdisciplinary Education and Research, Kyoto University, Yoshida, Sakyo-ku, Kyoto 606-8501, Japan.

Contents

1. General information.

All reactions were carried out in dry solvents under argon atmosphere. Unless otherwise noted, all substrates and solvents were purchased from commercial sources and were used without further purification. Flash column chromatography was performed with 40–50 or 63–210 μm Silica Gel 60 N (Kanto Chemical Co., Inc.). Melting points were measured on SANSHO SMP-300 or Yanaco MP-S3. IR spectra were recorded on SHIMADZU IRAffinity-1S as a thin film on NaCl or Bruker FT-IR ALPHA/SHIMADZU IRAffinity-1 as an ATR method. ^{1}H and ^{13}C NMR spectra were recorded on JEOL JNM-ECZ400 (^{1}H NMR: 400 MHz, ^{13}C NMR: 100 MHz) or JEOL JNM-ECA500 (^{1}H NMR: 500 MHz, ^{13}C NMR: 125 MHz, ^{2}H NMR: 77 MHz) with chemical shifts reported in δ (ppm) relative to an internal standard or the residual solvent signal for ^{1}H (tetramethylsilane: δ = 0.00 ppm, $CDCl_3$: δ = 7.26 ppm, $(CD_3)_2CO$: δ = 2.05 ppm) and relative to the deuterated solvent signal for ^{13}C ($CDCl_3$: δ = 77.0 ppm, $(CD_3)_2CO$: δ = 29.8 ppm). High resolution mass spectra were measured on JEOL JMS-S3000 (MALDI), JEOL JMS-700 (EI, FAB) or Shimadzu hybrid IT-TOF (ESI).

2. Optimization of reaction conditions.

Table S1. Optimization in the reaction of 1a with indole

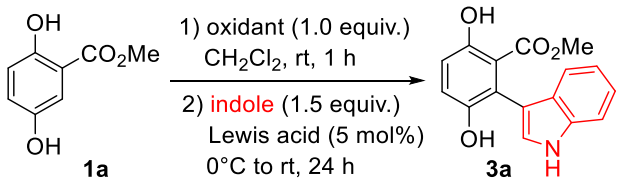

Entry	oxidant	Lewis acid	NMR yield (%)[a]
1	DDQ	$FeCl_3$	97[b]
2	DDQ	-	25
3	chloranil	$FeCl_3$	25
4	PIFA	$FeCl_3$	42
5	Ag_2O	$FeCl_3$	33
6	PIDA	$FeCl_3$	95
7	DDQ	$ZnCl_2$	80
8	DDQ	$InCl_3$	82
9	DDQ	$BF_3 \cdot Et_2O$	31

[a] Determined by ^{1}H NMR using 1,1,2,2-tetrachloroethane as an internal standard. [b] Isolated yield.

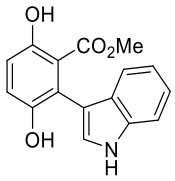

3a

Methyl 3,6-dihydroxy-2-(1*H*-indol-3'-yl)benzoate (3a)

(Entry 1)

DDQ (182 mg, 0.80 mmol) was added to a solution of methyl 2,5-dihydroxybenzoate (**1a**, 135 mg, 0.80 mmol) in CH_2Cl_2 (4.0 mL) at 0 ℃. After being stirred for 1 h at room temperature, indole (140 mg, 1.20 mmol), $FeCl_3$ (6,4 mg, 0.040 mmol), and CH_2Cl_2 (2.0 mL) were successively added to the reaction mixture at 0 ℃. The reaction mixture was stirred for 24 h at 0 ℃ to room temperature. After that, the reaction was quenched with aqueous $NaHCO_3$ solution. The resulting mixture was extracted with CH_2Cl_2. The combined organic layers were dried over Na_2SO_4 and concentrated in vacuo. The residue was purified by flash column chromatography on silica gel (hexane/EtOAc = 2/1) to afford **3a** (220 mg, 0.78 mmol) in 97% yield.

Pale yellow solid; ^{1}H NMR (500 MHz, $CDCl_3$): δ 10.36 (s, 1H), 8.50 (brs, 1H), 7.41 (d, J = 8.0 Hz, 1H), 7.30 (d, J = 8.0 Hz, 1H), 7.24 (dd, J = 8.0, 7.0 Hz, 1H), 7.17 (d, J = 9.0 Hz, 1H), 7.16 (s, 1H), 7.10 (dd, J = 8.0, 7.0 Hz, 1H), 6.99 (d, J = 9.0 Hz, 1H), 5.24 (s, 1H), 3.23 (s, 3H). Spectroscopic data of ^{1}H NMR was identical to that reported in the reference 1.

(Entry 2)

DDQ (45.4 mg, 0.20 mmol) was added to a solution of methyl 2,5-dihydroxybenzoate (**1a**, 33.6 mg, 0.20 mmol) in CH_2Cl_2 (1.5 mL) at 0 ℃. After being stirred for 1 h at room temperature, indole (35.1 mg, 0.30 mmol) was added to the mixture at 0 ℃. The reaction mixture was stirred for 24 h at 0 ℃ to room temperature. After that, the reaction was quenched with saturated aqueous $NaHCO_3$ solution. The resulting mixture was extracted with $CHCl_3$. The combined organic layers were dried over Na_2SO_4 and concentrated in vacuo. The yield was calculated by crude ^{1}H NMR using 1,1,2,2-tetrachloroethane (21 mL, 0.20 mmol) as an internal standard.

(Entries 3–9)

DDQ (45.4 mg, 0.20 mmol) was added to a solution of methyl 2,5-dihydroxybenzoate (**1a**, 33.6 mg, 0.20 mmol) in CH_2Cl_2 (1.5 mL) at 0 ℃. After being stirred for 1 h at room temperature, indole (35.1 mg, 0.30 mmol), and Lewis acid (5 mol%) were successively added to the mixture at 0 ℃. The reaction mixture was stirred for 24 h at 0 ℃ to room temperature. After that, the reaction was

quenched with saturated aqueous $NaHCO_3$ solution. The resulting mixture was extracted with $CHCl_3$. The combined organic layers were dried over Na_2SO_4 and concentrated in vacuo. The yield was calculated by crude ^1H NMR using 1,1,2,2-tetrachloroethane (21 mL, 0.20 mmol) as an internal standard.

3. Procedure in Schemes 2–4.

Experimental procedure A for Scheme 2:

DDQ (45.4 mg, 0.20 mmol) or PIDA (64.4 mg, 0.20 mmol) was added to a solution of methyl 2,5-dihydroxybenzoate (**1a**, 33.6 mg, 0.20 mmol) in CH_2Cl_2 (1.0–1.5 mL) at 0 °C. After being stirred for 1–1.5 h at room temperature, indoles or arenes (0.30 mmol), and $FeCl_3$ (1.6 mg, 0.010 mmol) were successively added to the mixture at 0 °C. The reaction mixture was stirred for 24 h at 0 °C to room temperature. After that, the reaction was quenched with saturated aqueous $NaHCO_3$ solution. The resulting mixture was extracted with CH_2Cl_2. The combined organic layers were dried over Na_2SO_4 and concentrated in vacuo. The residue was purified by flash column chromatography on silica gel to afford biaryl **3b**–**3k** and **4a**–**4e**.

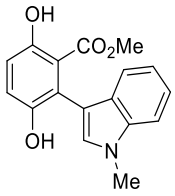

3b

Methyl 3,6-dihydroxy-2-(1'-methyl-1*H*-indol-3'-yl)benzoate (3b)

According to Experimental procedure A, DDQ (45.4 mg, 0.20 mmol), 1-methylindole (37 μL, 0.30 mmol), and CH_2Cl_2 (1.0 mL) were used. The rection time of oxidation step was 1.5 h. The crude product was purified by flash column chromatography on silica gel (hexane/EtOAc = 3/1) to afford **3b** (52.3 mg, 0.176 mmol) in 88% yield.

Purple oil; ^1H NMR (500 MHz, $CDCl_3$): δ 10.27 (s, 1H), 7.39 (d, J = 8.0 Hz, 1H), 7.30 (d, J = 7.5 Hz, 1H), 7.28 (dd, J = 8.0, 7.5 Hz, 1H), 7.17 (d, J = 9.5 Hz, 1H), 7.10 (t, J = 8.0 Hz, 1H), 7.06 (s, 1H), 6.98 (d, J = 9.5 Hz, 1H), 5.24 (s, 1H), 3.88 (s, 3H), 3.24 (s, 3H). Spectroscopic data of ^1H NMR was identical to that reported in the reference 1.

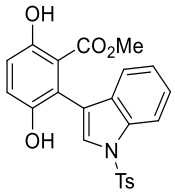

3c

Methyl 3,6-dihydroxy-2-(1'-tosyl-1*H*-indol-3'-yl)benzoate (3c)

According to Experimental procedure A, DDQ (45.4 mg, 0.20 mmol), 1-tosylindole (81.4 mg, 0.30 mmol), and CH_2Cl_2 (1.0 mL) were used. The reaction time of oxidation step was 1.5 h. The crude product was purified by flash column chromatography on silica gel (hexane/EtOAc = 3/1) to afford **3c** (52.5 mg, 0.120 mmol) in 60% yield.

White solid; m.p. 210.8–212.2 ºC; IR(ATR) cm^{-1}: 3508, 3111, 2950, 1666, 1593, 1445, 1369, 1445, 1369, 1332, 1174, 1113, 1090; ^1H NMR (500 MHz, $CDCl_3$): δ 10.54 (s, 1H), 8.11 (d, J = 9.0 Hz, 1H), 7.82 (d, J = 9.0 Hz, 2H), 7.55 (s, 1H), 7.39 (dd, J = 9.0, 8.0 Hz, 1H), 7.27 (d, J = 9.0 Hz, 2H), 7.22 (dd, J = 8.0, 7.5 Hz, 1H), 7.18 (d, J = 9.0 Hz, 1H), 7.16 (d, J = 7.5 Hz, 1H), 7.03 (d, J = 9.0 Hz, 1H), 4.74 (s, 1H), 2.91 (s, 3H), 2.36 (s, 3H); ^{13}C NMR (125 MHz, $CDCl_3$): δ 170.4, 156.2, 146.7, 145.3, 135.0, 134.9, 130.7, 129.9, 126.8, 125.5, 124.3, 123.9, 123.1, 119.8, 119.4, 117.9, 116.5, 113.8, 112.1, 51.3, 21.5; ESI-HRMS (*m*/*z*) calcd. for $C_{23}H_{19}NO_6SNa$ $[M+Na]^+$ 460.0825, found 460.0808.

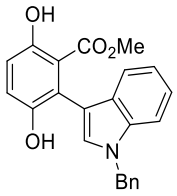

3d

Methyl 3,6-dihydroxy-2-(1'-benzyl-1*H*-indol-3'-yl)benzoate (3d)

According to Experimental procedure A, PIDA (64.4 mg, 0.20 mmol), 1-benzylindole (62.2 mg, 0.30 mmol), and CH_2Cl_2 (1.5 mL) were used. The reaction time of oxidation step was 1 h. The crude product was purified by flash column chromatography on silica gel (hexane/EtOAc = 4/1) to afford **3d** (69.2 mg, 0.185 mmol) in 93% yield.

Pale yellow solid; m.p. 130–131 ºC; IR (ATR) cm^{-1}: 3483, 3029, 2950, 1664, 1608, 1453, 1439, 1332, 1226, 1176, 1126, 1025; ^1H NMR (500 MHz, $CDCl_3$): δ 10.35 (s, 1H), 7.99 (d, J = 7.5 Hz, 1H), 7.33 (m, 5H), 7.27 (m, 5H), 5.45 (d, J = 16.0 Hz, 1H), 5.35 (d, J = 16.0 Hz, 1H), 5.18 (s, 1H), 3.22 (s, 3H); ^{13}C NMR (125 MHz, $CDCl_3$): δ 171.2, 155.5, 147.2, 137.2, 136.6, 128.9, 127.9, 126.6, 122.7, 122.1, 120.4, 119.5, 119.3, 118.2,113.1, 110.0, 109.5, 51.7, 50.1; ESI-HRMS (*m*/*z*)

calcd. for $C_{23}H_{20}NO_4$ $[M+H]^+$ 374.1387, found 374.1384.

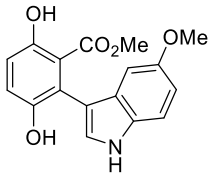

3e

Methyl 3,6-dihydroxy-2-(5'-methoxy-1*H*-indol-3'-yl)benzoate (3e)

According to Experimental procedure A, DDQ (45.4 mg, 0.20 mmol), 5-methoxyindole (44.2 mg, 0.30 mmol), and CH_2Cl_2 (1.0 mL) were used. The reaction time of oxidation step was 1.5 h. The crude product was purified by flash column chromatography on silica gel (hexane/EtOAc = 2/1) to afford **3e** (55.7 mg, 0.178 mmol) in 89% yield.

White solid; ^{1}H NMR (500 MHz, $CDCl_3$): δ 10.30 (s, 1H), 8.43 (s, 1H), 7.32 (d, J = 8.7 Hz, 1H), 7.20–7.16 (m, 2H), 7.01 (d, J = 8.7 Hz, 1H), 6.91 (dd, J = 8.7, 2.3 Hz, 1H), 6.71 (d, J = 2.3 Hz, 1H), 3.76 (s, 3H), 3.29 (s, 3H). Spectroscopic data of ^{1}H NMR was identical to that reported in the reference 1.

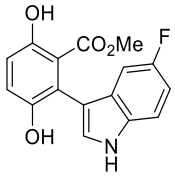

3f

Methyl 3,6-dihydroxy-2-(5'-fluoro-1*H*-indol-3'-yl)benzoate (3f)

According to Experimental procedure A, DDQ (45.4 mg, 0.20 mmol), 5-fluoroindole (40.5 mg, 0.30 mmol), and CH_2Cl_2 (1.0 mL) were used. The rection time of oxidation step was 1.5 h. The crude product was purified by flash column chromatography on silica gel (hexane/EtOAc = 2/1) to afford **3f** (53.0 mg, 0.176 mmol) in 88% yield.

Gray solid; ^{1}H NMR (500 MHz, $CDCl_3$): δ 10.42 (s, 1H), 8.53 (brs, 1H), 7.36 (dd, J = 9.0, 4.5 Hz, 1H), 7.22 (d, J = 2.5 Hz, 1H), 7.17 (d, J = 9.0 Hz, 1H), 7.01–6.97 (m, 2H), 6.95 (dd, J = 9.0, 2.5 Hz, 1H), 5.13 (s, 1H), 3.29 (s, 3H). Spectroscopic data of ^{1}H NMR was identical to that reported in the reference 1.

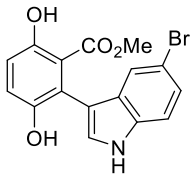

3g

Methyl 3,6-dihydroxy-2-(5'-bromo-1*H*-indol-3'-yl)benzoate (3g)

According to Experimental procedure A, DDQ (45.4 mg, 0.20 mmol), 5-bromoindole (58.5 mg, 0.30 mmol), and CH_2Cl_2 (1.0 mL) were used. The rection time of oxidation step was 1.5 h. The crude product was purified by flash column chromatography on silica gel (hexane/EtOAc = 2/1) to afford **3f** (55.1 mg, 0.152 mmol) in 76% yield.

Gray solid; ^{1}H NMR (500 MHz, $CDCl_3$): δ 10.45 (s, 1H), 8.45 (brs, 1H), 7.43 (s, 1H), 7.35–7.32 (m, 2H), 7.21–7.17 (m, 2H), 7.00 (d, J = 9.0 Hz, 1H), 4.99 (s, 1H), 3.30 (s, 3H). Spectroscopic data of ^{1}H NMR was identical to that reported in the reference 1.

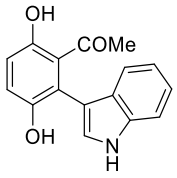

3h

1-(3,6-dihydroxy-2-(1*H*-indol-3'-yl)phenyl)ethan-1-one (3h)

According to Experimental procedure A, 2',5'-dihydroxyacetophenone (30.4 mg, 0.20 mmol), DDQ (45.4 mg, 0.20 mmol), indole (35.1 mg, 0.30 mmol), and THF (1.5 mL) were used. The reaction time of oxidation step was 1 h. The crude product was purified by flash column chromatography on silica gel (hexane/Et_2O = 3/2) to afford **3h** (33.1 mg, 0.124 mmol) in 62% yield.

Yellow solid; m.p. 228–229 °C; IR(NaCl) cm^{-1}: 3353, 1687, 1615, 1459, 1286, 1207; ^{1}H NMR (500 MHz, $CDCl_3$): δ 10.62 (brs, 1H), 10.45 (s, 1H), 7.51 (d, J = 8.0 Hz, 1H), 7.37–7.35 (m, 2H), 7.20–7.17 (m, 1H), 7.11 (d, J = 8.9 Hz, 1H), 7.09–7.06 (m, 2H), 6.87 (d, J = 8.9 Hz, 1H), 1.76 (s, 3H); ^{13}C NMR (125 MHz, $CDCl_3$): δ 206.9, 153.5, 149.2, 137.6, 128.5, 126.9, 125.7, 122.9, 122.3, 121.6, 120.7, 120.3, 117.7, 112.6, 111.3, 30.7; MALDI-HRMS (*m*/*z*) calcd. for $C_{16}H_{13}NO_3$ $[M]^+$ 267.0890, found 267.0884.

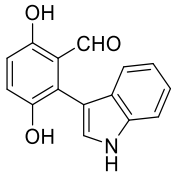

3i

3,6-dihydroxy-2-(1*H*-indol-3'-yl)benzaldehyde (3i)

According to Experimental procedure A, 2,5-dihydroxybenzaldehyde (27.6 mg, 0.20 mmol), DDQ (45.4 mg, 0.20 mmol), indole (35.1 mg, 0.30 mmol), and CH_2Cl_2 (1.5 mL) were used. The reaction time of oxidation step was 1 h. The crude product was purified by flash column chromatography on silica gel (hexane/EtOAc = 2/1) to afford **3i** (32.3 mg, 0.128 mmol) in 64% yield.

Orange solid; m.p. 248 °C (decomp.); IR(NaCl) cm^{-1}: 3384, 1640, 1579, 1458, 1277, 1178; ^1H NMR (500 MHz, $(CD_3)_2CO$): δ 11.44 (s, 1H), 10.70 (brs, 1H), 9.71 (s, 1H), 7.55 (d, *J* = 2.3 Hz, 1H), 7.53 (d, *J* = 8.6 Hz, 1H), 7.36 (brs, 1H), 7.33 (d, *J* = 8.0 Hz, 1H), 7.29 (d, *J* = 8.9 Hz, 1H), 7.21–7.18 (m, 1H), 7.08 (td, *J* = 7.4, 1.1 Hz, 1H), 6.88 (d, *J* = 8.9 Hz, 1H); ^{13}C NMR (125 MHz, $(CD_3)_2CO$): δ 198.7, 157.2, 148.9, 137.4, 129.4, 127.9, 126.5, 125.1, 122.9, 120.8, 120.0, 117.4, 112.6, 107.0; MALDI-HRMS (*m*/*z*) calcd. for $C_{15}H_{11}NO_3$ $[M]^+$ 253.0733, found 253.0735.

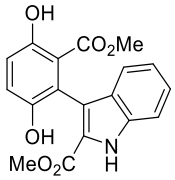

3k

Methyl 3-(3',6'-dihydroxy-2'-(methoxycarbonyl)phenyl)-1*H*-indole-2-carboxylate (3k)

According to Experimental procedure A, DDQ (45.4 mg, 0.20 mmol), methyl 1*H*-indole-2-carboxylate (52.5 mg, 0.30 mmol), and CH_2Cl_2 (1.0 mL) were used. The reaction time of oxidation step was 1.5 h. The crude product was purified by flash column chromatography on silica gel (hexane/EtOAc = 1/1) to afford **3k** (61.4 mg, 0.180 mmol) in 90% yield.

Pink solid; m.p. 188.7–189.6 °C; IR(ATR) cm^{-1}: 3381, 3312, 2946, 1694, 1465, 1438, 1319, 1278, 1243, 1191, 1146, 1064; ^1H NMR (500 MHz, $CDCl_3$): δ 10.55 (s, 1H), 9.17 (brs, 1H), 7.47 (d, *J* = 8.0 Hz, 1H), 7.38 (t, *J* = 8.0 Hz, 1H), 7.32 (d, *J* = 8.0 Hz, 1H), 7.21 (d, *J* = 9.0 Hz, 1H), 7.14 (t, *J* = 8.0 Hz, 1H), 7.05 (d, *J* = 9.0 Hz, 1H), 4.87 (brs, 1H), 3.77 (s, 3H), 3.26 (s, 3H); ^{13}C NMR (125 MHz, $CDCl_3$): δ 170.9, 162.1, 156.0, 146.7, 135.9, 127.5, 126.3, 123.9, 123.1, 121.5, 121.5, 121.1, 118.9, 116.7, 112.5, 111.9, 52.2, 51.8; ESI-HRMS (*m*/*z*) calcd. for $C_{18}H_{15}NO_6Na$ $[M+Na]^+$ 364.0792, found 364.0776.

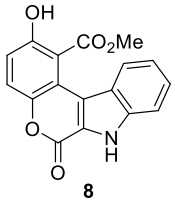

8

Methyl 2-hydroxy-6-oxo-6,7-dihydrochromeno[3,4-*b*]indole-1-carboxylate (8)

K_2CO_3 (69.1 mg, 0.50 mmol) was added to a solution of **3k** (34.1 mg, 0.10 mmol) in THF (1.0 mL) at room temperature. After being stirred for 12 h at room temperature, distilled water was added to the mixture. The resulting mixture was filtered through a pad of Celite. The filtrate was concentrated in vacuo to afford **8** (13.9 mg, 0.0449 mmol) in 45% yield.

Pale yellow solid; m.p. 248.6–250.8 ºC; IR(ATR) cm^{-1}: 3258, 2951, 1707, 1672, 1620, 1591, 1571, 1522, 1435, 1380, 1331, 1286, 1212, 1012; ^1H NMR (500 MHz, $(CD_3)_2SO$): δ 7.79 (d, J = 8.5 Hz, 1H), 7.62 (d, J = 8.5 Hz, 1H), 7.45 (t, J = 8.5 Hz, 1H), 7.37 (d, J = 9.2 Hz, 1H), 7.26 (t, J = 8.5 Hz, 1H), 6.95 (d, J = 9.2 Hz, 1H), 3.88 (s, 3H); ^{13}C NMR (125 MHz, $(CD_3)_2SO$): δ 169.8, 156.9, 155.4, 141.3, 139.9, 126.3, 123.1, 122.9, 121.8, 120.9, 119.5, 118.3, 116.6, 116.5, 115.5, 113.6, 52.0; ESI-HRMS (*m*/*z*) calcd. for $C_{17}H_{11}NO_5Na$ $[M+Na]^+$ 332.0529, found 332.0504.

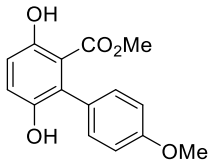

4a

Methyl 3,6-dihydroxy-4'-methoxy-[1,1'-biphenyl]-2-carboxylate (4a)

According to Experimental procedure A, DDQ (45.4 mg, 0.20 mmol), anisole (32.4 mg, 0.30 mmol), and CH_2Cl_2 (1.0 mL) were used. The reaction time of oxidation step was 1.5 h. The crude product was purified by flash column chromatography on silica gel (hexane/EtOAc = 1/1) to afford **4a** (41.6 mg, 0.152 mmol) in 76% yield.

Orange solid; m.p. 86.9–87.9 ℃. IR(ATR) cm^{-1}: 3443, 2953, 2838, 1667, 1609, 1514, 1456, 1336, 1246, 1177, 1129, 830; ^1H NMR (500 MHz, $CDCl_3$): δ 10.45 (s, 1H), 7.13 (d, J = 8.2 Hz, 2H), 7.12 (d, J = 9.2 Hz, 1H), 7.00 (d, J = 8.2 Hz, 2H), 6.96 (d, J = 9.2 Hz, 1H), 4.62 (s, 1H), 3.87 (s, 3H), 3.46 (s, 3H); ^{13}C NMR (125 MHz, $CDCl_3$): δ 170.9, 159.2, 155.6, 146.1, 130.4, 127.8, 127.0, 122.5, 118.1, 114.3, 111.8, 55.2, 51.8; ESI-HRMS (*m*/*z*) calcd. for $C_{15}H_{14}O_5Na$ $[M+Na]^+$ 297.0733, found 297.0731.

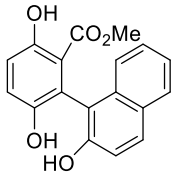

4b

Methyl 3,6-dihydroxy-2-(2'-hydroxynaphthalen-1'-yl)benzoate (4b)

According to Experimental procedure A, DDQ (45.4 mg, 0.20 mmol), 2-naphthol (43.2 mg, 0.30 mmol), and CH_2Cl_2 (1.0 mL) were used. The reaction time of oxidation step was 1.5 h. The crude product was purified by flash column chromatography on silica gel (hexane/EtOAc = 1/1) to afford **4b** (37.8 mg, 0.122 mmol) in 61% yield.

White solid; ^{1}H NMR (500 MHz, $CDCl_3$): δ 10.81 (s, 1H), 7.86 (d, J = 9.5 Hz, 1H), 7.84–7.82 (m, 1H), 7.37–7.35 (m, 2H), 7.30 (d, J = 9.0 Hz, 1H), 7.27 (d, J = 9.5 Hz, 1H), 7.18–7.16 (m, 1H), 7.15 (d, J = 9.0 Hz, 1H), 3.20 (s, 3H). Spectroscopic data of ^{1}H NMR was identical to that reported in the reference 2.

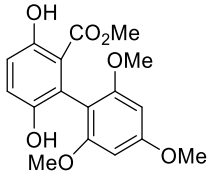

4c

Methyl 3,6-dihydroxy-2',4',6'-trimethoxy-[1,1'-biphenyl]-2-carboxylate (4c)

According to Experimental procedure A, PIDA (64.4 mg, 0.20 mmol), 1,3,5-trimethoxybenzene (50.5 mg, 0.30 mmol), and CH_2Cl_2 (1.5 mL) were used. The reaction time of oxidation step was 1 h. The crude product was purified by flash column chromatography on silica gel (hexane/EtOAc = 1/1) to afford **4c** (47.2 mg, 0.141 mmol) in 71% yield.

White solid; m.p. 133.4–135.3 °C; IR(ATR) cm^{-1}: 3466, 2950, 2839, 1663, 1607, 1582, 1506, 1453, 1335, 1224, 1121, 1053; ^{1}H NMR (500 MHz, $CDCl_3$): δ 10.41 (s, 1H), 7.13 (d, J = 9.3 Hz, 1H), 6.94 (d, J = 9.3 Hz, 1H), 6.23 (s, 2H), 4.90 (s, 1H), 3.88 (s, 3H), 3.70 (s, 6H), 3.50 (s, 3H); ^{13}C NMR (125 MHz, $CDCl_3$): δ 171.1, 161.7, 158.3, 155.6, 146.4, 122.7, 120.1, 117.9, 113.0, 105.3, 90.9, 55.9, 55.3, 51.7; ESI-HRMS (*m*/*z*) calcd. for $C_{17}H_{19}O_7$ $[M+H]^+$ 335.1125, found 335.1104.

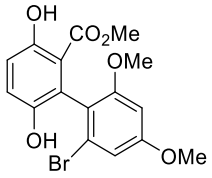

4d

Methyl 2'-bromo-3,6-dihydroxy-4',6'-dimethoxy-[1,1'-biphenyl]-2-carboxylate (4d)

According to Experimental procedure A, PIDA (64.4 mg, 0.20 mmol), 1-bromo-3,5-dimethoxybenzene (65.1 mg, 0.30 mmol), and CH_2Cl_2 (1.5 mL) were used. The reaction time of oxidation step was 1 h. The crude product was purified by flash column chromatography on silica gel (hexane/EtOAc = 2/1) to afford **4d** (44.4 mg, 0.116 mmol) in 58% yield.

Colorless oil; m.p. 107.1–110.2 °C; IR(ATR) cm^{-1}: 3448, 3008, 2951, 1665 1602, 1561, 1496, 1462, 1436, 1212, 1152, 1033; ^1H NMR (500 MHz, $CDCl_3$): δ 10.72 (s, 1H), 7.16 (d, J = 9.0 Hz, 1H), 7.00 (d, J = 9.0Hz, 1H), 6.85 (d, J = 2.5 Hz, 1H), 6.51 (d, J = 2.5 Hz, 1H), 4.47 (s, 1H), 3.86 (s, 3H), 3.68 (s, 3H), 3.52 (s, 3H); ^{13}C NMR (125 MHz, $CDCl_3$): δ 170.6, 160.9, 158.8, 156.3, 145.8, 125.3, 123.1, 122.8, 118.9, 118.1, 111.7, 108.9, 98.2, 56.0, 55.6, 52.2; ESI-HRMS (*m*/*z*) calcd. for $C_{16}H_{15}O_6BrNa$ $[M+Na]^+$ 404,9944, found 404,9947.

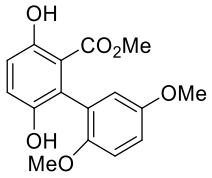

4e

Methyl 3,6-dihydroxy-2',5'-dimethoxy-[1,1'-biphenyl]-2-carboxylate (4e)

According to Experimental procedure A, DDQ (45.4 mg, 0.20 mmol), 1,4-dimethoxybenzene (41.4 mg, 0.30 mmol), and CH_2Cl_2 (1.0 mL) were used. The reaction time of oxidation step was 1.5 h. The crude product was purified by flash column chromatography on silica gel (hexane/EtOAc = 1/1) to afford **4b** (28.4 mg, 0.0933 mmol) in 47% yield.

Brown solid; m.p. 122.6–124.2 °C; IR(ATR) cm^{-1}: 3437, 2952, 2834, 1667, 1605, 1459, 1438, 1271, 1221, 1044; ^1H NMR (500 MHz, $CDCl_3$): δ 10.35 (s, 1H), 7.15 (d, J = 9.0 Hz, 1H), 6.97 (d, J = 9.0 Hz, 1H), 6.95 (d, J = 9.5 Hz, 1H), 6.91 (dd, J = 9.5, 3.0 Hz, 1H), 6.67 (d, J = 3.0 Hz, 1H), 4.95 (s, 1H), 3.77 (s, 3H), 3.72 (s, 3H), 3.47 (s, 3H); ^{13}C NMR (125 MHz, $CDCl_3$): δ 170.8, 155.6, 153.9, 150.7, 145.8, 125.8, 123.8, 123.2, 118.4, 116.1, 114.3, 112.5, 112.2, 56.4, 55.7, 51.8; ESI-HRMS (*m*/*z*) calcd. for $C_{16}H_{17}O_6$ $[M+H]^+$ 305.1020, found 305.1022.

Experimental procedure for Scheme 3:

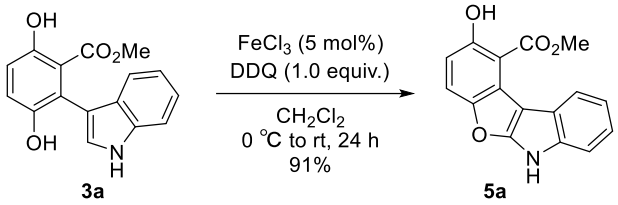

Methyl 2-hydroxy-6*H*-benzofuro[2,3-*b*]indole-1-carboxylate (5a)

$FeCl_3$ (1.4 mg, 9.0 μmol), DDQ (40 mg, 0.18 mmol), and CH_2Cl_2 (1.0 mL) were successively added to a solution of **3a** (50 mg, 0.18 mol) in CH_2Cl_2 (1.0 mL) at 0 ℃. After being stirred for 24 h at 0 ℃ to room temperature, saturated aqueous $NaHCO_3$ solution was added to the mixture. The resulting mixture was extracted with CH_2Cl_2. The combined organic layers were dried over Na_2SO_4 and concentrated in vacuo. The residue was purified by flash column chromatography on silica gel (hexane/EtOAc = 2/1) to afford **5a** (46 mg, 0.164 mmol) in 91% yield.

Yellow solid; ^{1}H NMR; (500 MHz, $CDCl_3$): δ 11.10 (s, 1H), 8.40 (s, 1H), 7.93–7.89(m, 1H), 7.56 (d, J = 8.5 Hz, 1H), 7.44–7.42 (m, 1H), 7.31–7.27 (m, 2H), 6.80 (d, J = 8.5 Hz, 1H), 4.23 (s, 3H). Spectroscopic data of ^{1}H NMR was identical to that reported in the reference 3.

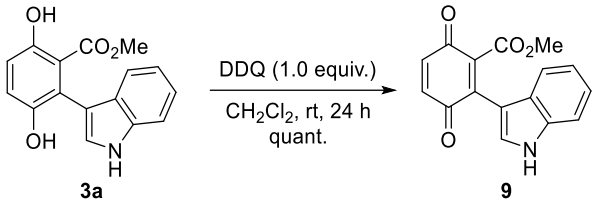

Methyl 2-(1*H*-indol-3'-yl)-3,6-dioxocyclohexa-1,4-diene-1-carboxylate (9)

DDQ (23 mg, 0.10 mmol) was added to a solution of **3a** (28 mg, 0.10 mmol) in CH_2Cl_2 (1.0 mL) at room temperature. After being stirred for 24 h at room temperature, saturated aqueous $NaHCO_3$ solution was added to the mixture. The resulting mixture was extracted with CH_2Cl_2. The combined organic layers were concentrated in vacuo to afford **9** (35 mg, 0.12 mmol) in quantitatively yield.

Purple solid; ^{1}H NMR (500 MHz, $CDCl_3$): δ 8.67 (brs, 1H), 7.51–7.47 (m, 2H), 7.39 (d, J = 8.2 Hz, 1H), 7.25–7.16 (m, 2H), 6.95–6.87 (m, 2H), 3.68 (s, 3H). Spectroscopic data of ^{1}H NMR was identical to that reported in the reference 4.

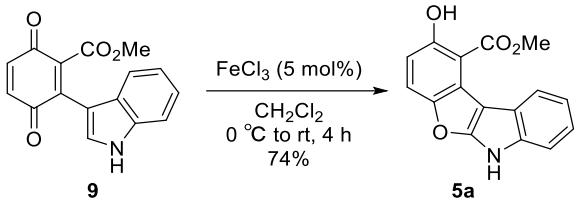

9 **5a**

Methyl 2-hydroxy-6*H*-benzofuro[2,3-*b*]indole-1-carboxylate (5a)

$FeCl_3$ (0.75 mg, 5.0 μmol) was added to a solution of **9** (26 mg, 0.090 mmol) in CH_2Cl_2 (0.5 mL) at 0 ℃. After being stirred for 4 h at 0 ℃ to room temperature, saturated aqueous $NaHCO_3$ solution was added to the mixture. The resulting mixture was extracted with CH_2Cl_2. The combined organic layers were dried over Na_2SO_4 and concentrated in vacuo. The residue was purified by flash column chromatography on silica gel (hexane/EtOAc = 1/1) to afford **5a** (20 mg, 0.70 mmol) in 78% yield.

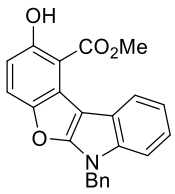

5b

Methyl 6-benzyl-2-hydroxy-6*H*-benzofuro[2,3-*b*]indole-1-carboxylate (5b)

$FeCl_3$ (0.80 mg, 5.0 μmol) and DDQ (22.7 mg, 0.10 mmol) were added to a solution of **3d** (37.3 mg, 0.10 mmol) in CH_2Cl_2 (1.0 mL) at 0 ℃. After being stirred for 24 h at 0 ℃ to room temperature, saturated aqueous $NaHCO_3$ solution was added to the mixture. The resulting mixture was extracted with CH_2Cl_2. The combined organic layers were dried over Na_2SO_4 and concentrated in vacuo. The residue was purified by flash column chromatography on silica gel (hexane/EtOAc = 3/1) to afford **5b** (26.9 mg, 0.072 mmol) in 72% yield.

Yellow solid; m.p. 155–156 ºC; IR (ATR) cm^{-1}: 3030, 2952, 1659, 1622, 1572, 1553, 1511, 1495, 1474, 1453, 1440, 1359, 1203, 1112, 1026; ^1H NMR (500 MHz, $CDCl_3$): δ 11.1 (s, 1H), 7.90 (d, *J* = 8.0 Hz, 1H), 7.52 (d, *J* = 8.6 Hz, 1H), 7.33–7.23 (m, 8H) , 6.76 (d, *J* = 8.6 Hz, 1H), 5.43 (s, 2H), 4.19 (s, 3H); ^{13}C NMR (125 MHz, $CDCl_3$): δ 171.0, 159.1, 158.4, 149.9, 137.6, 128.9, 127.9, 126.8, 125.2, 121.5, 121.3, 120.9, 118.3, 110.4,109.5, 103.8, 98.6, 52.8, 46.5; ESI-HRMS (*m*/*z*) calcd. for $C_{23}H_{18}NO_4$ $[M+H]^+$ 372.1230, found 372.1228.

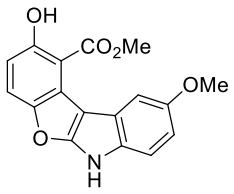

5c

Methyl 2-hydroxy-9-methoxy-6*H*-benzofuro[2,3-*b*]indole-1-carboxylate (5c)

$FeCl_3$ (0.80 mg, 5.0 μmol) and DDQ (22.7 mg, 0.10 mmol) were added to a solution of **3e** (31.3 mg, 0.10 mmol) in CH_2Cl_2 (1.0 mL) at 0 ℃. After being stirred for 24 h at 0 ℃ to room temperature, saturated aqueous $NaHCO_3$ solution was added to the mixture. The resulting mixture was extracted with CH_2Cl_2. The combined organic layers were dried over Na_2SO_4 and concentrated in vacuo. The residue was purified by flash column chromatography on silica gel (hexane/EtOAc = 2/1) to afford **5c** (23.3 mg, 0.075 mmol) in 75% yield.

Yellow solid; m.p. 162–163 ºC; IR (ATR) cm^{-1}: 3302, 2952, 1658, 1626, 1579, 1550, 1519, 1461, 1438, 1287, 1205, 1112, 1104; ^1H NMR (500 MHz, $CDCl_3$): δ 11.1 (s, 1H), 8.29 (s, 1H), 7.53 (d, J = 8.6 Hz, 1H), 7.44 (d, J = 2.3 Hz 1H), 7.30 (d, J = 9.2 Hz, 1H), 6.90 (dd, J = 8.6, 2.3 Hz, 1H), 6.78 (d, J = 9.2 Hz, 1H), 4.19 (s, 3H), 3.93 (s, 3H); ^{13}C NMR (125 MHz, $CDCl_3$): δ 170.9, 159.0, 158.3, 154.9, 149.8, 131.6, 124.8, 122.7, 118.3, 112.4, 109.8, 109.7, 106.0, 103.9, 100.1, 56.0, 52.9; ESI-HRMS (*m*/*z*) calcd. for $C_{16}H_{14}NO_5$ $[M+H]^+$ 312.0866, found 312.0866.

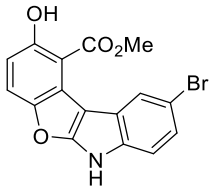

5d

Methyl 9-bromo-2-hydroxy-6*H*-benzofuro[2,3-*b*]indole-1-carboxylate (5d)

$FeCl_3$ (0.80 mg, 5.0 μmol) and DDQ (22.7 mg, 0.10 mmol) were added to a solution of **3g** (36.2 mg, 0.10 mmol) in CH_2Cl_2 (1.0 mL) at 0 ℃. After being stirred for 24 h at 0 ℃ to room temperature, saturated aqueous $NaHCO_3$ solution was added to the mixture. The resulting mixture was extracted with CH_2Cl_2. The combined organic layers were dried over Na_2SO_4 and concentrated in vacuo. The residue was purified by flash column chromatography on silica gel (hexane/EtOAc = 2/1) to afford **5d** (21.3 mg, 0.059 mmol) in 59% yield.

Yellow solid; m.p. 260–263 ℃, IR (ATR) cm^{-1}: 3247, 1651, 1623, 1461, 1438, 1419, 1359, 1257, 1212, 1208, 1178, 1156; 1H NMR (500 MHz, $(CD_3)_2SO$): δ 10.30 (s, 1H), 7.99 (d, J = 2.3 Hz, 1H), 7.66 (d, J = 8.6 Hz, 1H), 7.39 (d, J = 8.6 Hz, 1H), 7.29 (dd, J = 8.6, 1.7 Hz, 1H), 6.73 (d, J

= 9.2 Hz, 1H), 4.05 (s, 3H); ^{13}C NMR (125 MHz, $(CD_3)_2SO$): δ 169.3, 159.0, 156.0, 149.9, 136.3, 124.9, 124.0, 123.5, 123.0, 117.5, 114.8, 113.3, 110.4, 107.0, 97.9, 53.1; ESI-HRMS (*m*/*z*) calcd. for $C_{16}H_{11}NO_4Br$ $[M+H]^+$ 359.9866, found 359.9872.

Experimental procedure for Scheme 4:

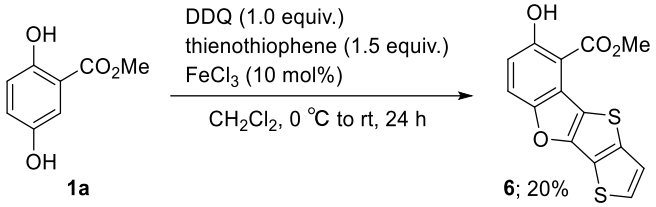

Methyl 5-hydroxy-thieno[2',3':4,5]thieno[3,2-*b*]benzofuran-4-carboxylate (6)

Thienothiophene (42 mg, 0.30 mmol), $FeCl_3$ (3.2 mg, 0.020 mmol), DDQ (45.4 mg, 0.20 mmol), and CH_2Cl_2 (1.0 mL) were added to a solution of **1a** (34 mg, 0.20 mmol) in CH_2Cl_2 (1.0 mL) at 0 ℃. After being stirred for 24 h at 0 ℃ to room temperature, saturated aqueous $NaHCO_3$ solution was added to the mixture. The resulting mixture was extracted with CH_2Cl_2. The combined organic layers were dried over Na_2SO_4 and concentrated in vacuo. The residue was purified by flash column chromatography on silica gel (hexane/EtOAc = 5/1) to afford **6** (12 mg, 0.039 mmol) in 20% yield.

Yellow solid; m.p. 198–205 ℃; IR (NaCl) cm^{-1}: 2922, 1679, 1610, 1491, 1464, 1426, 1355, 1304, 1256, 1232, 1222, 1112; ^{1}H NMR (500 MHz, $CDCl_3$): δ 11.01 (s, 1H), 7.66 (d, J = 9.0 Hz, 1H), 7.47 (d, J = 5.0 Hz, 1H), 7.34 (d, J = 5.0 Hz, 1H), 6.94 (d, J = 9.0 Hz, 1H), 4.16 (s, 3H); ^{13}C NMR (125 MHz, $CDCl_3$): δ 170.4, 159.4. 152.4, 151.4, 144.1, 127.8, 124.3, 122.4, 122.1, 121.1, 119.5, 113.5, 102.5, 52.3; MALDI-HRMS (*m*/*z*) calcd. for $C_{14}H_8O_4S_2$ $[M]^+$ 303.9859, found 303.9857.

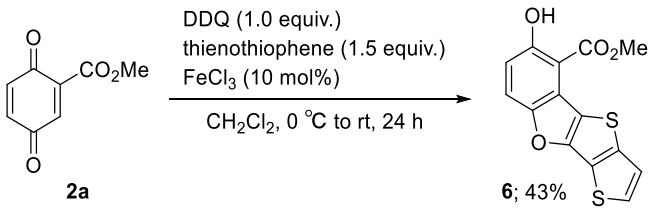

Thienothiophene (21 mg, 0.15 mmol), $FeCl_3$ (1.6 mg, 0.010 mmol), DDQ (22.7 mg, 0.10 mmol), and CH_2Cl_2 (0.5 mL) were added to a mixture of **2a** (17 mg, 0.10 mmol) in CH_2Cl_2 (0.5 mL) at 0 ℃. After being stirred for 24 h at 0 ℃ to room temperature, saturated aqueous $NaHCO_3$ was added to the mixture. The resulting mixture was extracted with CH_2Cl_2. The combined organic layers were dried over Na_2SO_4 and concentrated in vacuo. The residue was purified by flash

column chromatography on silica gel (hexane/EtOAc = 5/1) to afford **6** (13 mg, 0.043 mmol) in 43% yield.

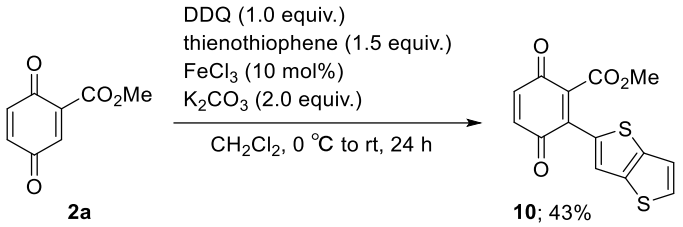

Methyl 3,6-dioxo-2-(thieno[3,2-*b*]thiophen-2-yl)cycloxexa-1,4-diene-1-carboxylate (10)

Thienothiophene (63 mg, 0.45 mmol), DDQ (68 mg, 0.30 mmol), and CH_2Cl_2 (1.5 mL) were added to a solution of **2a** (48 mg, 0.30 mmol) and K_2CO_3 (81 mg, 0.60 mmol) in CH_2Cl_2 (1.5 mL) at 0 ℃. After being stirred for 24 h at 0 ℃ to room temperature, saturated aqueous $NaHCO_3$ solution was added to the mixture. The resulting mixture was extracted with CH_2Cl_2. The combined organic layers were dried over Na_2SO_4 and concentrated in vacuo. The residue was purified by flash column chromatography on silica gel (hexane/EtOAc = 4/1) to afford **10** (40 mg, 0.13 mmol) in 43% yield.

Dark red solid; m.p. 135–140 ℃; IR (NaCl) cm^{-1}:1735, 1667, 1650, 1560, 1486, 1448, 1435, 1419, 1379, 1308, 1280, 1230, 1099, 1046; ^1H NMR (500 MHz, $CDCl_3$): δ 7.70 (s, 1H), 7.54 (d, J = 5.5 Hz, 1H), 7.28 (d, J = 5.5 Hz, 1H), 6.84–6.91 (m, 2H), 3.90 (s, 3H); ^{13}C NMR (125 MHz, $CDCl_3$): δ 185.7, 183.5, 165.2, 146.0, 139.8, 136.4, 136.0, 134.5, 133.0, 131.4, 124.9, 119.5, 53.2; MALDI-HRMS (*m*/*z*) calcd. for $C_{14}H_8O_4S_2$ $[M]^+$ 303.9853, found 303.9858.

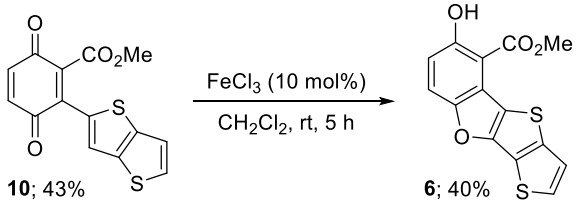

$FeCl_3$ (1,5 mg, 9.2 μmol) was added to a mixture of **10** (28 mg, 0.092 mmol) in CH_2Cl_2 (1.0 mL) at room temperature. After being stirred for 5 h at room temperature, water was added to the mixture. The resulting mixture was extracted with CH_2Cl_2. The combined organic layers were dried over Na_2SO_4 and concentrated in vacuo. The yield was calculated by crude ^1H NMR using dimethyl sulfone (8.7 mg, 0.092 mmol) as an internal standard.

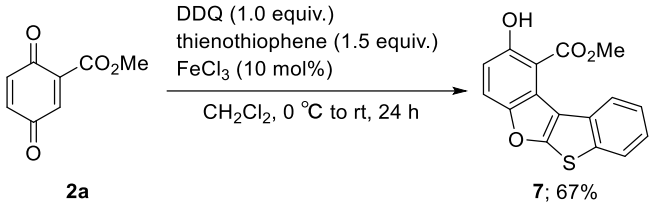

2a **7**; 67%

Methyl 2-hydroxybenzo[4,5]thieno[2,3-*b*]benzofuran-1-carboxylate (7)

Benzothiophene (20 mg, 0.15 mmol), $FeCl_3$ (1.6 mg, 0.010 mmol), DDQ (22.7 mg, 0.10 mmol), and CH_2Cl_2 (0.5 mL) were successively added to a solution of **2a** (17 mg, 0.10 mmol) in CH_2Cl_2 (0.5 mL) at 0 ℃. After being stirred for 24 h at 0 ℃ to room temperature, saturated aqueous $NaHCO_3$ solution was added to the mixture. The resulting mixture was extracted with CH_2Cl_2. The combined organic layers were dried over Na_2SO_4 and concentrated in vacuo. The residue was purified by flash column chromatography on silica gel (hexane/EtOAc = 5/1) to afford **7** (20 mg, 0.067 mmol) in 67% yield.

Pale yellow solid; m.p. 136–140 ºC; IR (NaCl) cm^{-1}: 2952, 1667, 1612, 1577, 1493, 1457, 1439, 1433, 1421, 1327, 1276, 1255, 1255, 1213, 1117, 1032; ^1H NMR (400 MHz, $CDCl_3$): δ 10.53 (s, 1H), 7.92 (d, *J* = 8.2 Hz, 1H), 7.82 (d, *J* = 8.2 Hz, 1H), 7.68 (d, *J* = 9.1 Hz, 1H), 7.49–7.46 (m, 1H), 7.38–7.35 (m, 1H), 6.98 (d, *J* = 9.1 Hz, 1H), 4.13 (s, 3H); ^{13}C NMR (125 MHz, $CDCl_3$): δ 170.3, 162.1, 158.3, 154.2, 137.8, 131.1, 124.9, 124.1, 124.0, 123.8, 122.8, 120.0, 118.6, 113.1, 104.9, 52,4; MALDI-HRMS (*m*/*z*) calcd. for $C_{16}H_{10}O_4S$ $[M]^+$ 298.0294, found 298.0294.

4. Structure determination of compound 6.

4-1. Determination by MicroED.

MicroED data collection;

The microcrystals of **6**, as obtained in S14 or recrystallized as follows, were used to prepare two MicroED grids. Crystals in the two grids were isomorphic and merged during data processing. For recrystallization, the compound **6** was dissolved in a small amount of hot MeOH. After 12 h at room temperature, resulting precipitates were filtrated and dried in the air.

A Quantifoil grid (Cu R 1.2/1.3) containing the crystals was loaded into a CRYO ARM 300 II (JEOL Ltd.) equipped with an XF416 camera (TVIPS). The CRYO ARM 300 II had an omega filter set at a slit width of 20 eV and was operated at an acceleration voltage of 300 kV while being cooled at liquid nitrogen temperature. The emission and illumination conditions were as follows: CL aperture at 100 µm, spot 7, alpha 1, emission at 2.0 µA and A2 at 4.8 kV for parallel beam illumination, leading to the beam diameter of *ca.* 2.0 µm. The virtual camera distance was set to nominal 600 mm, calibrated to be 715 mm. Automatic data collection was carried out by SerialEM[5] with a strategy similar to those reported in the references 6–8. Crystals identified on montage maps were centered by stage shifts and brought to the eucentric height at a view magnification of x2500. Continuous rotation diffraction patterns were then collected at a rotation rate of 1°/sec, 1 frame/sec, with an electron flux of 0.05 electron/Å^2/sec, spanning 60° per crystal. To mitigate preferred orientations of crystals on a grid, the starting angles of rotation were varied from -50° to -20° among crystals. Images were recorded at 2x binning (2048 x 2048 pixels) with a pedestal of 100 and the image correction parameter LC_ROW 1[9].

Diffraction patterns from more than 550 crystals were measured. Typical images of crystals and diffraction patterns are shown in Supplementary Figure S2 The crystals were thin plates and tended to be bent and curly. Diffraction spots were streaky.

MicroED data processing;

Diffraction patterns were processed with DIALS[10,11] with parallelization provided by GNU parallel[12]. 26 crystals that diffracted to high resolutions and showed similar unit cell parameters were scaled with dials.scale[13]. Merging statistics are shown in Supplementary Table S2. Structure solution by SHELXD[14] and kinematical refinement by SHELXL[15] were carried out in the Olex2 GUI[16]. Twin refinement with a twinning operator h,-k,-h-l was employed. Anisotropic atomic displacement factor (ADP) refinement was unstable, leading to many non-positive definite ADP

tensors. Thus we refined only isotropic ADP. Probably this is caused by the limited data quality (diffraction spot streaking and unit cell variability), crystal twinning and/or multiple scattering. The resulting MicroED structure should be interpreted qualitatively, not quantitatively.

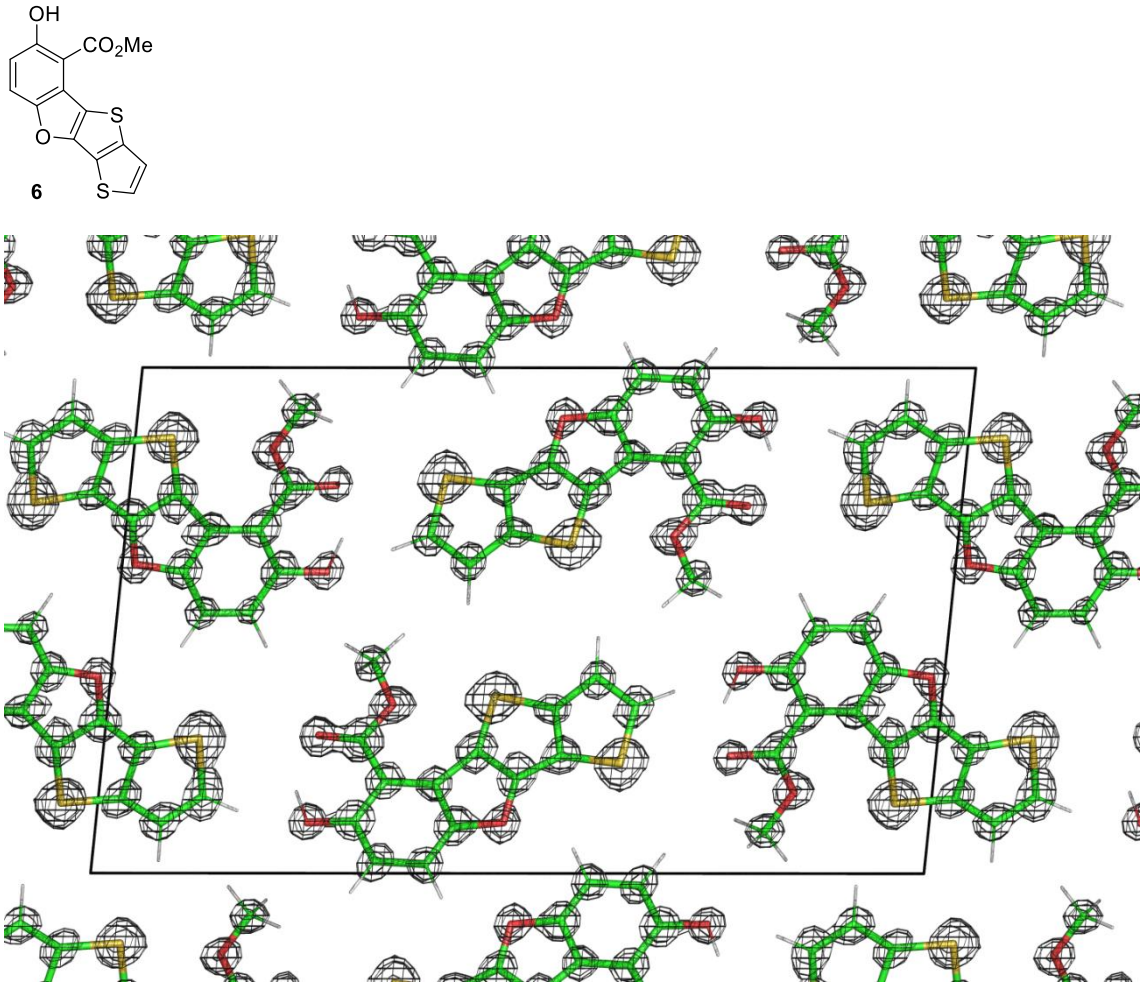

Figure S1: MicroED structure and map of 6 showing the bc plane.
The figure was rendered by PyMOL 2.5.0 (Schrödinger LLC).

Supplementary Figure S2:

(A) A square montage showing microcrystals of **6**. Note the crystal bending.

(B) A diffraction pattern of compound **6**.

(C) Raw distributions of the unit cell parameters for crystals diffracted better than 1.2 Å. These are from an early step of processing before using prior cell information in the indexing routine and include bad crystals and mis-indexed crystals. Note the broad angle distributions, probably due to streaky diffraction spots.

(A)

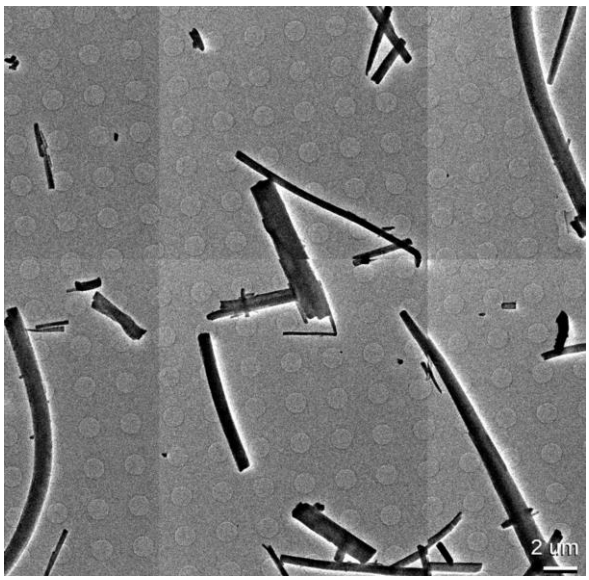

(B)

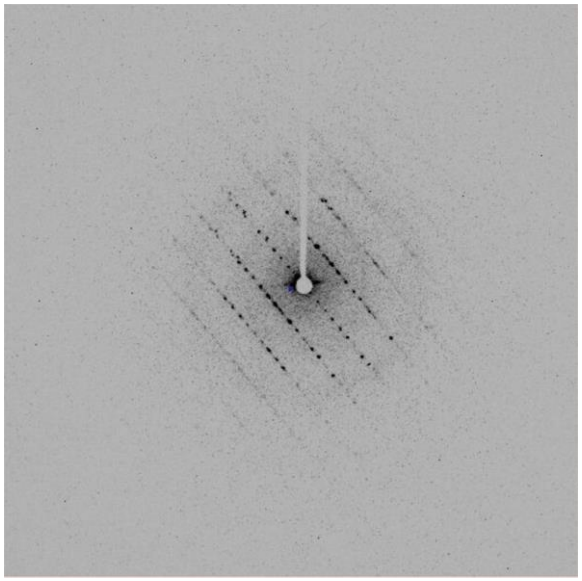

(C)

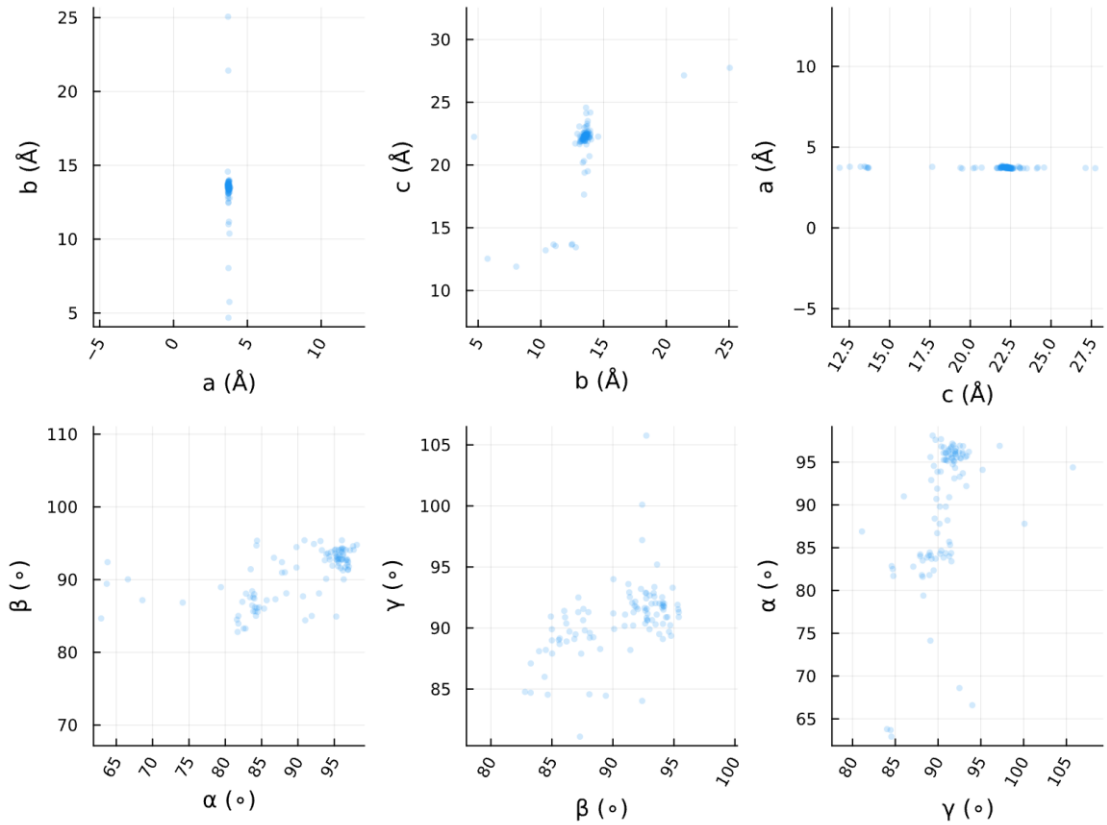

Supplementary Table S2: Merging statistics of the MicroED dataset for compound **6**.

d_max	d_min	#obs	#uniq	mult.	%comp	<I>	<I/sI>	r_mrg	r_meas	r_pim	cc1/2
8.15	2.29	1752	179	9.79	94.71	68.60	33.40	0.12	0.12	0.04	0.992*
2.29	1.83	1644	164	10.02	94.25	33.40	20.80	0.22	0.24	0.07	0.977*
1.83	1.60	2848	208	13.69	97.20	28.30	18.70	0.26	0.27	0.07	0.968*
1.60	1.45	2225	186	11.96	95.38	19.10	11.10	0.33	0.34	0.10	0.945*
1.45	1.35	1874	167	11.22	95.43	12.50	7.30	0.42	0.44	0.13	0.880*
1.35	1.27	1711	158	10.83	95.76	11.50	6.10	0.45	0.47	0.14	0.842*
1.27	1.21	2622	183	14.33	94.82	11.40	6.20	0.47	0.49	0.13	0.923*
1.21	1.15	2954	195	15.15	96.53	10.20	5.40	0.48	0.50	0.13	0.917*
1.15	1.11	2829	197	14.36	95.63	12.70	6.20	0.47	0.49	0.13	0.893*
1.11	1.07	2552	198	12.89	96.59	9.40	4.50	0.52	0.54	0.14	0.832*
1.07	1.04	2163	175	12.36	96.69	6.90	3.30	0.57	0.60	0.16	0.859*
1.04	1.01	2162	171	12.64	96.07	6.10	2.70	0.59	0.61	0.17	0.817*
1.01	0.98	2016	171	11.79	94.48	5.80	2.30	0.60	0.63	0.17	0.743*
0.98	0.96	1871	167	11.20	95.43	4.60	1.80	0.66	0.69	0.20	0.801*
0.96	0.94	1876	162	11.58	95.86	3.90	1.50	0.71	0.74	0.21	0.450*
0.94	0.92	2621	190	13.79	96.94	3.60	1.40	0.71	0.74	0.20	0.554*
0.92	0.90	3263	199	16.40	96.60	3.30	1.40	0.73	0.76	0.18	0.577*
0.90	0.88	2874	189	15.21	94.50	2.80	1.10	0.74	0.77	0.19	0.674*
0.88	0.86	2766	200	13.83	96.62	2.40	0.90	0.73	0.76	0.19	0.375*
0.86	0.85	2514	176	14.28	96.17	2.70	1.00	0.76	0.79	0.19	0.310*
8.15	0.85	47137	3635	12.97	95.83	12.90	6.90	0.35	0.37	0.10	0.982*

Supplementary Table S3: Crystallographic refinement statistics of compound **6**.

Compound	**6**
Chemical formula	C_{14} H_8 O_4 S_2
Formula wt	304.34
Cryst syst	Triclinic
Space group	*P*-1
T, K	79
a, Å	3.711
b, Å	13.550
c, Å	22.244
α, deg	95.74
β, deg	92.86
γ, deg	91.59
Z	4
V, Å^3	1110.8
D_{calc}, g cm^{-3}	1.820
R1[I > 2(I)]	0.2074
wR2 (all)	0.4785
GOF	1.639
Data collection	Talos Arctica microscope
High resolution limit for refinement, Å	0.90
COD ID.	3000464
CCDC no.	2294744
XRDa ID	162

4-2. Determination by chemical modification.

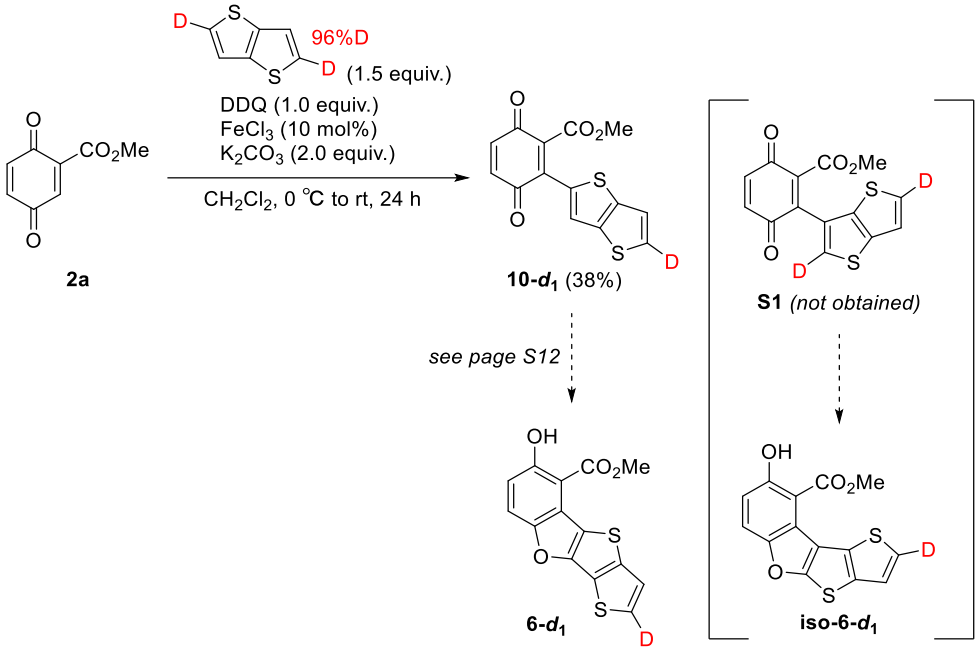

The reaction with **2a** and thieno[3,2-*b*]thiophene-2,5-d_2 provided mono-deuterated **10-d_1** as the reaction intermediate of compound **6-d_1** (see page S12). If di-duterated product **S1** are obtained during this step, **iso-6-d_1** would be produced. These results indirectly proved the structure of **6**.

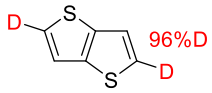

Thieno[3,2-*b*]thiophene-2,5-d_2

n-BuLi (2.64 M in *n*-hexane; 758 mL, 2.00 mmol) was added to a mixture of thieno[3,2-*b*]thiophene (140 mg, 1.00 mmol) in THF (5.0 mL) at -78 °C. After being stirred for 2 h at -78 °C to room temperature, D_2O was added to the mixture. The resulting mixture was extracted with hexane. The combined organic layers were dried over Na_2SO_4 and concentrated in vacuo to afford thieno[3,2-*b*]thiophene-2,5-d_2 (120 mg, 0.86 mmol) in 86% yield.

Gray solid; ^{1}H NMR (500 MHz, $CDCl_3$): δ 7.39 (d, J = 5.0 Hz, 0.08 H), 7.27 (s, 2H); ^{2}H NMR (77 MHz, $CDCl_3$): δ 7.44 (brs).

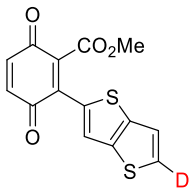

10-d_1

Thieno[3,2-*b*]thiophene-2,5-d_2 (42 mg, 0.40 mmol), $FeCl_3$ (3.2 mg, 0.020 mmol), DDQ (45.4 mg, 0.20 mmol), and CH_2Cl_2 (1.0 mL) were added to a mixture of **2a** (33 mg, 0.20 mmol) in CH_2Cl_2 (1.0 mL) at 0 ℃. After being stirred for 24 h at 0 ℃ to room temperature, saturated aqueous $NaHCO_3$ was added to the mixture. The resulting mixture was extracted with CH_2Cl_2. The combined organic layers were dried over Na_2SO_4 and concentrated in vacuo. The residue was purified by flash column chromatography on silica gel (hexane/EtOAc = 4/1) to afford **S1** (23 mg, 0.075 mmol) in 38% yield.

Dark red solid; ^{1}H NMR (500 MHz, CDCl3): δ 7.71 (s, 1H), 7.29 (s. 1H), 6.92–6.85 (m, 2H), 3.91 (s, 3H); ^{2}H NMR (77 MHz, CDCl3): δ 7.44 (brs).

5. Fluorescence test of compounds 5a, 6, and 7.

Fluorescence and absorption measurement. All solvents for spectrophotometry were purchased from Nacalai Tesque. The solution- and solid-state fluorescence spectra were collected on a Hitachi F-7100 fluorescence spectrophotometer. To obtain an accurate spectrum, spectrum correction was carried out with a concentrated solution of rhodamine B. The solid-state fluorescence spectra were measured by surface photometric method. A cut filter was used to eliminate multiple lights due to the effects of light scattering. The absolute fluorescence quantum yields in the solid state were determined by Hitachi F-7100 fluorescence spectrophotometer by using a calibrated integrating sphere system. UV/Vis spectra were recorded on a HITACHI UH-5700 spectrophotometer at room temperature using a 1 mm quartz cuvette.

Computational details. All calculations were carried with the Gaussian 16 program[17]. Structural optimizations were carried out at the B3LYP level in the gas phase using the 6-31G(d) basis set. The vibrational frequencies were computed at the same level to check whether each optimized structure is an energy minimum (no imaginary frequency). Excitation wavelengths and oscillator strengths were obtained at the density functional level using time-dependent perturbation theory (TDDFT) approach.

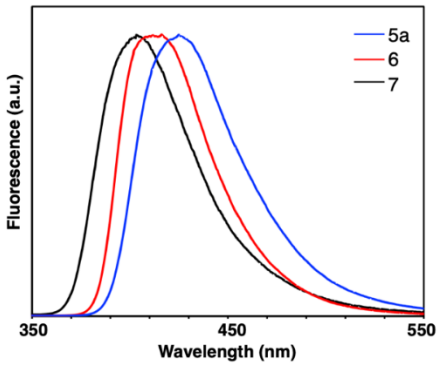

Figure. S3. Normalized fluorescence spectra of **5a**, **6**, and **7** in toluene.

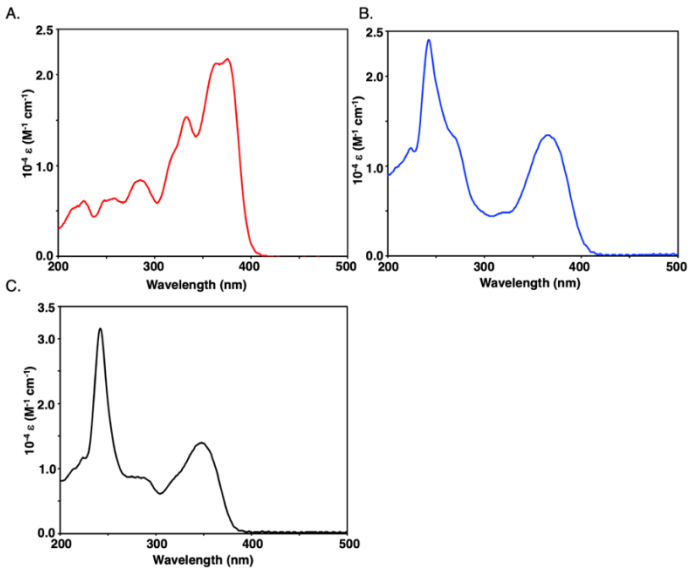

Figure S4. Absorption spectra of (A) **6**, (B) **5a**, and (C) **7** in $CHCl_3$.

All generated absorption bands in the 300 to 400 nm UV region. Compound **6** had a wide and large absorption band, whereas **5a** and **7** had a weak absorption band. Regarding the prediction by time-dependent DFT calculations, the large absorption band of **6** corresponded to the HOMO→LUMO transition and was attributable to the π-π* transition (See Figure S5).

A.

λ_{abs} (nm)	*f*	*Contribution (%)*
342	0.4783	HOMO→LUMO (48%)

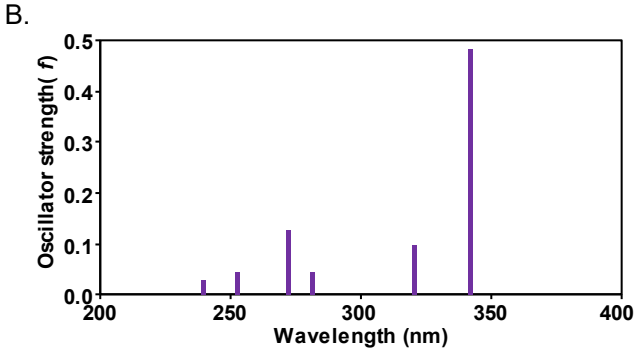

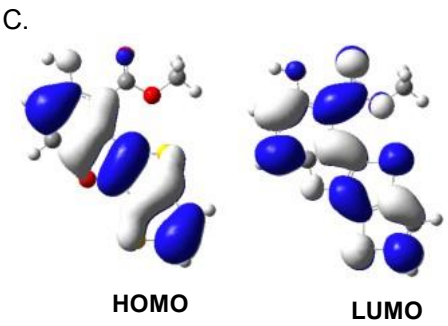

Figure S5. (A) Calculated excitation wavelength (λ_{abs}), oscillator strength (*f*) and major contribution for **6**. (B) Calculated absorption spectra. (C) Frontier molecular orbitals of **6**.

Cartesian Coordination

6

Sum of electronic and thermal Free Energies
= -1635.40999 A.U

C	-1.47393609	-2.20522482	-0.14341031
C	-0.09817779	-2.54911158	-0.15844407
C	0.92249001	-1.62355729	-0.05533917
C	0.55682240	-0.28792318	0.06523415
C	-0.79438611	0.10845538	0.07622161
C	-1.84217686	-0.83751594	-0.02874223
H	1.96227449	-1.93261086	-0.06961212
H	1.32750599	0.47474178	0.15159541
C	-3.25551908	-0.38577800	-0.02766041
O	-3.64948936	0.75811951	-0.10407248
O	-4.11749446	-1.43811313	0.07479680
C	-5.50832282	-1.08333239	0.07482245
H	-6.04896967	-2.02652581	0.15740873
H	-5.73613152	-0.43245679	0.92279427
H	-5.77364253	-0.56557865	-0.85060119
O	0.10474850	-3.90907152	-0.29208949
C	-2.13860569	-3.47340679	-0.27863643
C	-1.14656410	-4.43600625	-0.36429221
S	-3.73621123	-4.18959121	-0.37764453
C	-3.01032474	-5.78561809	-0.53951827
C	-1.61481536	-5.75855810	-0.51248642
S	-0.94174103	-7.35473706	-0.66959794
C	-3.54423870	-7.09844950	-0.68704780
C	-2.55212790	-8.03626561	-0.76960986
H	-4.60052907	-7.33784496	-0.72974320
H	-2.66335417	-9.10616743	-0.88516124
O	-1.10518981	1.42518959	0.20213082
H	-0.27865065	1.92734615	0.28094589

6. References.

1. X. Yuan, X. Wu, F. Peng, H. Yang, C. Zhu, H. Fu, *Chem*. *Commun*., **2020**, *56*, 12648–12651.

2. C. Xu, H. Zheng, B. Hu, X. Liu, L. Lin, X. Feng, *Chem*. *Commun*., **2017**, *53*, 9741–9744.

3. M. A. Bashir, Y. Zhang, H. Yu, B. Wang, W. Zhao, F. Zhong, *Green Chem*., **2021**, *23*, 5031–5036.

4. J. N. Tsaklidis, A. Hofer, C. H. Eugster, *Helv*. *Chim*. *Acta*., **1977**, *60*, 1033–1060.

5. D. N. Mastronarde, *Micro. Microanal.*, **2003**, *9.S02*, 1182–1183.

6. K Takaba, S. Maki-Yonekura, K. Yonekura. *J. Struct. Biol.*, **2020**, *211.2*, 107549.

7. H. Hamada, T. Nakamuro, K. Yamashita, H. Yanagisawa, O. Nureki, M. Kikkawa, K. Harano, R. Shang, E. Nakamura, *Bull. Chem. Soc. Jpn.,* **2020**, *93*, 776–782.

8. H. Lu, T. Nakamuro, K. Yamashita, H. Yanagisawa, O. Nureki, M. Kikkawa, H. Gao, J. Tian, R. Shang, E. Nakamura, *J. Am. Chem. Soc.*, **2020**, *142*, 18990–18996.

9. Maki-Yonekura, Saori, et al. "Advances in cryo-EM and ED with a cold-field emission beam and energy filtration—Refinements of the CRYO ARM 300 system in RIKEN SPring-8 center—." Microscopy 70.2 (2021): 232-240.

10. G. Winter, D. G. Waterman, J. M. Parkhurst, A. S. Brewster, R. J. Gildea, M. Gerstel, L. Fuentes-Montero, M. Vollmar, T. Michels-Clark, I. D. Young, N. K. Sauter, G. Evans, *Acta Cryst.*, **2018**, *D74*, 85–97.

11. M. T. B. Clabbers, T. Gruene, J. M. Parkhurst, J. P. Abrahams, D. G. Waterman, *Acta Cryst.*, **2018**, *D74*, 506–518.

12. O. Tange (2011): GNU Parallel - The Command-Line Power Tool,;login: The USENIX Magazine, February 2011:42–47.

13. J. Beilsten-Edmands, G. Winter, R. Gildea, J. Parkhurst, D. Waterman, G. Evans, *Acta Cryst.*, **2020**, *D76*, 385–399.

14. T. R. Schneider, G. M. Sheldrick. *Acta Crystallogr. D: Biol. Crystallogr.*, **2002**, , 1772–1779.

15. G. M. Sheldrick, *Acta Cryst.*, **2015**, C*71*, 3–8.

16. O. V. Dolomanov, L. J. Bourhis, R. J. Gildea, J. A. K. Howard, H. Puschmann, *J. Appl. Cryst.*, **2009**, *42*, 339–341.

17. Gaussian 16, Revision C.01, M. J. Frisch, G. W. Trucks, H. B. Schlegel, G. E. Scuseria, M. A. Robb, J. R. Cheeseman, G. Scalmani, V. Barone, G. A. Petersson, H. Nakatsuji, X. Li, M. Caricato, A. V. Marenich, J. Bloino, B. G. Janesko, R. Gomperts, B. Mennucci, H. P. Hratchian, J. V. Ortiz, A. F. Izmaylov, J. L. Sonnenberg, D. Williams-Young, F. Ding, F. Lipparini, F. Egidi, J. Goings, B. Peng, A. Petrone, T. Henderson, D. Ranasinghe, V. G. Zakrzewski, J. Gao, N. Rega, G. Zheng, W. Liang, M. Hada, M. Ehara, K. Toyota, R. Fukuda, J. Hasegawa, M. Ishida, T. Nakajima, Y. Honda, O. Kitao, H. Nakai, T. Vreven, K. Throssell, J. A., Jr. Montgomery, J. E. Peralta, F. Ogliaro, M. J. Bearpark, J. J. Heyd, E. N. Brothers, K. N. Kudin, V. N. Staroverov, T. A. Keith, R. Kobayashi, J. Normand, K. Raghavachari, A. P. Rendell, J. C. Burant, S. S. Iyengar, J. Tomasi, M. Cossi, J. M. Millam, M. Klene, C. Adamo, R. Cammi, J. W. Ochterski, R. L. Martin, K. Morokuma, O. Farkas, J. B. Foresman, D. J. Fox, Gaussian, Inc., Wallingford CT, 2016.

7. ^{1}H and ^{13}C NMR spectra of newly synthesized compounds.

^{1}H NMR of methyl 3,6-dihydroxy-2-(1*H*-indol-3'-yl)benzoate (**3a**)

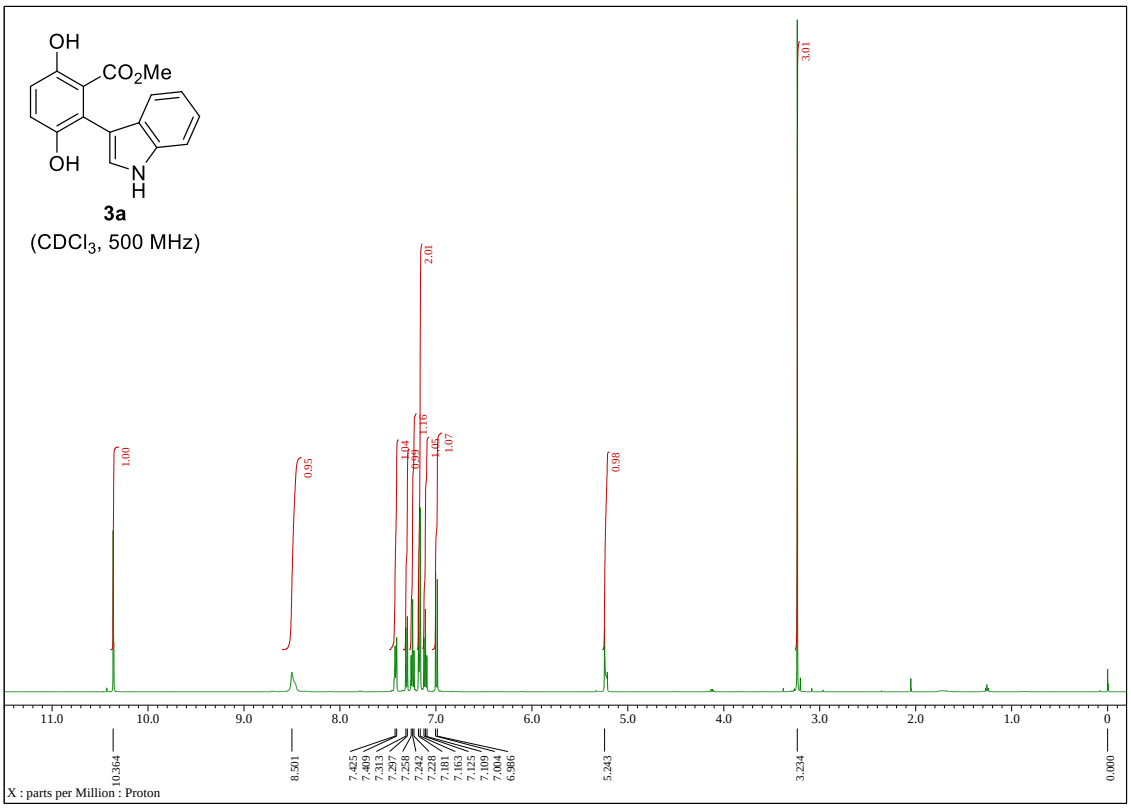

^{1}H NMR of methyl 3,6-dihydroxy-2-(1'-methyl-1*H*-indol-3'-yl)benzoate (**3b**)

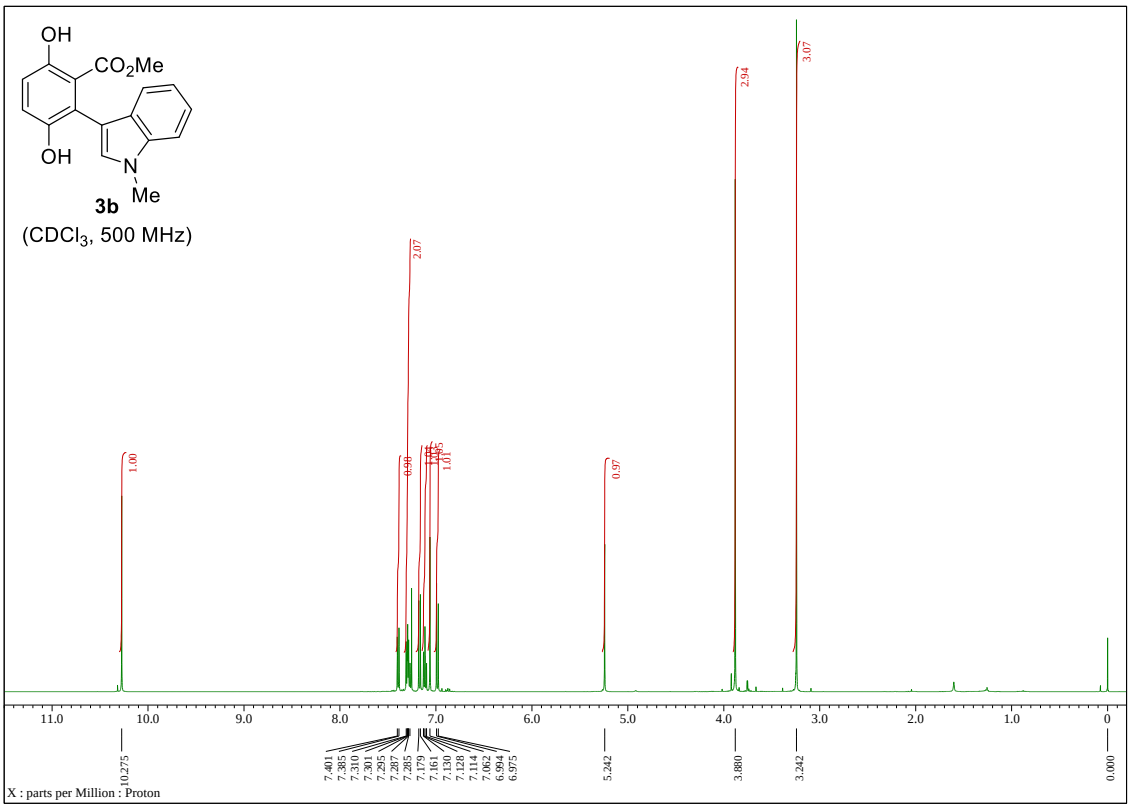

[1]H NMR of methyl 3,6-dihydroxy-2-(1'-tosyl-1*H*-indol-3'-yl)benzoate (**3c**)

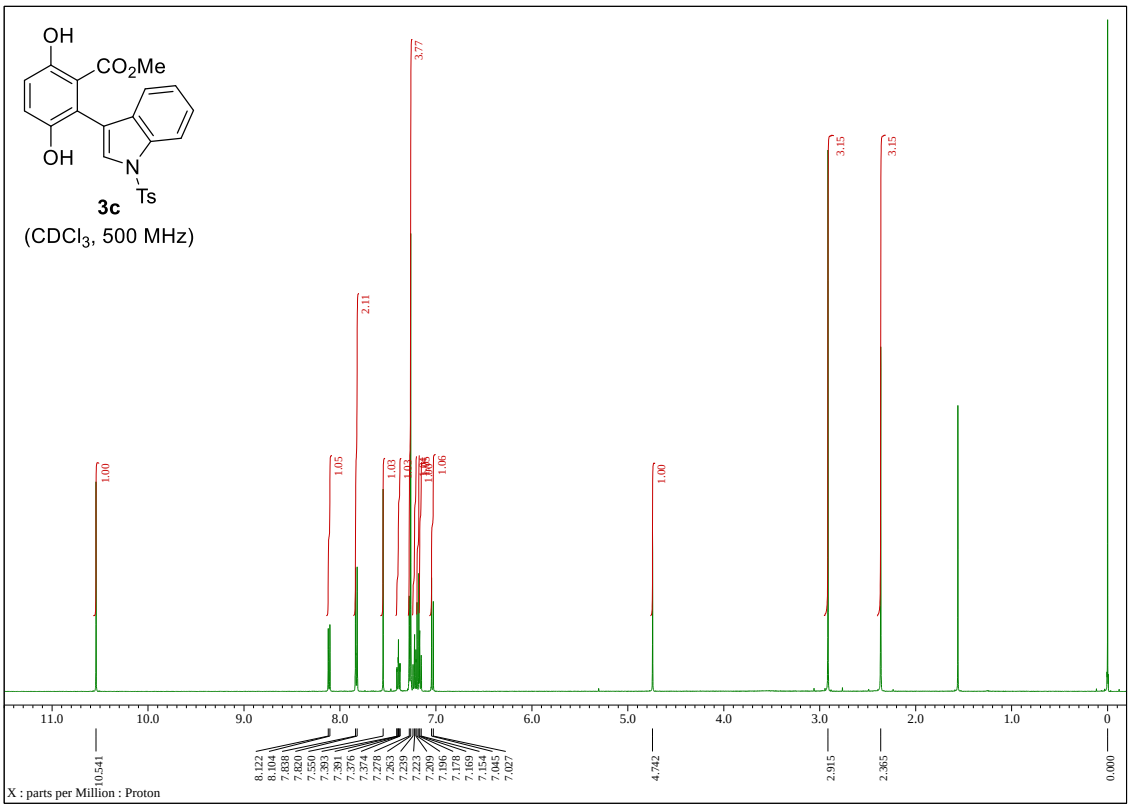

[13]C NMR of methyl 3,6-dihydroxy-2-(1'-tosyl-1*H*-indol-3'-yl)benzoate (**3c**)

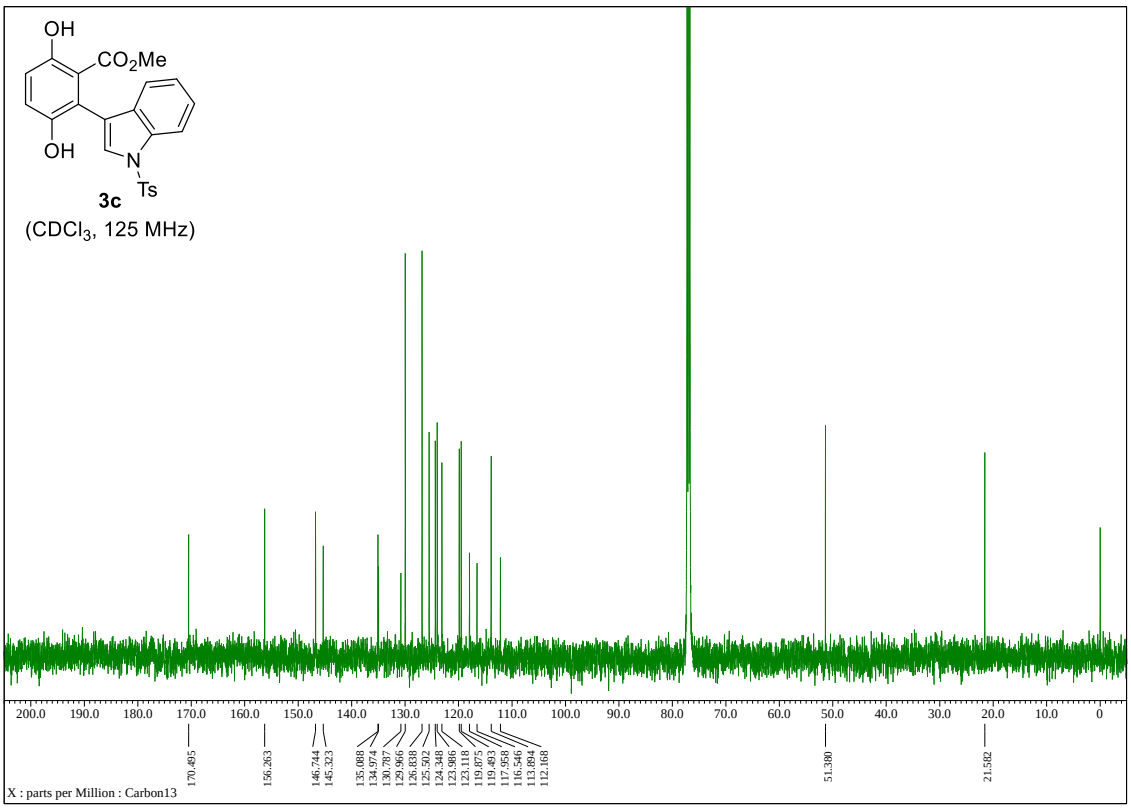

^{1}H NMR of methyl 3,6-dihydroxy-2-(1'-benzyl-1*H*-indol-3'-yl)benzoate (**3d**)

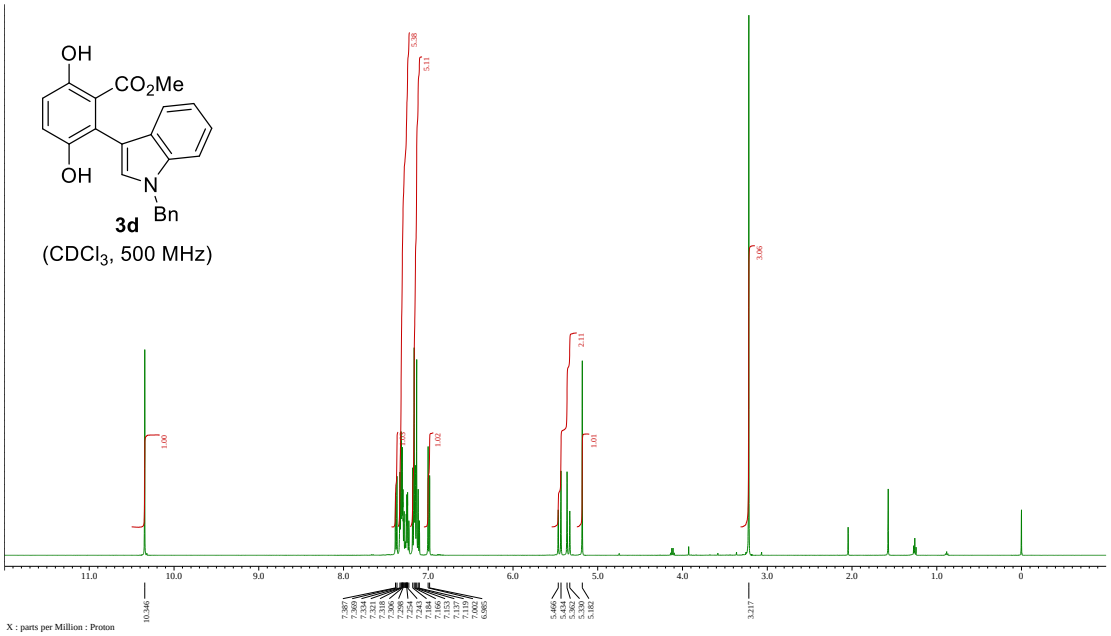

^{13}C NMR of methyl 3,6-dihydroxy-2-(1'-benzyl-1*H*-indol-3'-yl)benzoate (**3d**)

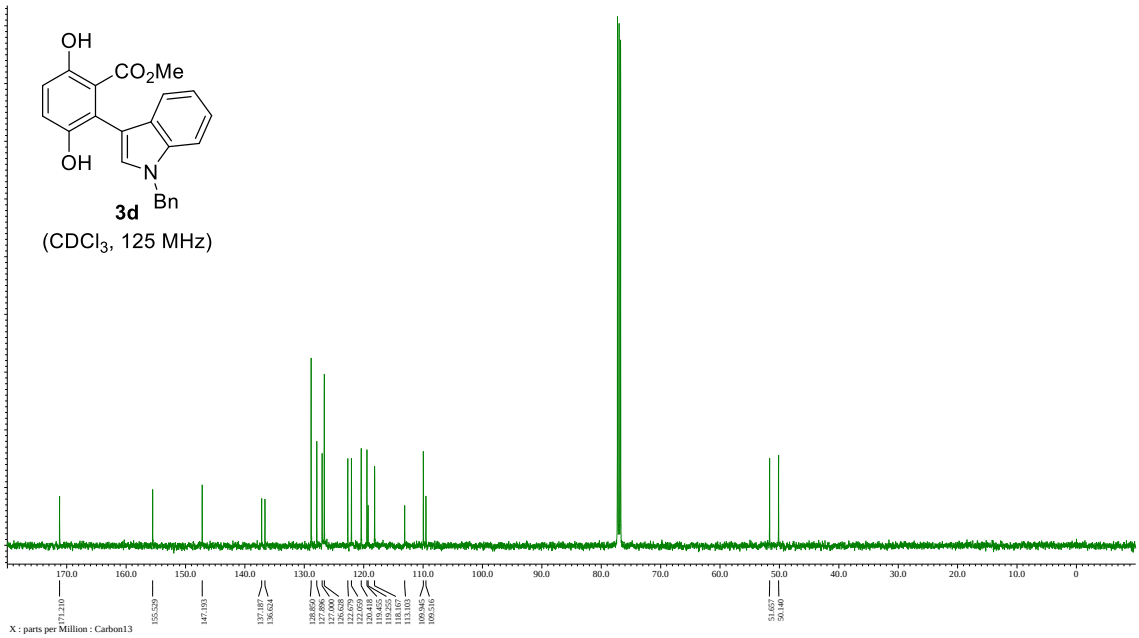

^{1}H NMR of methyl 3,6-dihydroxy-2-(5'-methoxy-1*H*-indol-3'-yl)benzoate (**3e**)

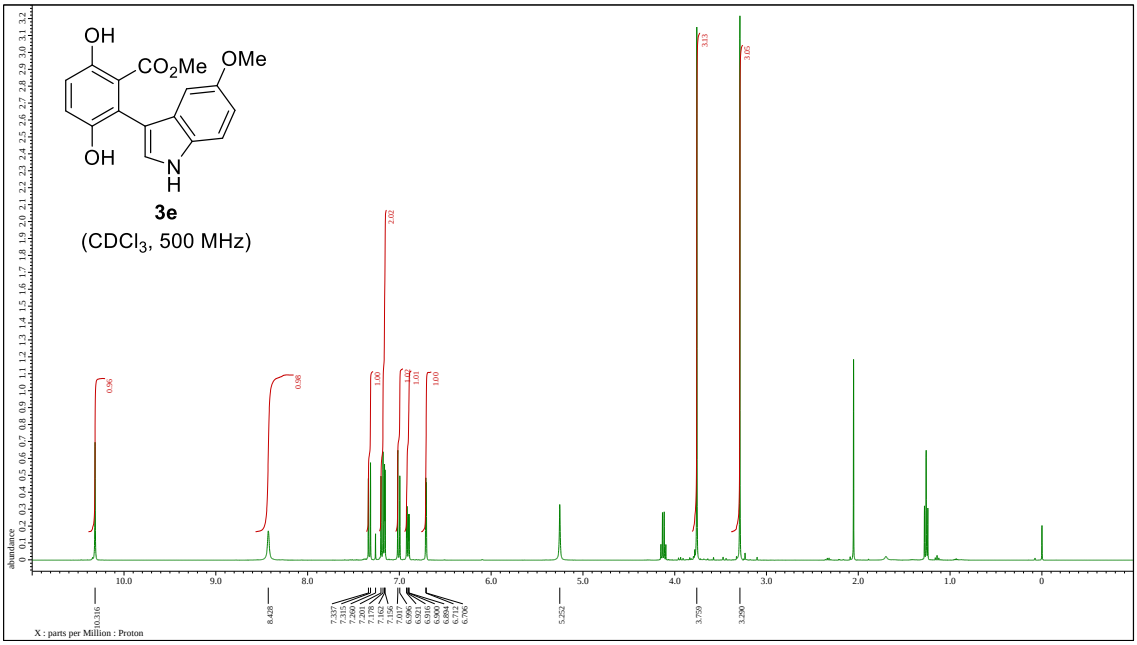

^{1}H NMR of methyl 3,6-dihydroxy-2-(5'-fluoro-1*H*-indol-3'-yl)benzoate (**3f**)

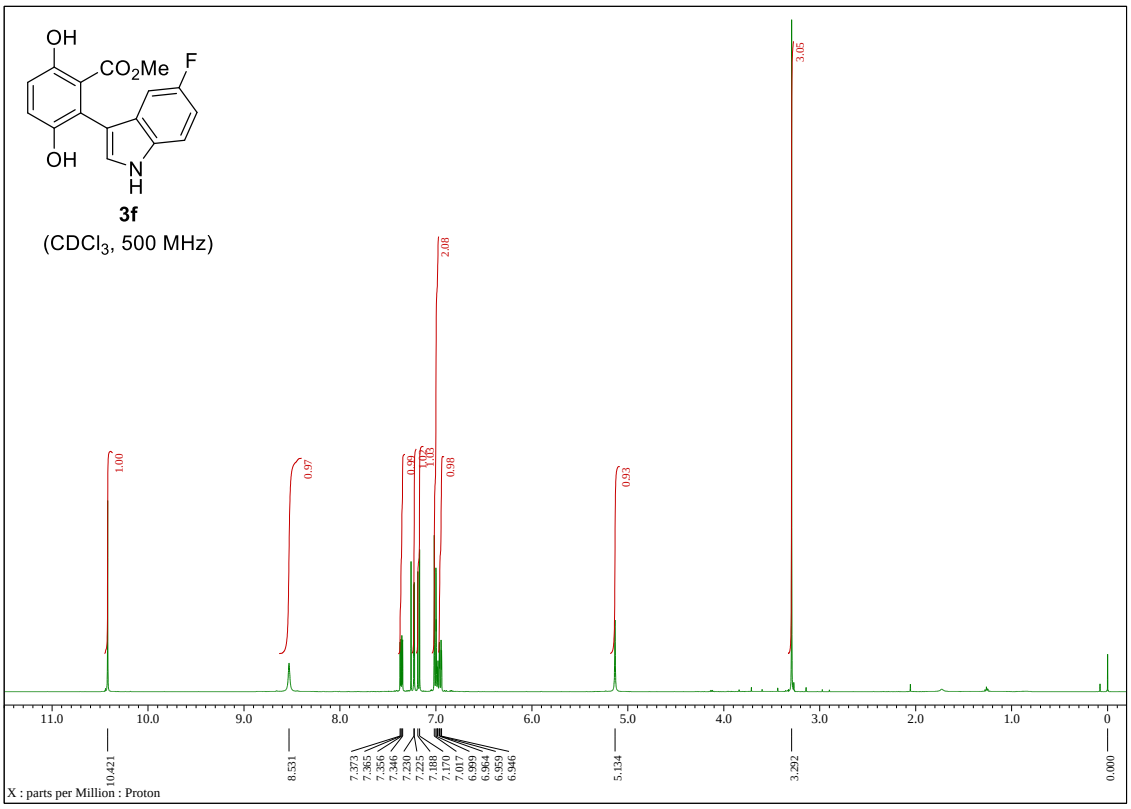

^{1}H NMR of methyl 3,6-dihydroxy-2-(5'-bromo-1*H*-indol-3'-yl)benzoate (**3g**)

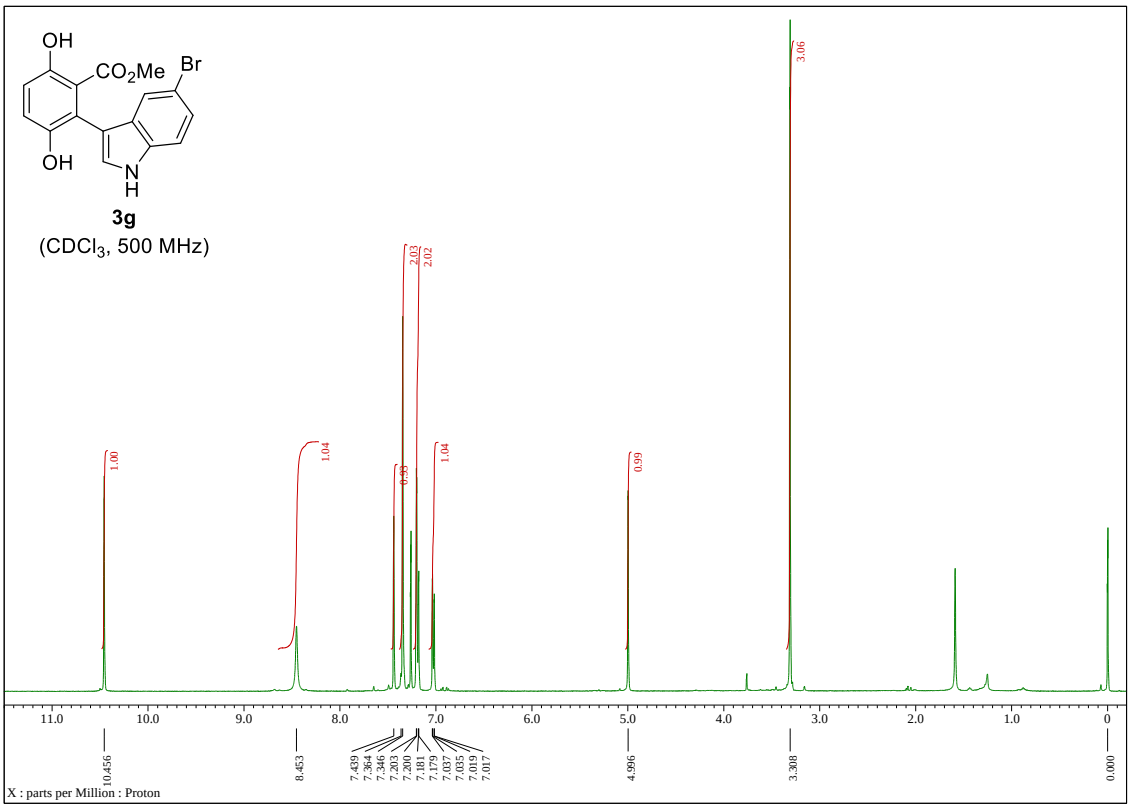

^{1}H NMR of 1-(3,6-dihydroxy-2-(1*H*-indol-3'-yl)phenyl)ethan-1-one (**3h**)

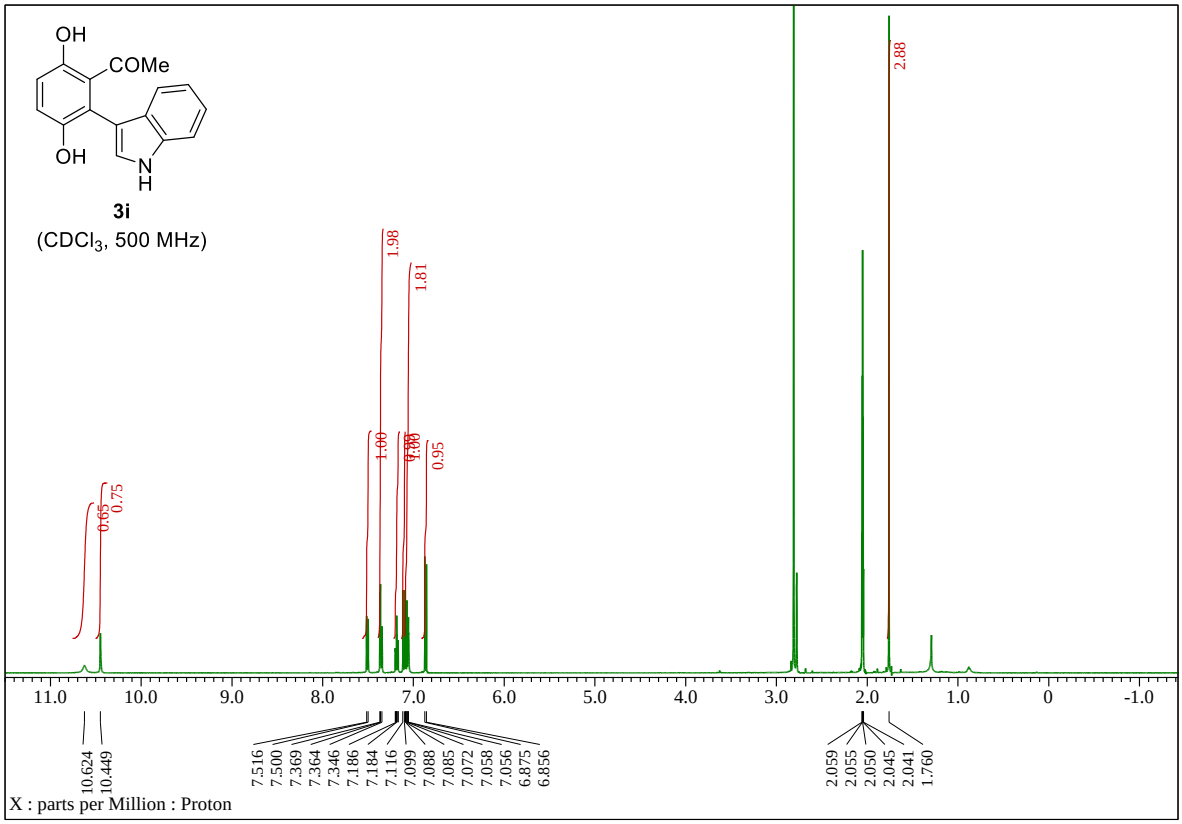

^{13}C NMR of 1-(3,6-dihydroxy-2-(1*H*-indol-3'-yl)phenyl)ethan-1-one (**3h**)

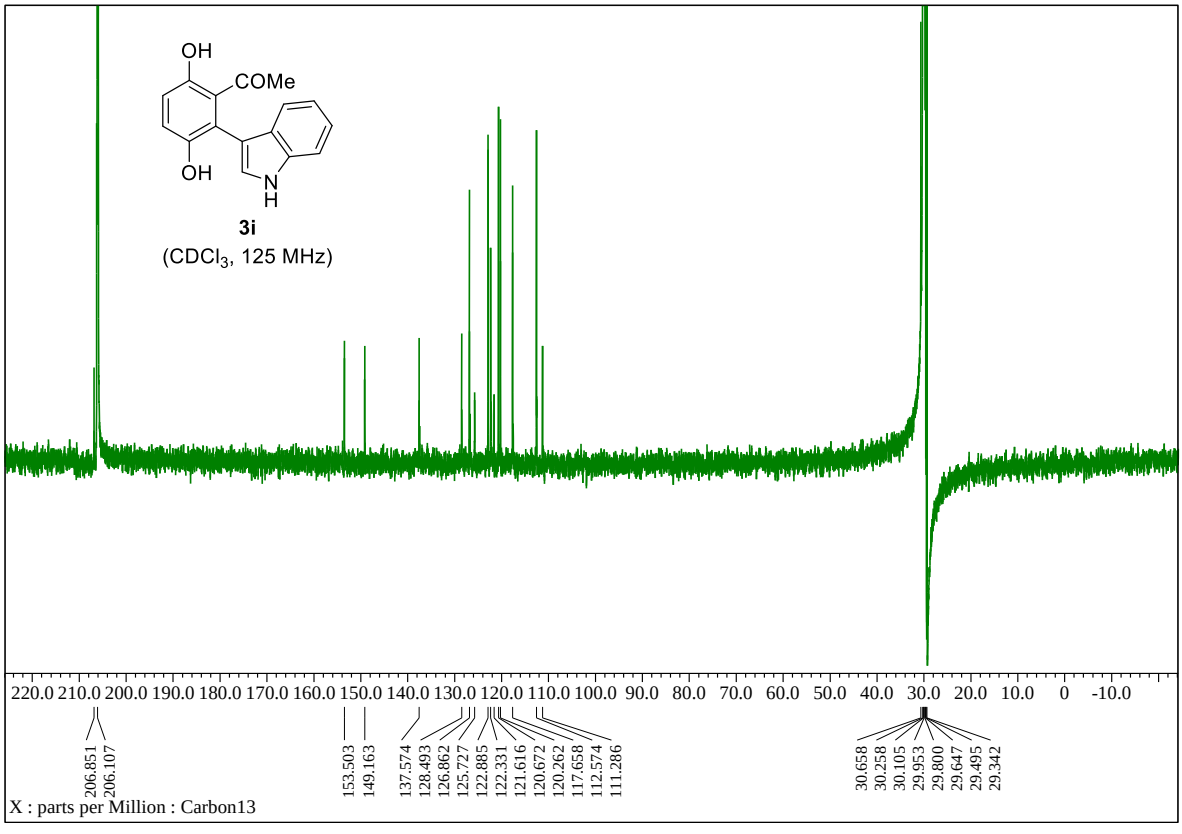

^{1}H NMR of 3,6-dihydroxy-2-(1*H*-indol-3'-yl)benzaldehyde (**3i**)

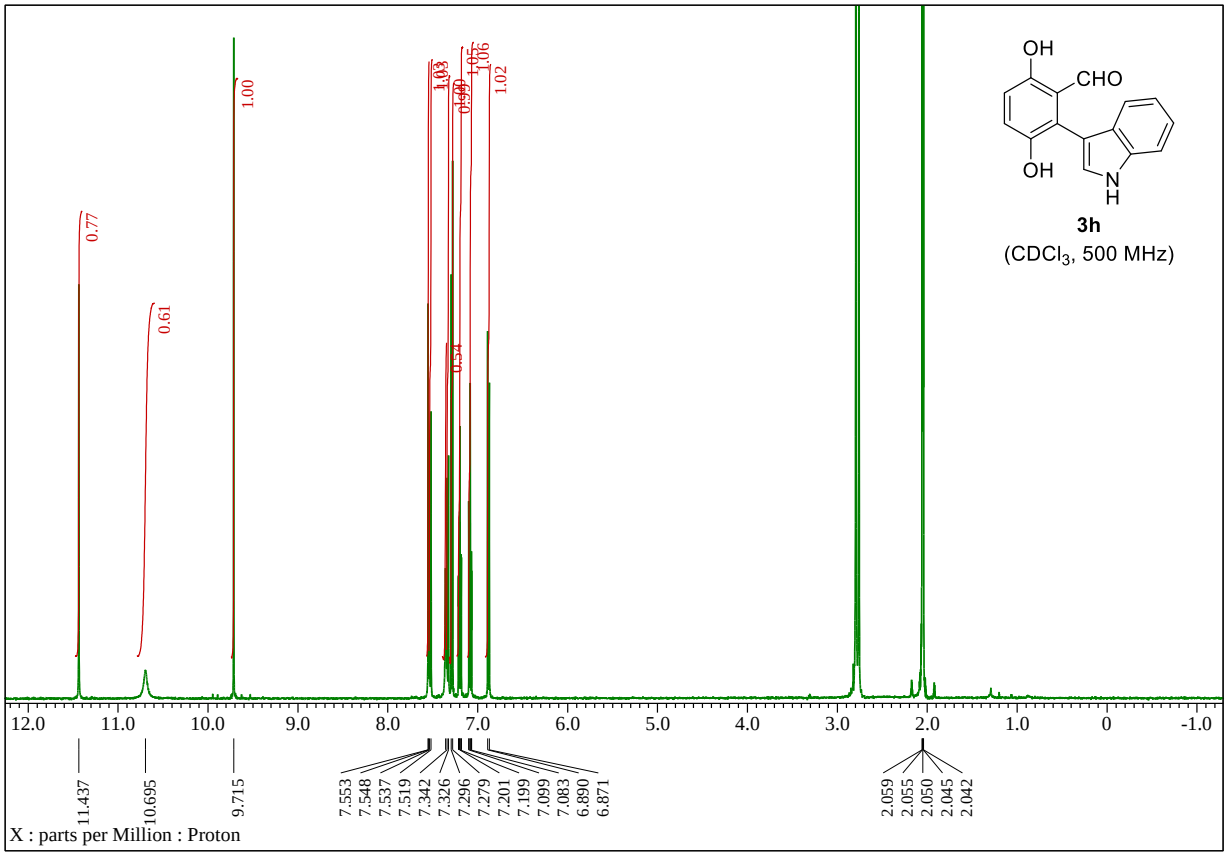

^{13}C NMR of 3,6-dihydroxy-2-(1*H*-indol-3'-yl)benzaldehyde (**3i**)

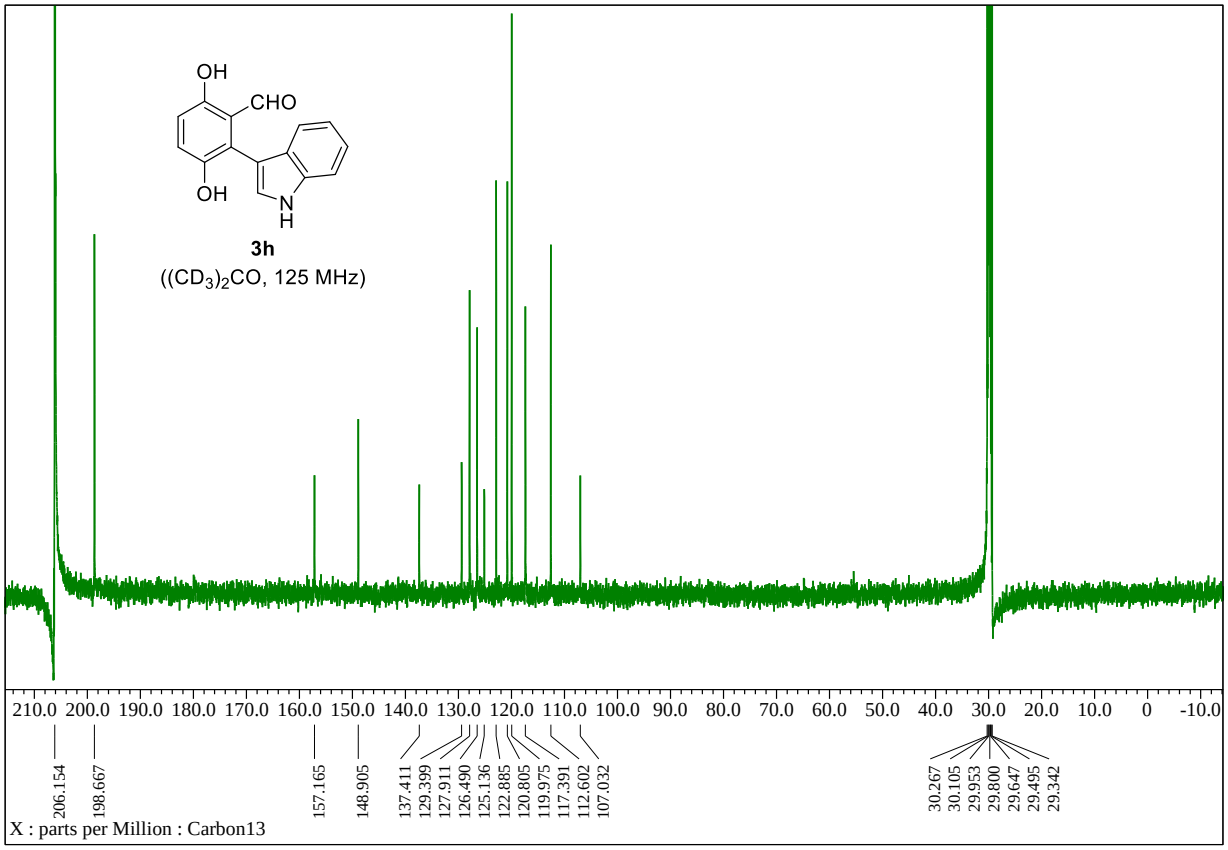

^{1}H NMR of methyl 3-(3',6'-dihydroxy-2'-(methoxycarbonyl)phenyl)-1*H*-indole-2-carboxylate (**3k**)

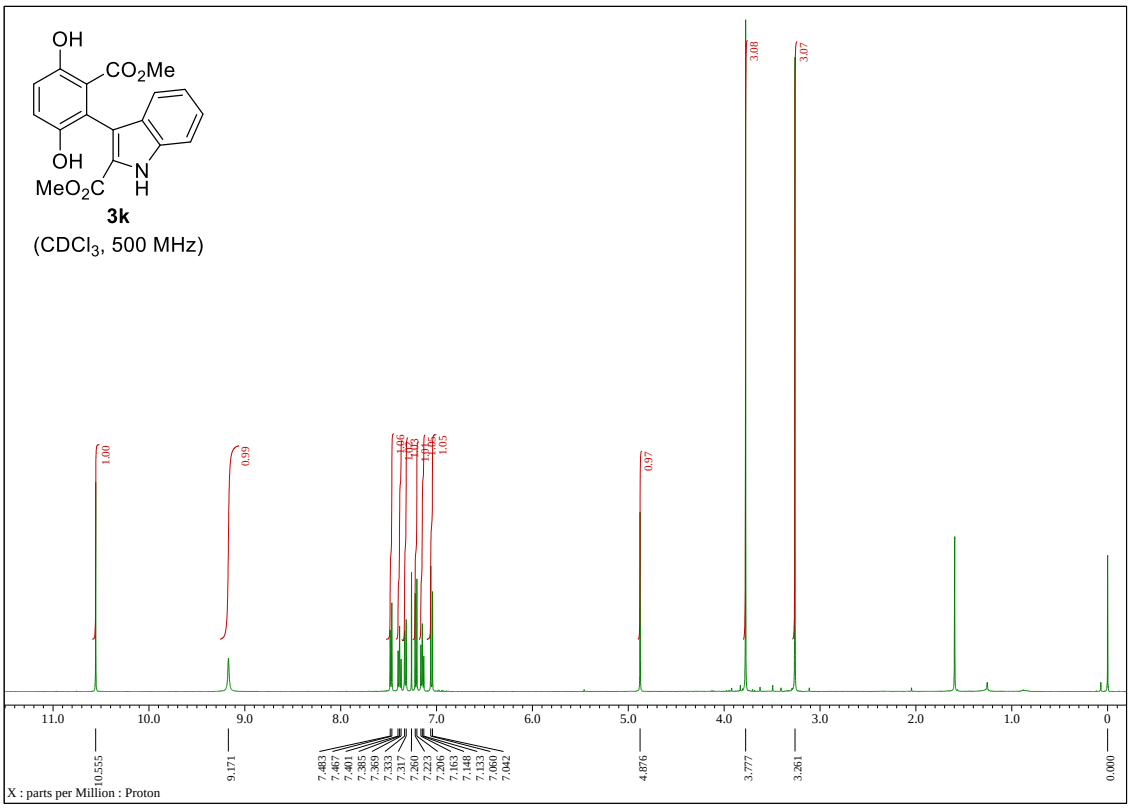

^{13}C NMR of methyl 3-(3',6'-dihydroxy-2'-(methoxycarbonyl)phenyl)-1*H*-indole-2-carboxylate (**3k**)

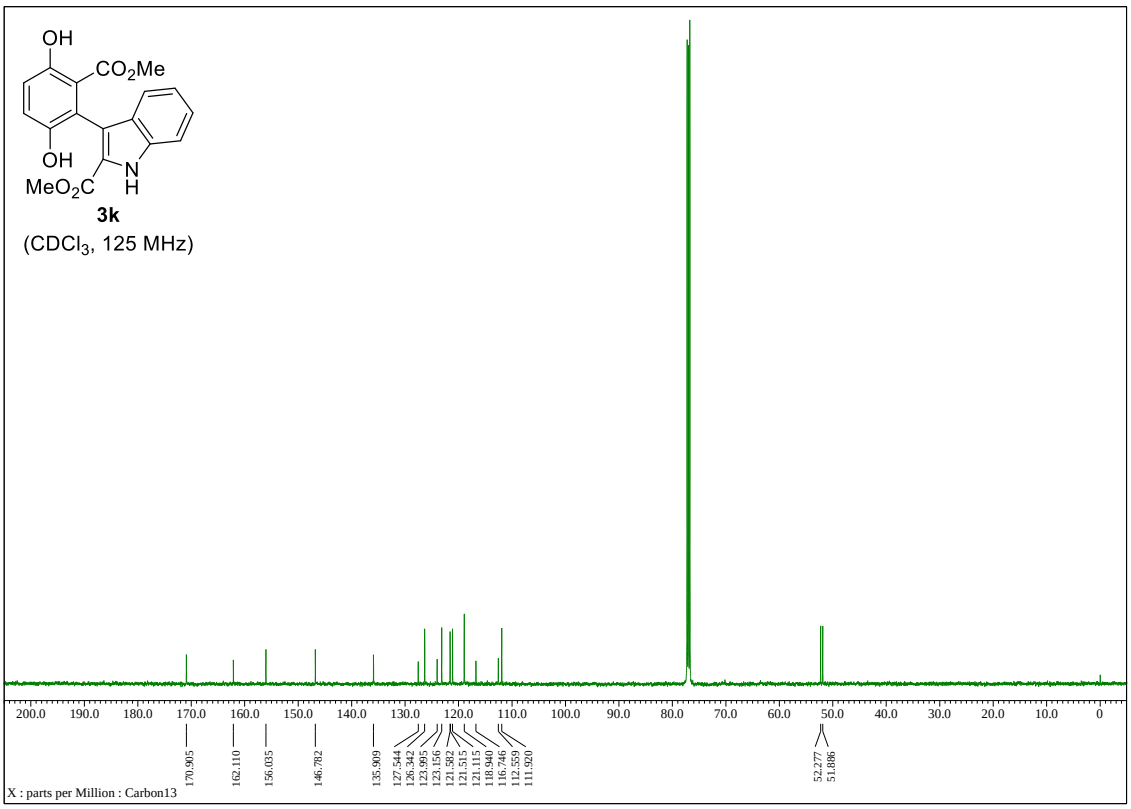

[1]H NMR of methyl 2-hydroxy-6-oxo-6,7-dihydrochromeno[3,4-*b*]indole-1-carboxylate (**8**)

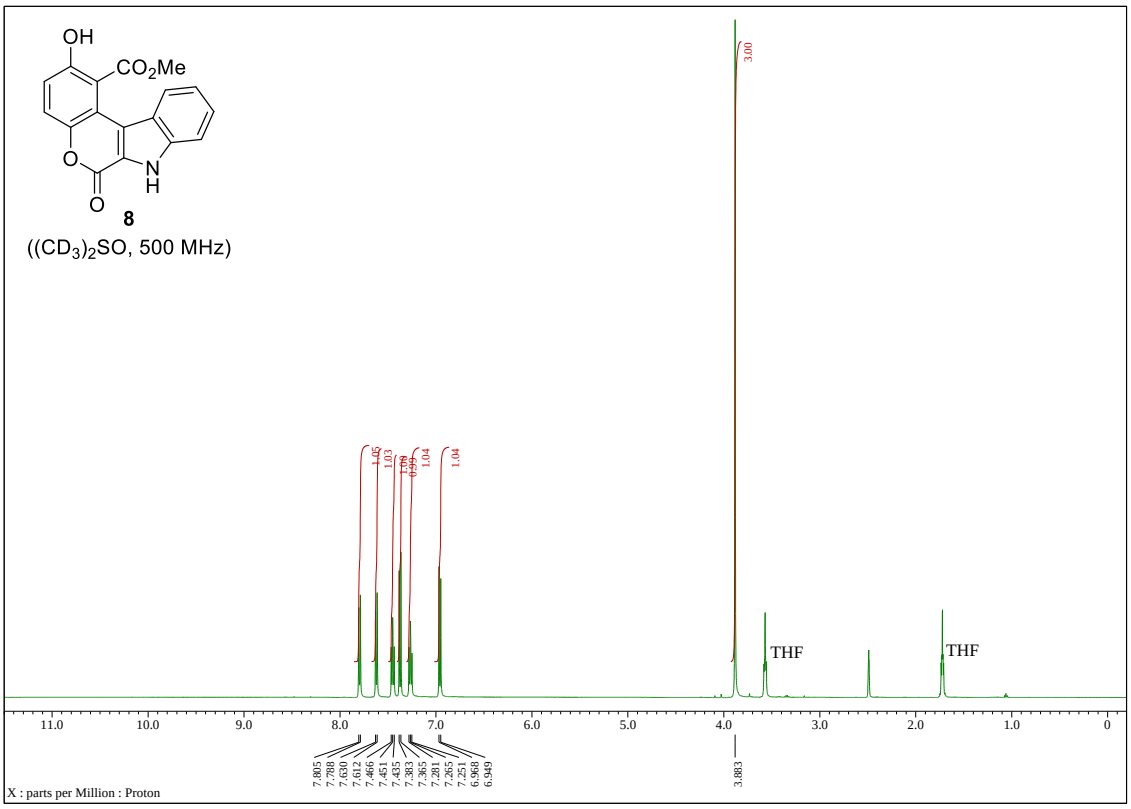

[13]C NMR of methyl 2-hydroxy-6-oxo-6,7-dihydrochromeno[3,4-*b*]indole-1-carboxylate (**8**)

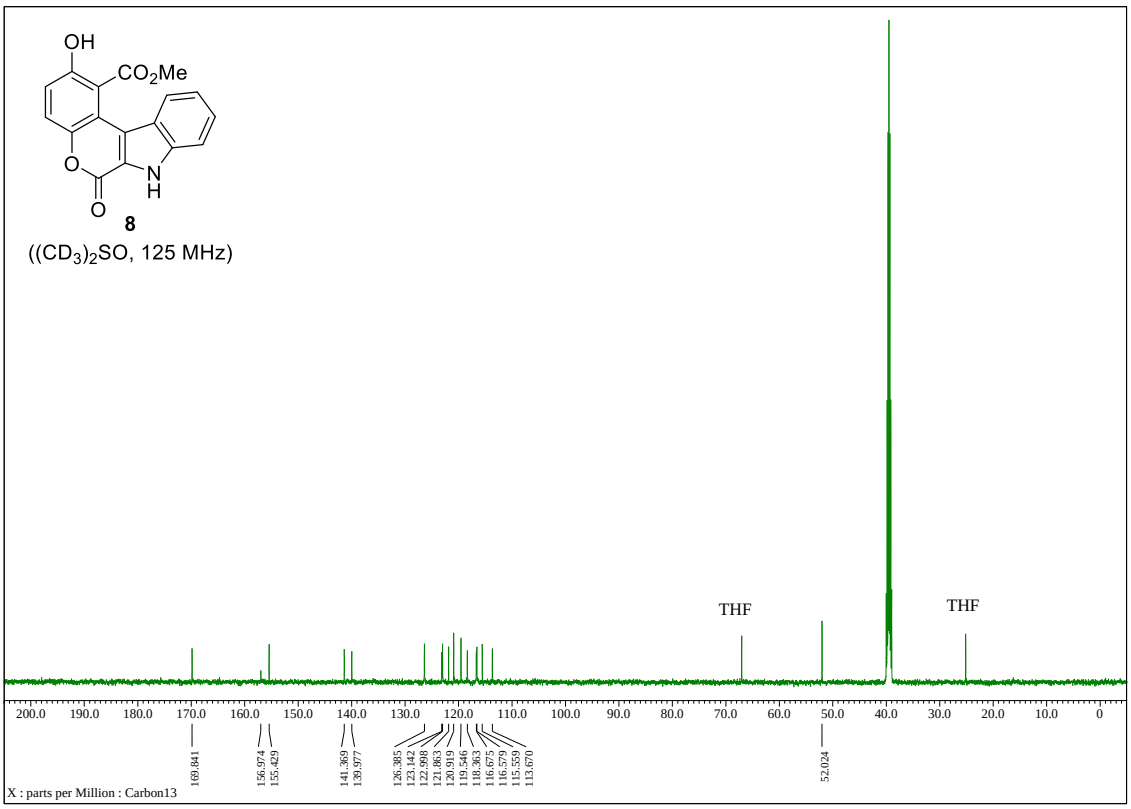

^{1}H NMR of methyl 3,6-dihydroxy-4’-methoxy-[1,1’-biphenyl]-2-carboxylate (**4a**)

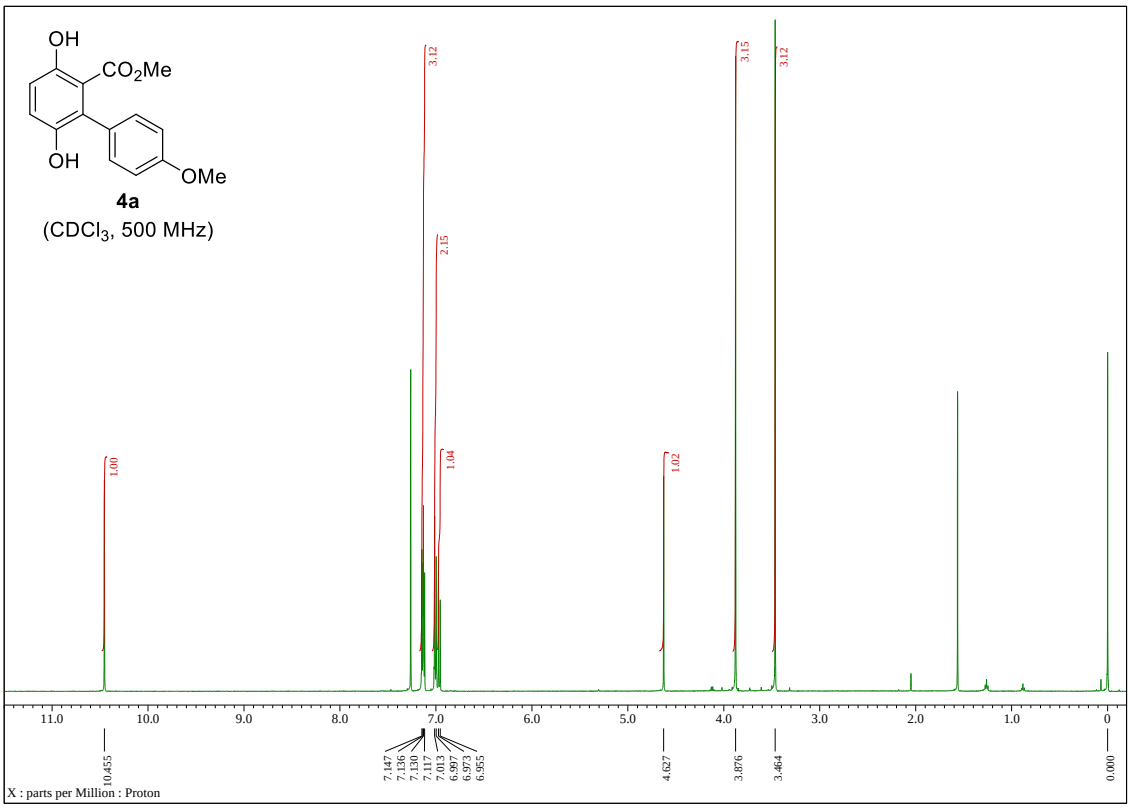

^{13}C NMR of methyl 3,6-dihydroxy-4’-methoxy-[1,1’-biphenyl]-2-carboxylate (**4a**)

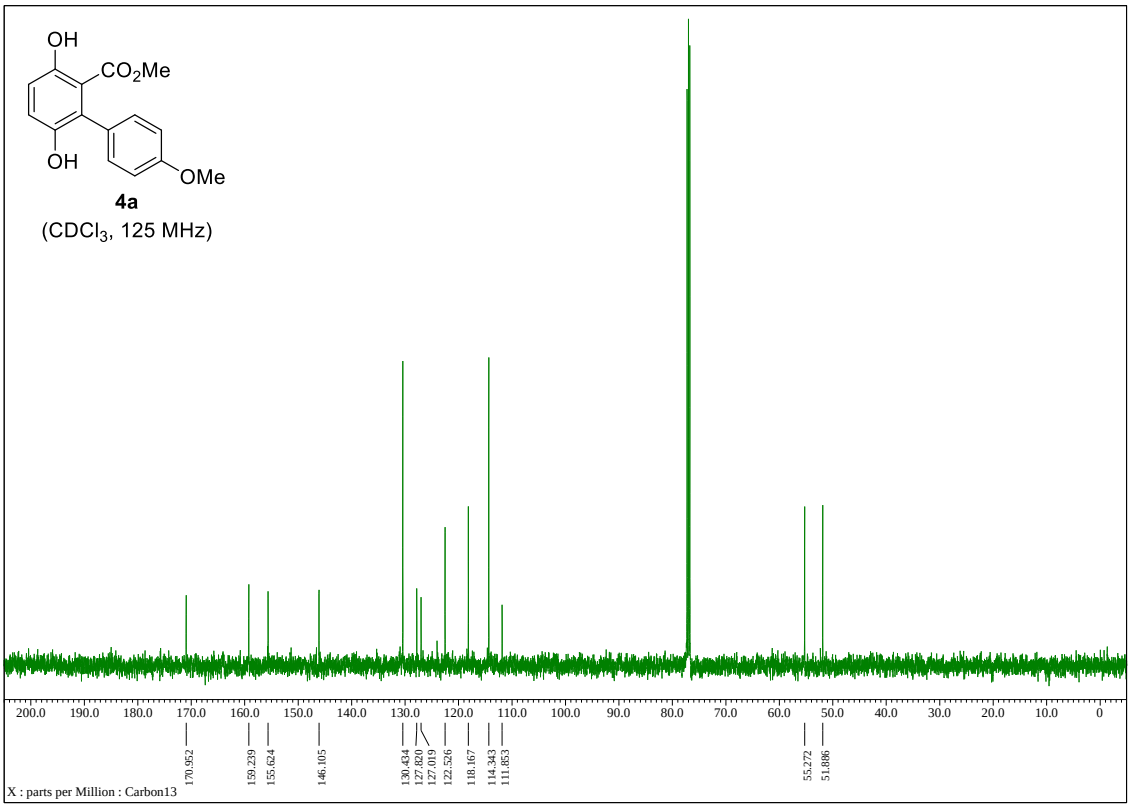

^{1}H NMR of methyl 3,6-dihydroxy-2-(2'-hydroxynaphthalen-1'-yl)benzoate (**4b**)

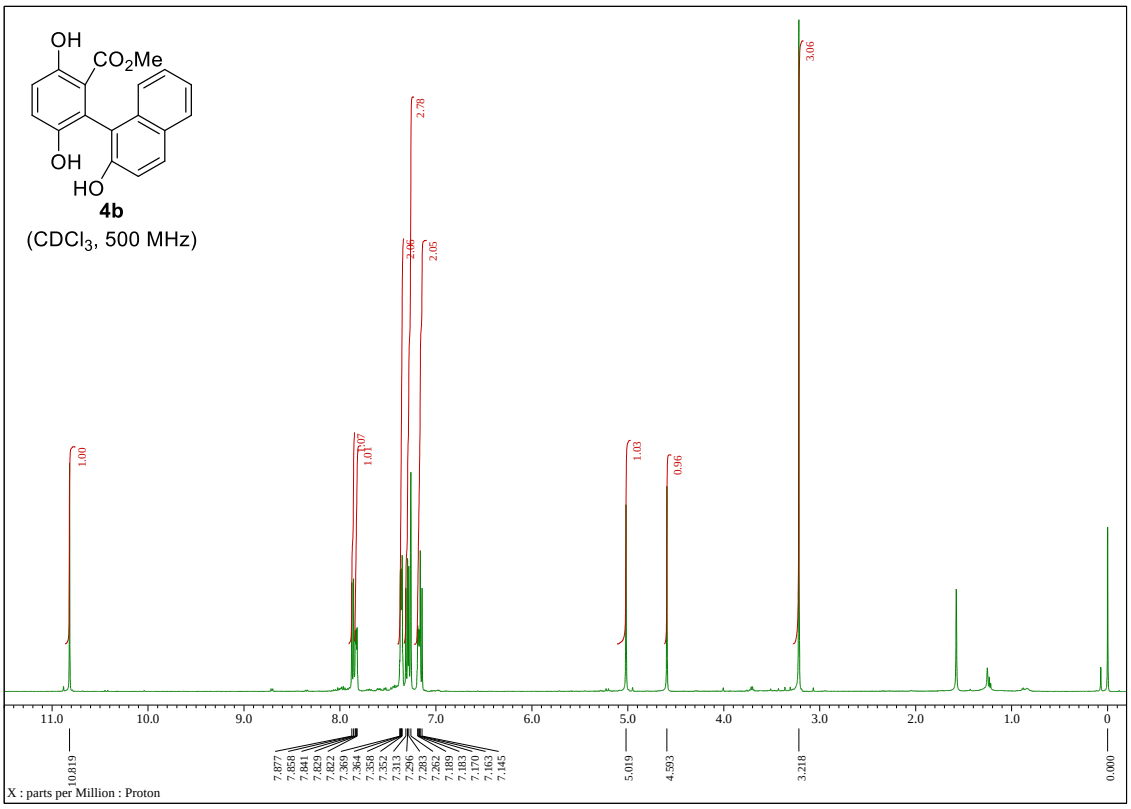

^{1}H NMR of methyl 3,6-dihydroxy-2',4',6'-trimethoxy-[1,1'-biphenyl]-2-carboxylate (**4c**)

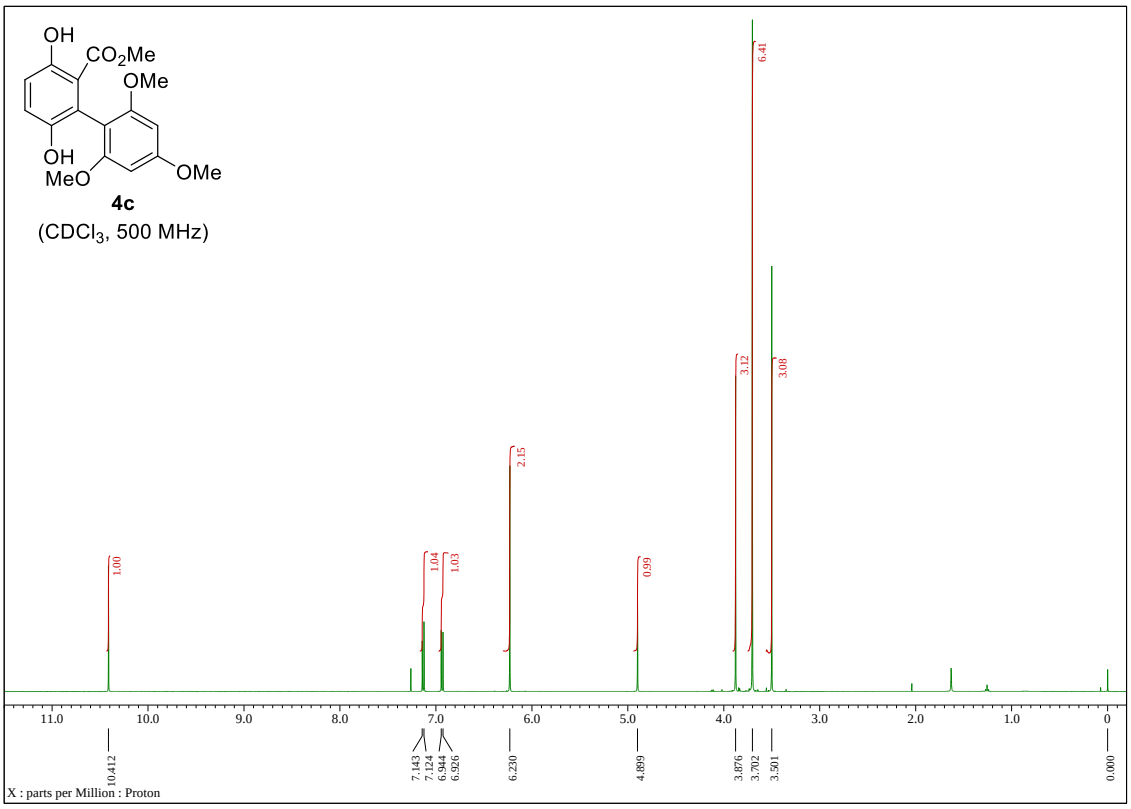

^{13}C NMR of methyl 3,6-dihydroxy-2',4',6'-trimethoxy-[1,1'-biphenyl]-2-carboxylate (**4c**)

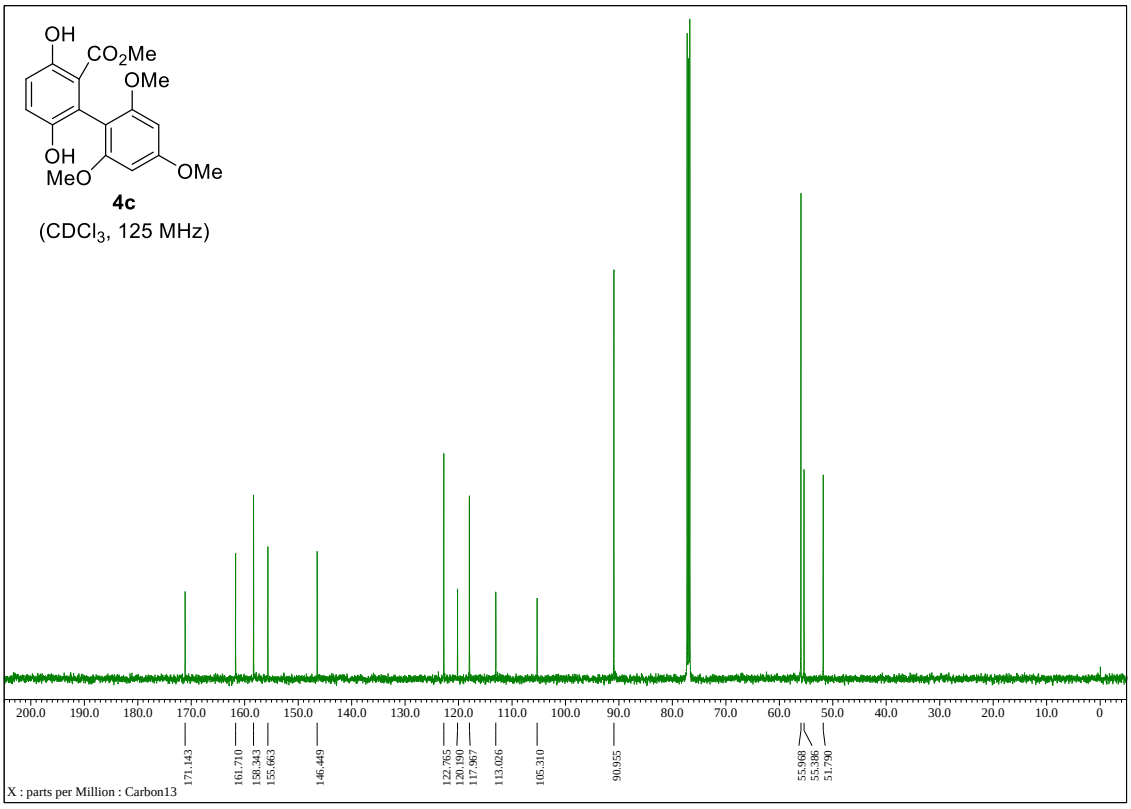

^{1}H NMR of methyl 2’-bromo-3,6-dihydroxy-4’,6’-dimethoxy-[1,1’-biphenyl]-2-carboxylate (**4d**)

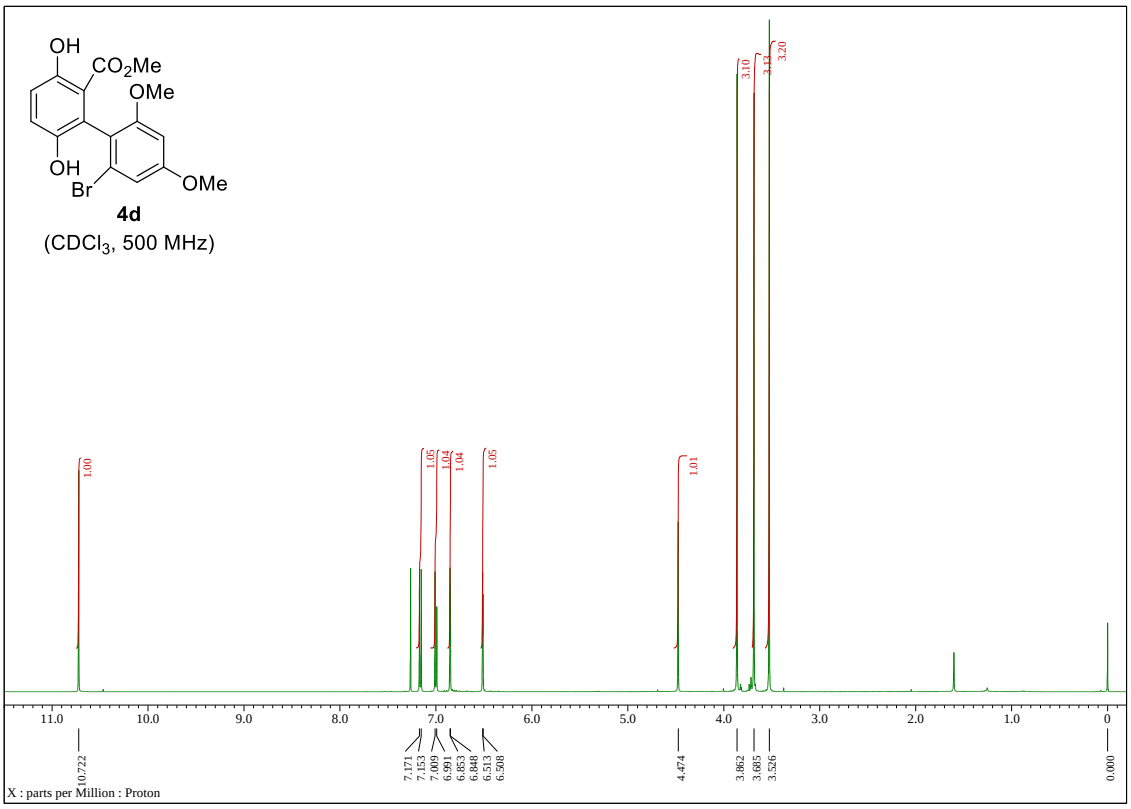

^{13}C NMR of methyl 2’-bromo-3,6-dihydroxy-4’,6’-dimethoxy-[1,1’-biphenyl]-2-carboxylate (**4d**)

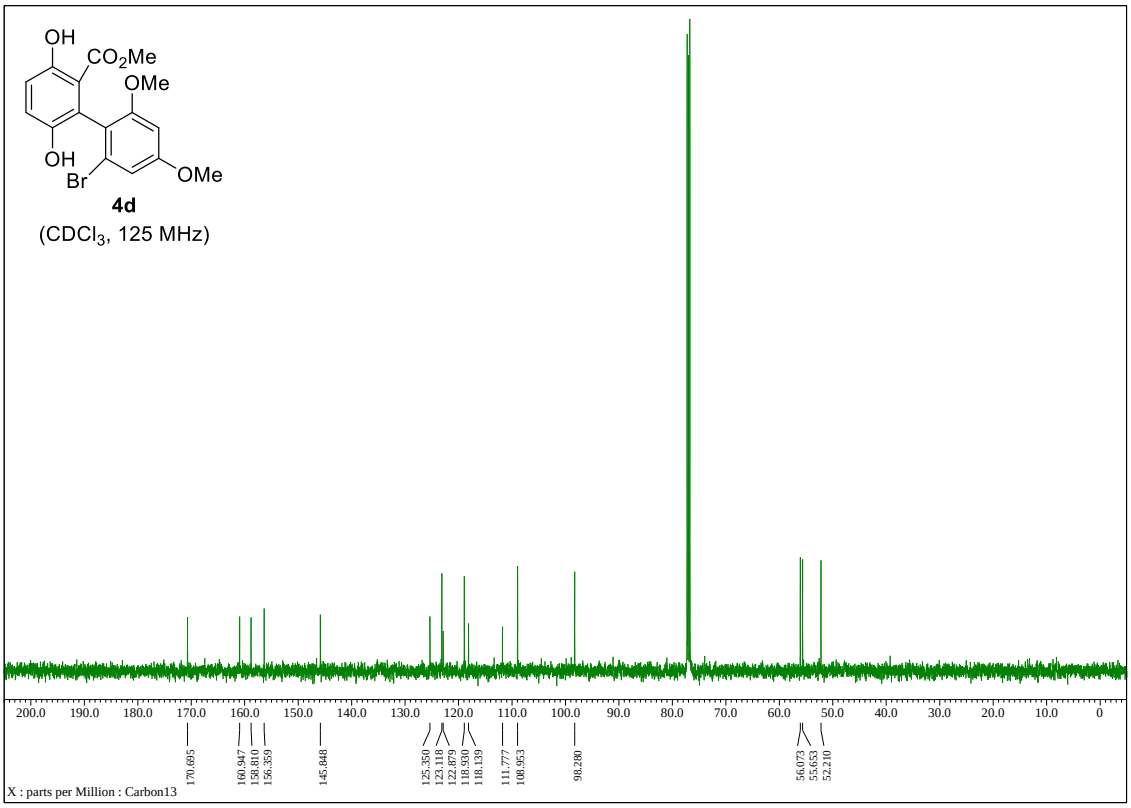

^{1}H NMR of methyl 3,6-dihydroxy-2',5'-dimethoxy-[1,1'-biphenyl]-2-carboxylate (**4e**)

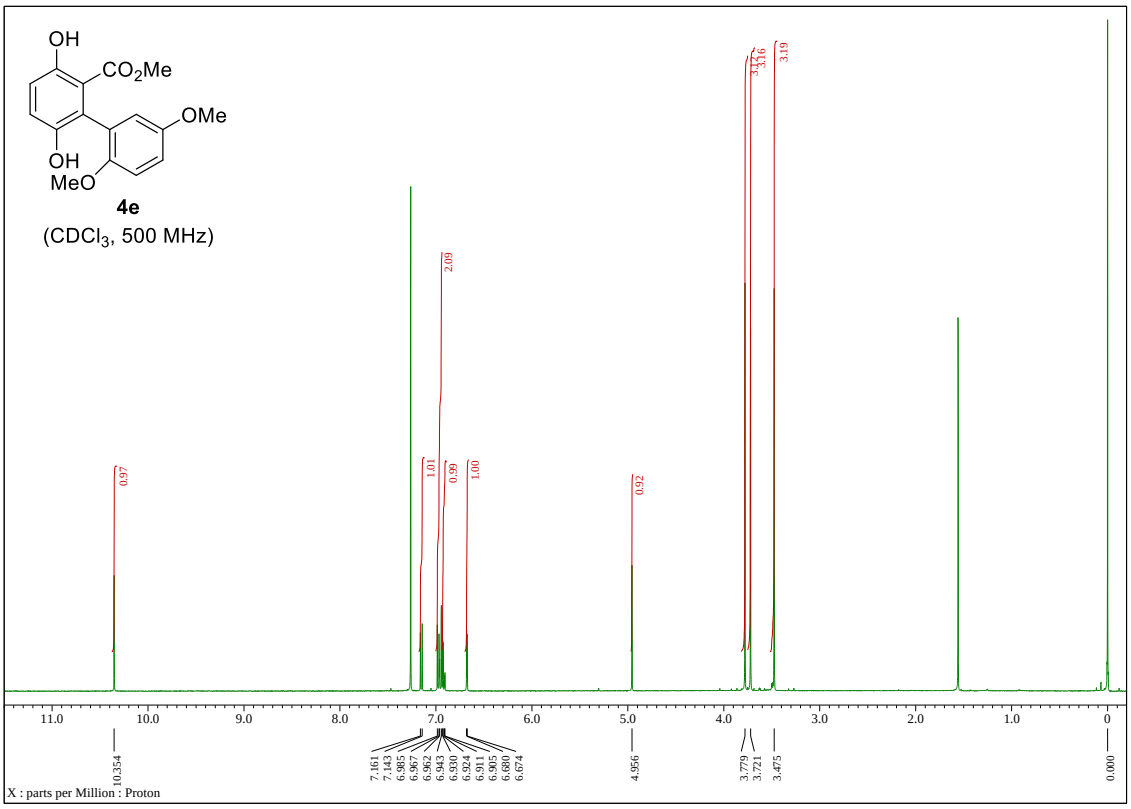

^{13}C NMR of methyl 3,6-dihydroxy-2',5'-dimethoxy-[1,1'-biphenyl]-2-carboxylate (**4e**)

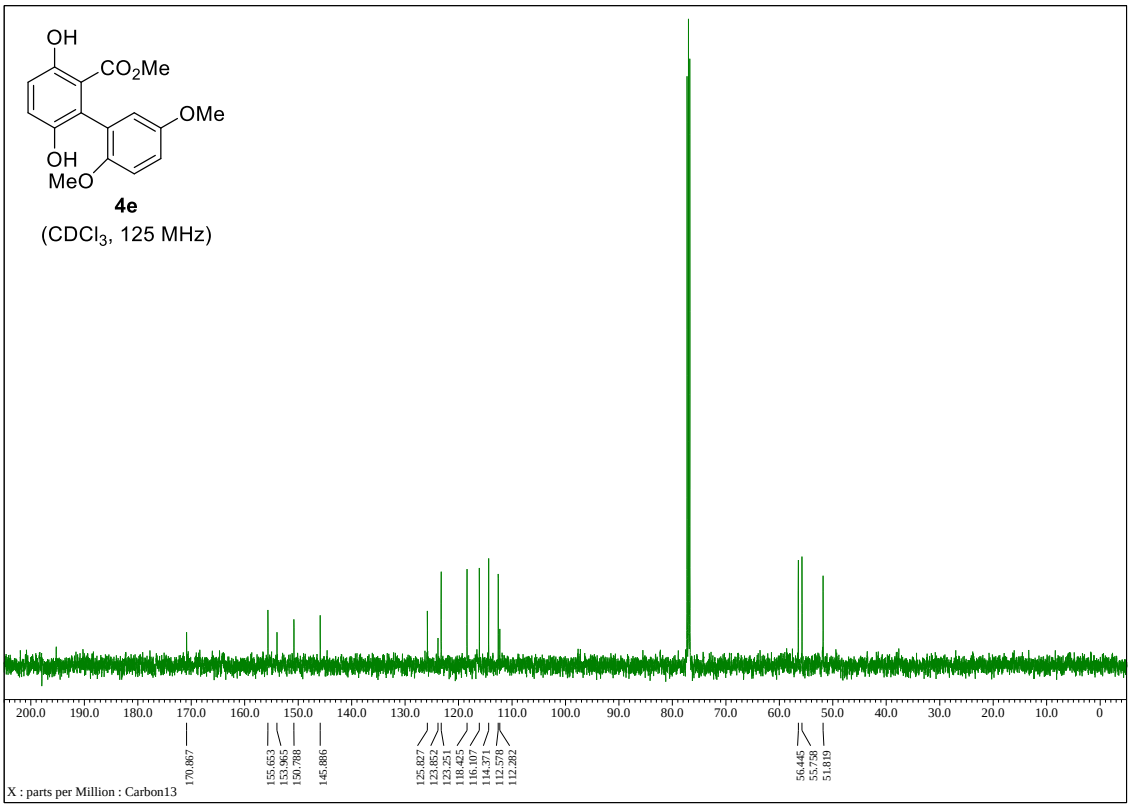

^{1}H NMR of methyl 2-hydroxy-6*H*-benzofuro[2,3-*b*]indole-1-carboxylate (**5a**)

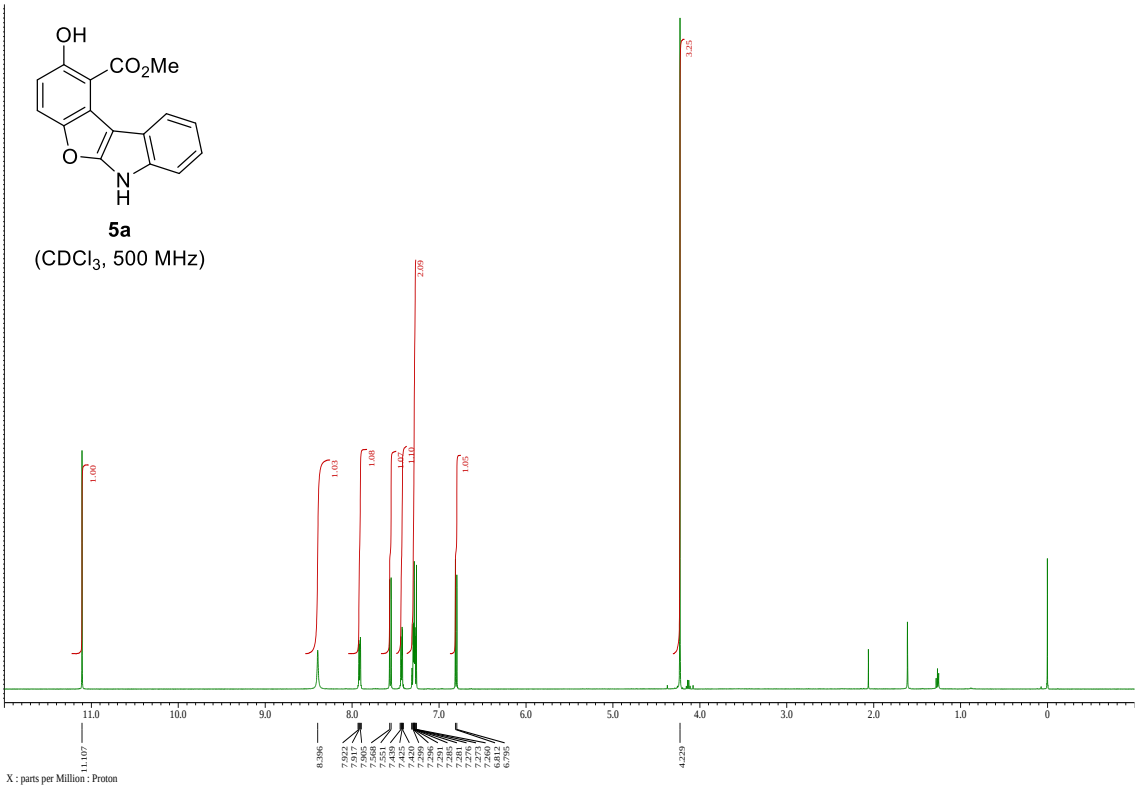

^{1}H NMR of methyl 2-(1*H*-indol-3'-yl)-3,6-dioxocyclohexa-1,4-diene-1-carboxylate (**9**)

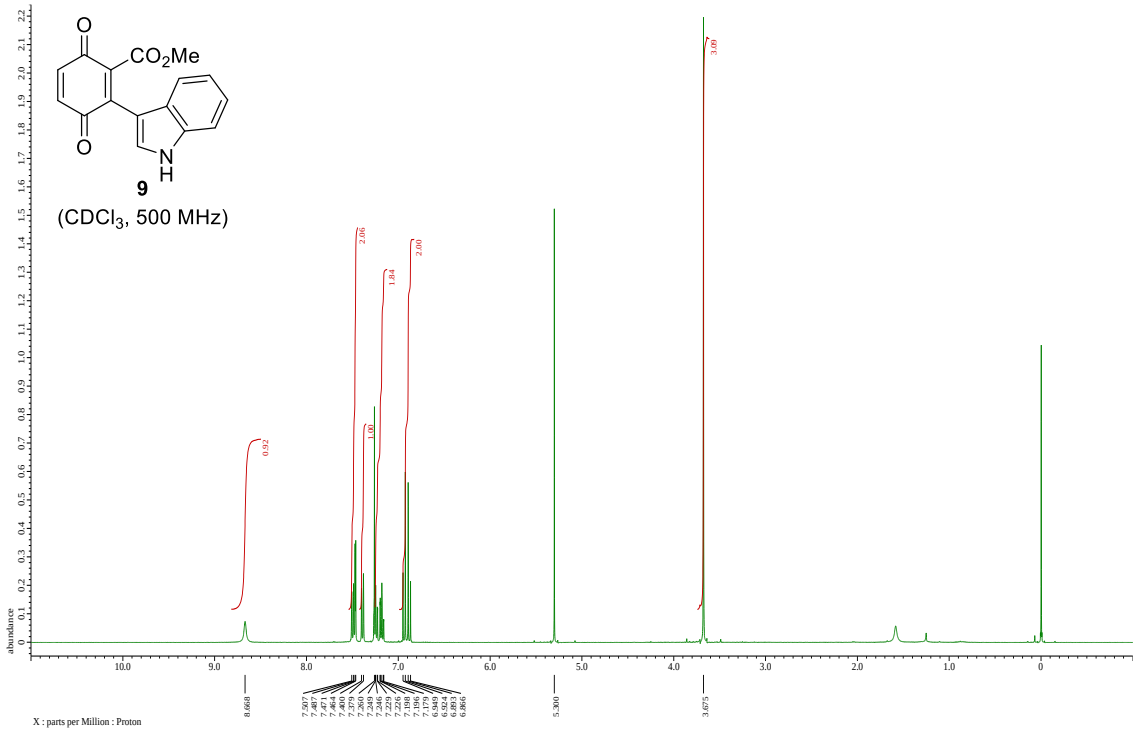

[1]H NMR of methyl 6-benzyl-2-hydroxy-6*H*-benzofuro[2,3-*b*]indole-1-carboxylate (**5b**)

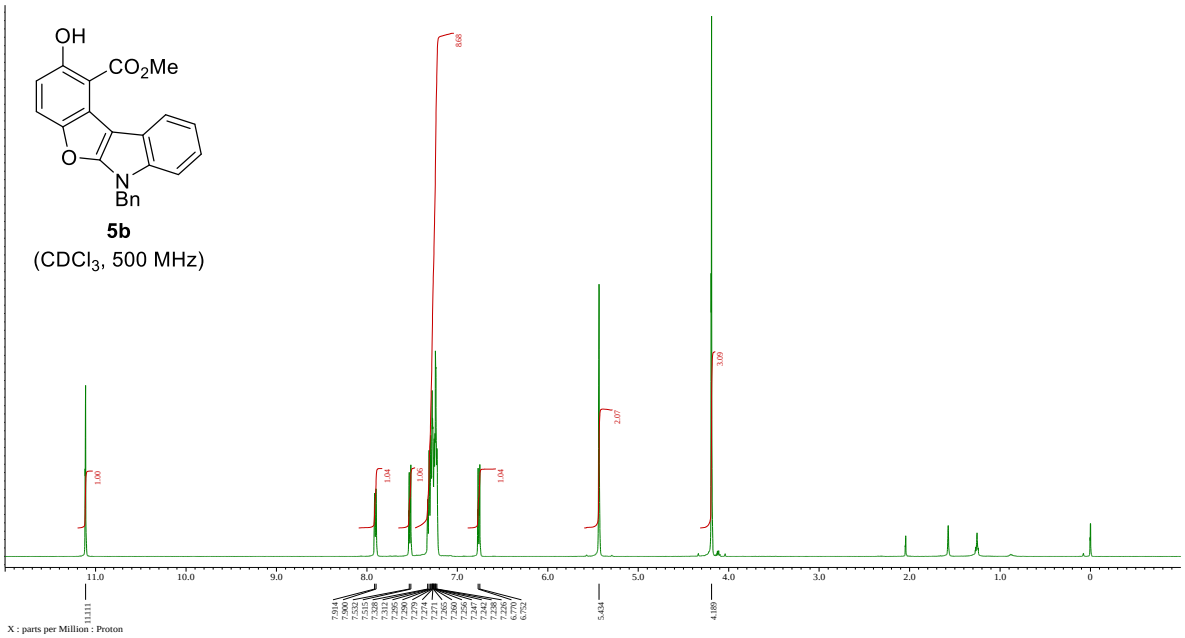

[13]C NMR of methyl 6-benzyl-2-hydroxy-6*H*-benzofuro[2,3-*b*]indole-1-carboxylate (**5b**)

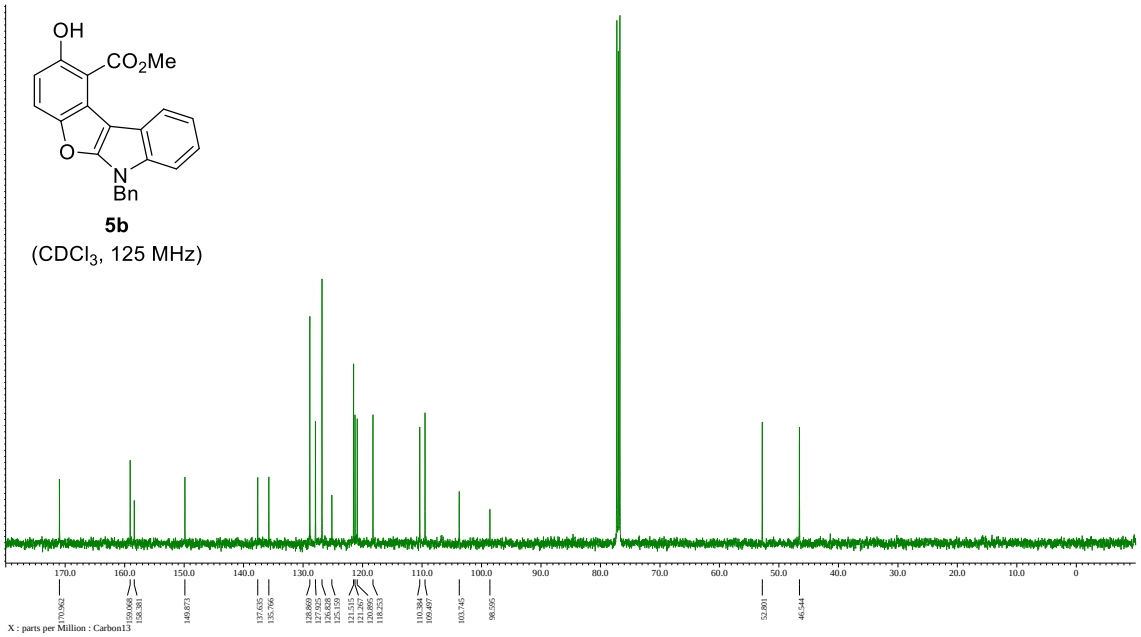

^{1}H NMR of methyl 2-hydroxy-9-methoxy-6*H*-benzofuro[2,3-*b*]indole-1-carboxylate (**5c**)

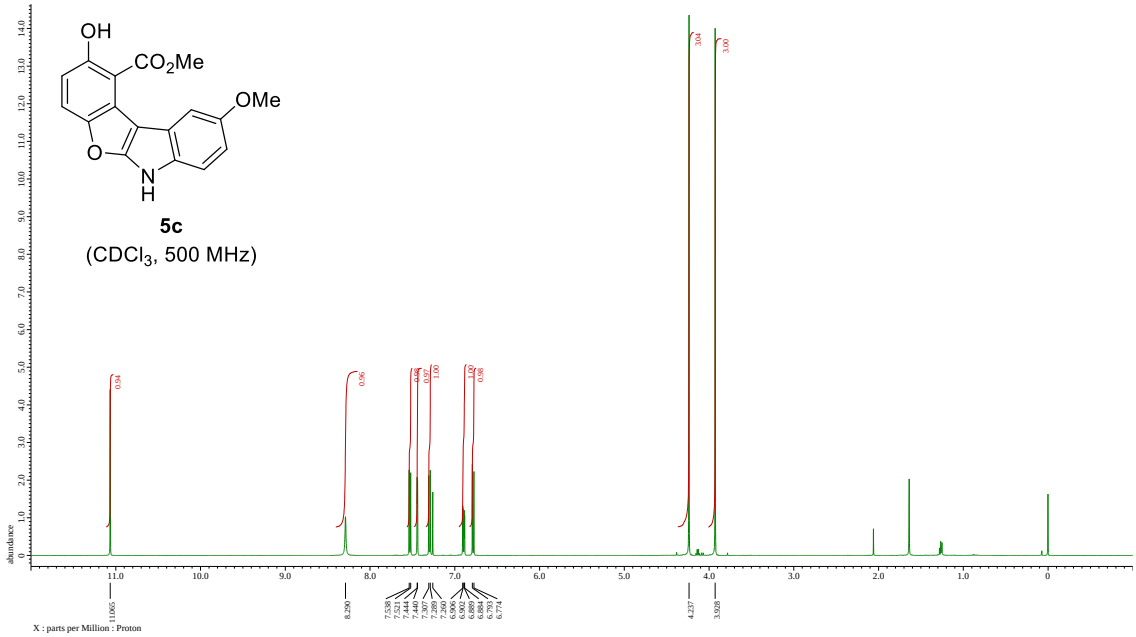

^{13}C NMR of methyl 2-hydroxy-9-methoxy-6*H*-benzofuro[2,3-*b*]indole-1-carboxylate (**5c**)

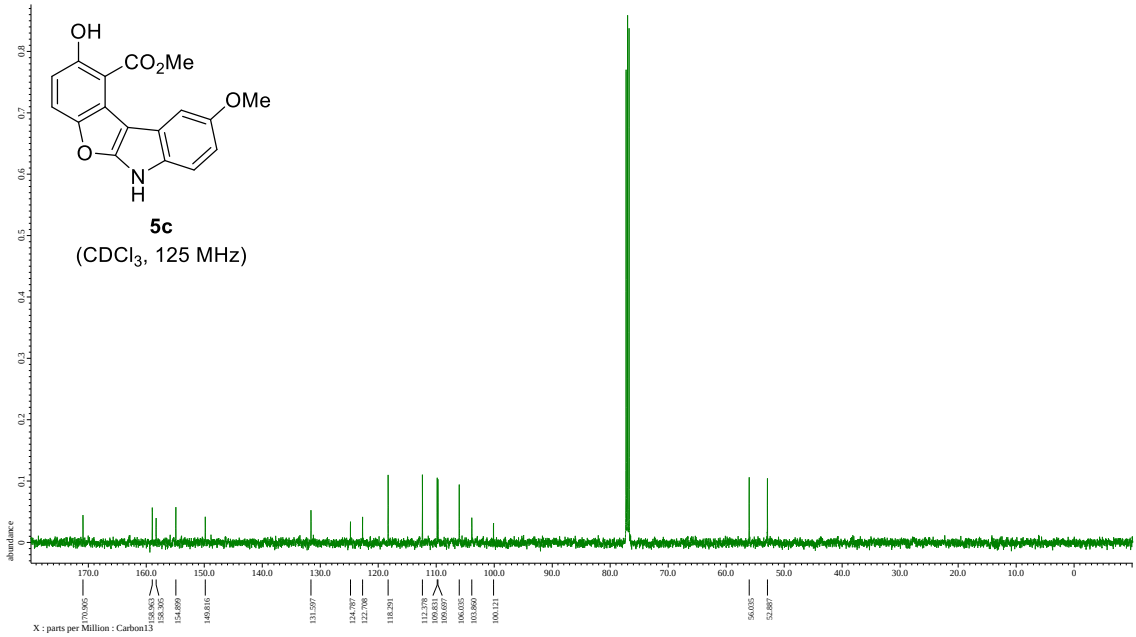

^{1}H NMR of methyl 9-bromo-2-hydroxy-6*H*-benzofuro[2,3-*b*]indole-1-carboxylate (**5d**)

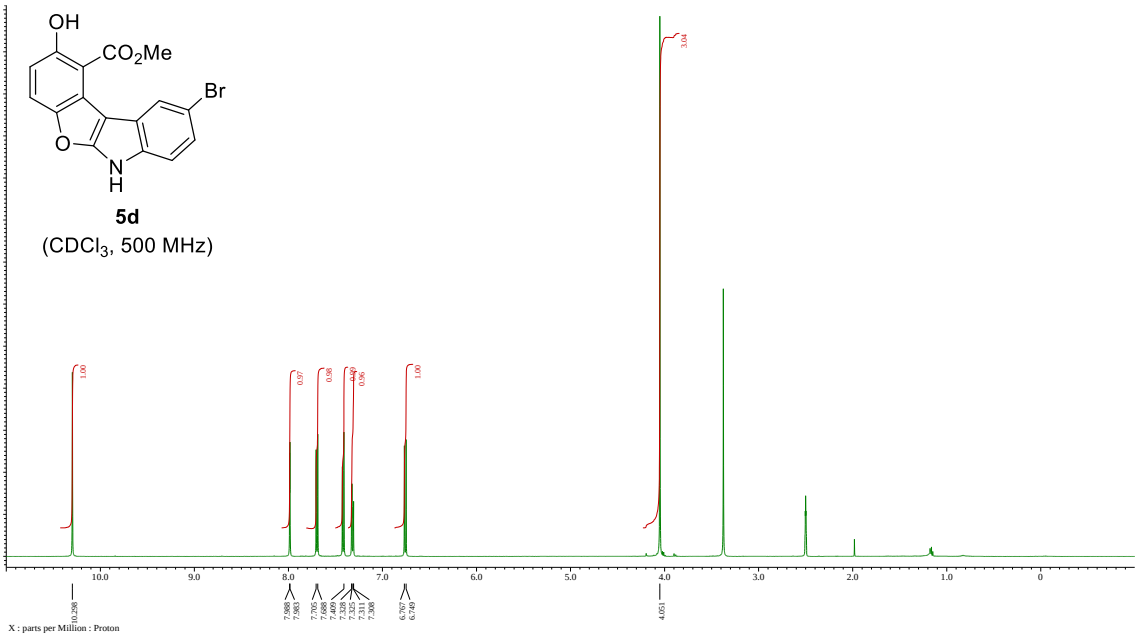

^{13}C NMR of methyl 9-bromo-2-hydroxy-6*H*-benzofuro[2,3-*b*]indole-1-carboxylate (**5d**)

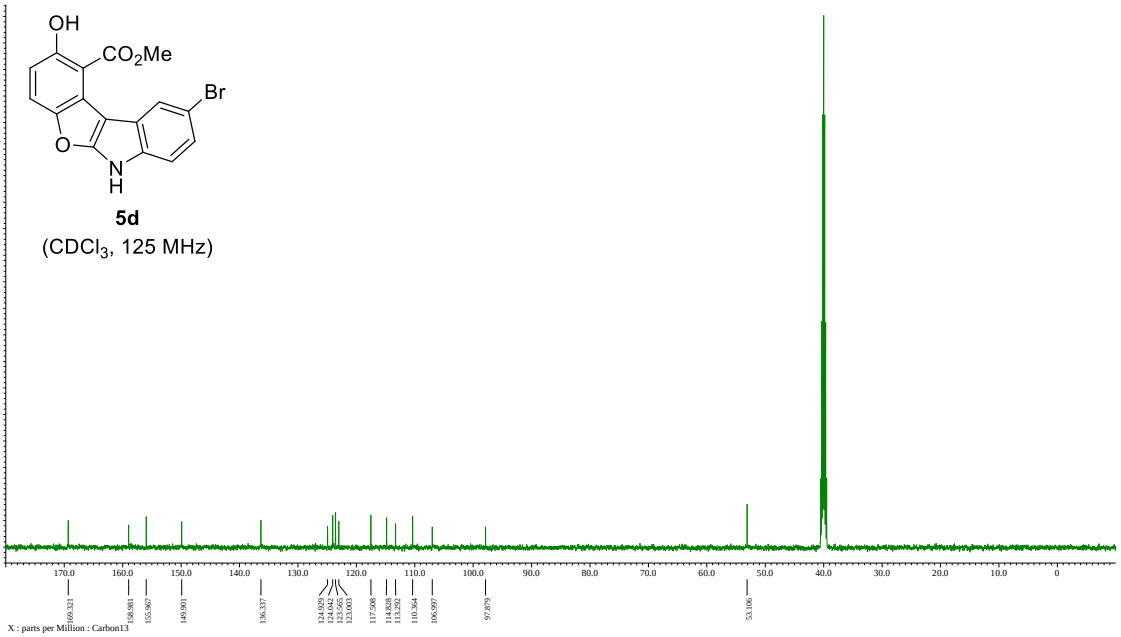

^{1}H NMR of methyl 5-hydroxy-thieno[2',3':4,5]thieno[3,2-*b*]benzofuran-4-carboxylate (**6**)

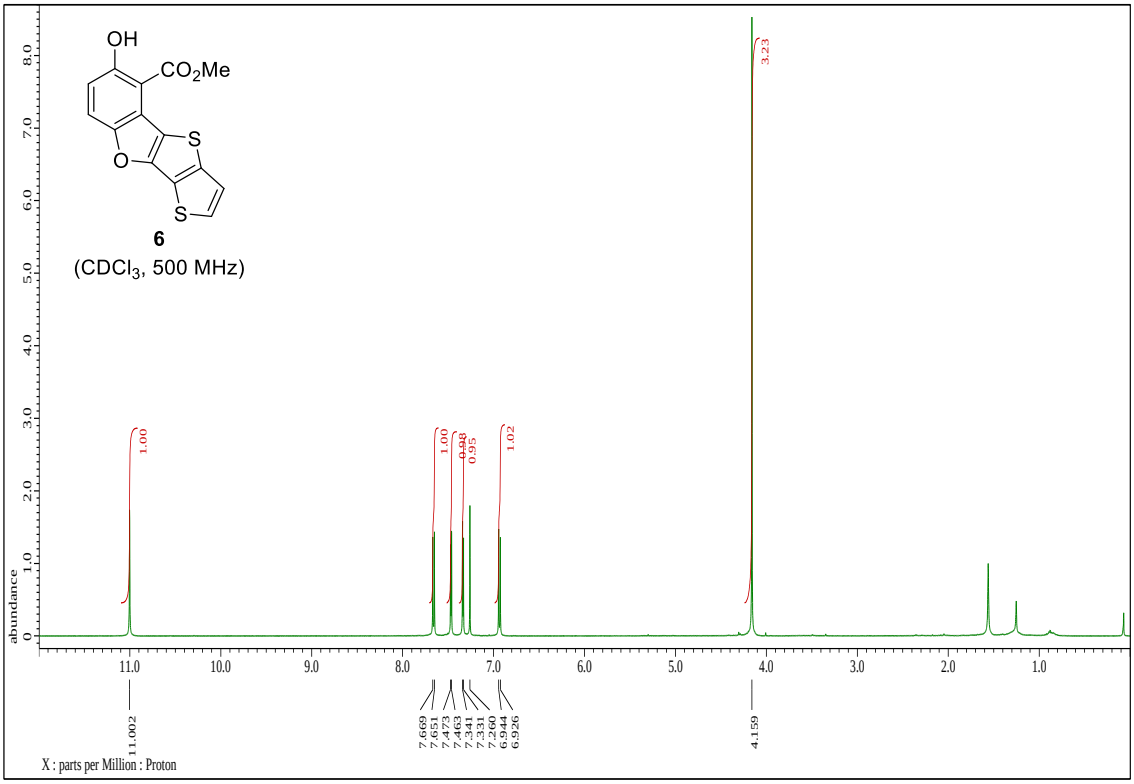

^{13}C NMR of methyl 5-hydroxy-thieno[2',3':4,5]thieno[3,2-*b*]benzofuran-4-carboxylate (**6**)

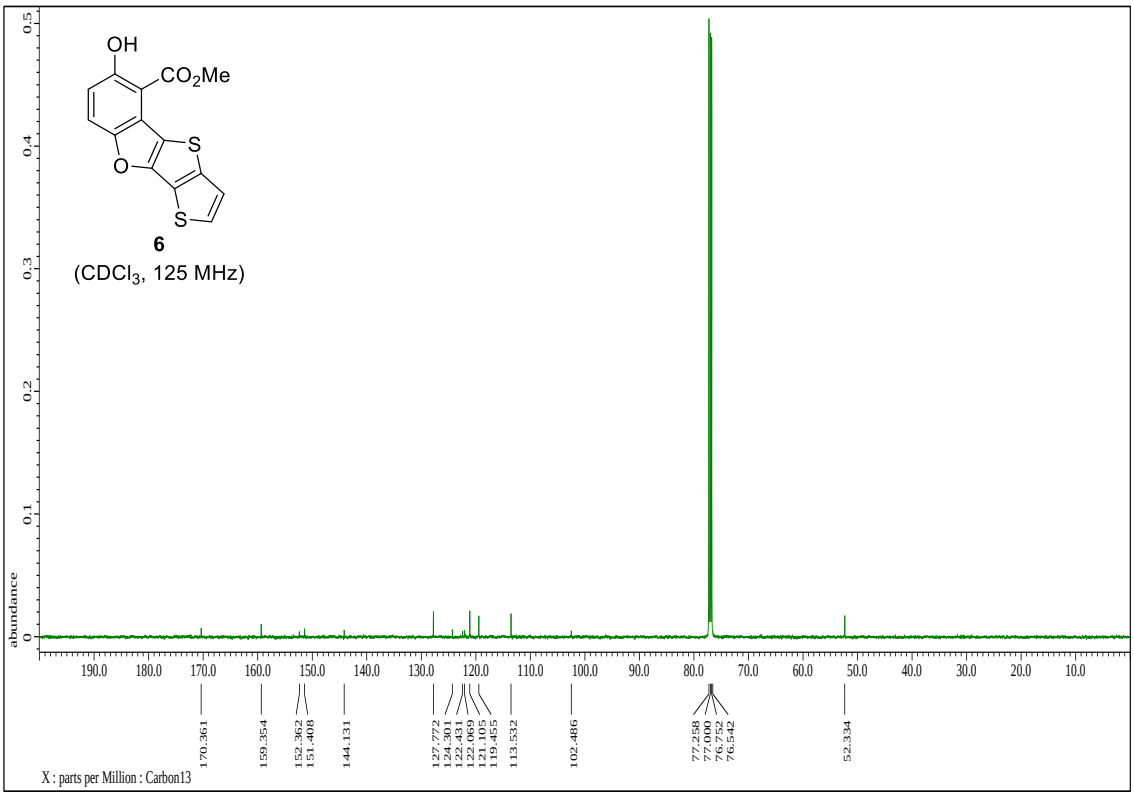

^{1}H NMR of methyl 3,6-dioxo-2-(thieno[3,2-*b*]thiophen-2-yl)cycloxexa-1,4-diene-1-carboxylate (**10**)

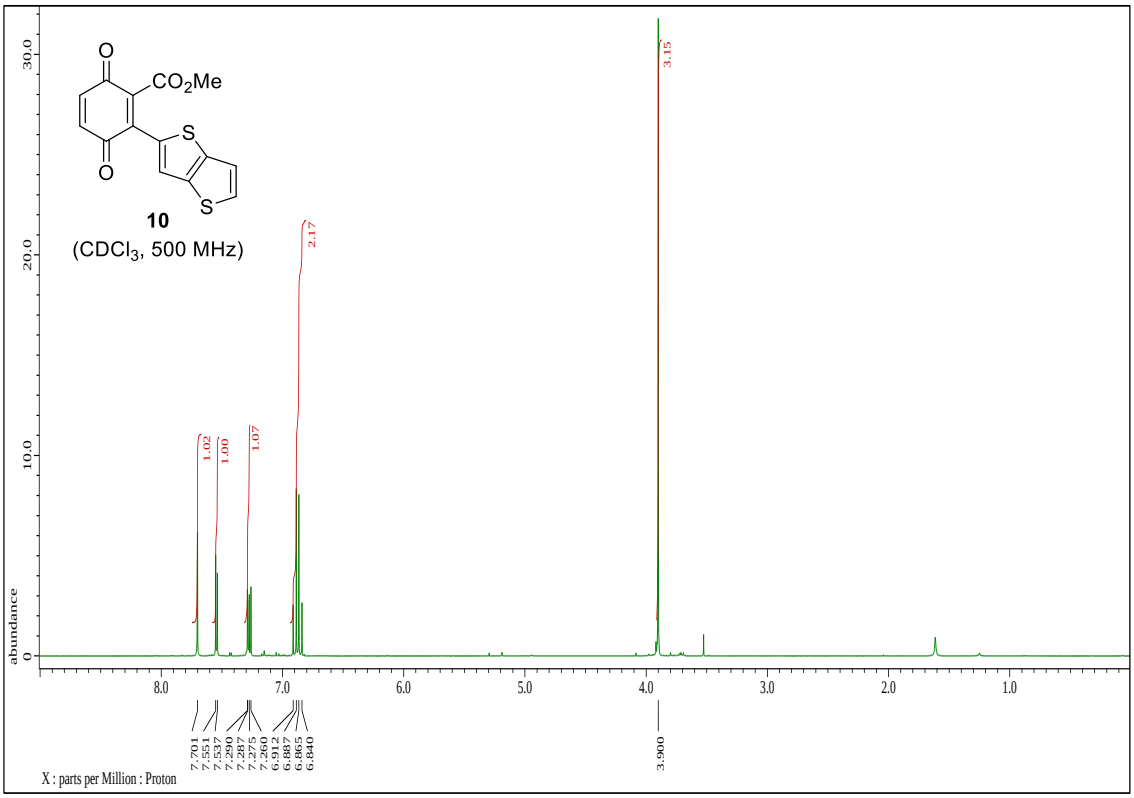

^{13}C NMR of methyl 3,6-dioxo-2-(thieno[3,2-*b*]thiophen-2-yl)cycloxexa-1,4-diene-1-carboxylate (**10**)

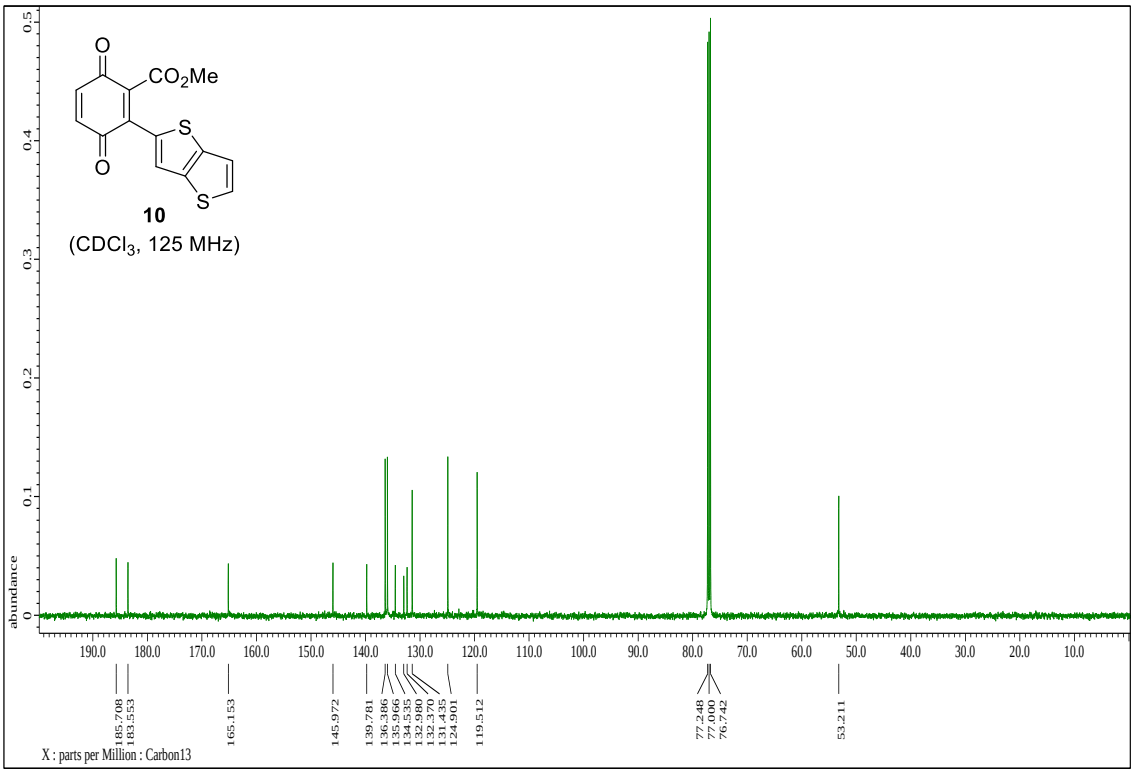

^{1}H NMR of methyl 2-hydroxybenzo[4,5]thieno[2,3-*b*]benzofuran-1-carboxylate (**7**)

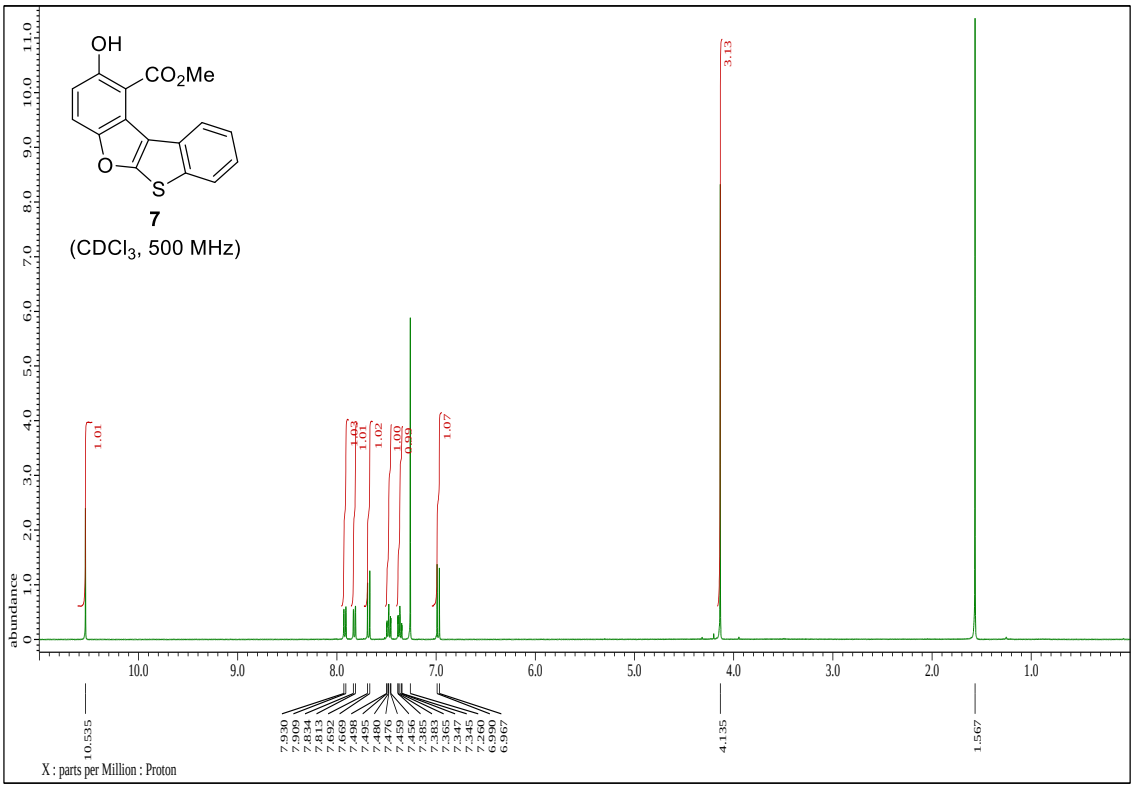

^{13}C NMR of methyl 2-hydroxybenzo[4,5]thieno[2,3-*b*]benzofuran-1-carboxylate (**7**)

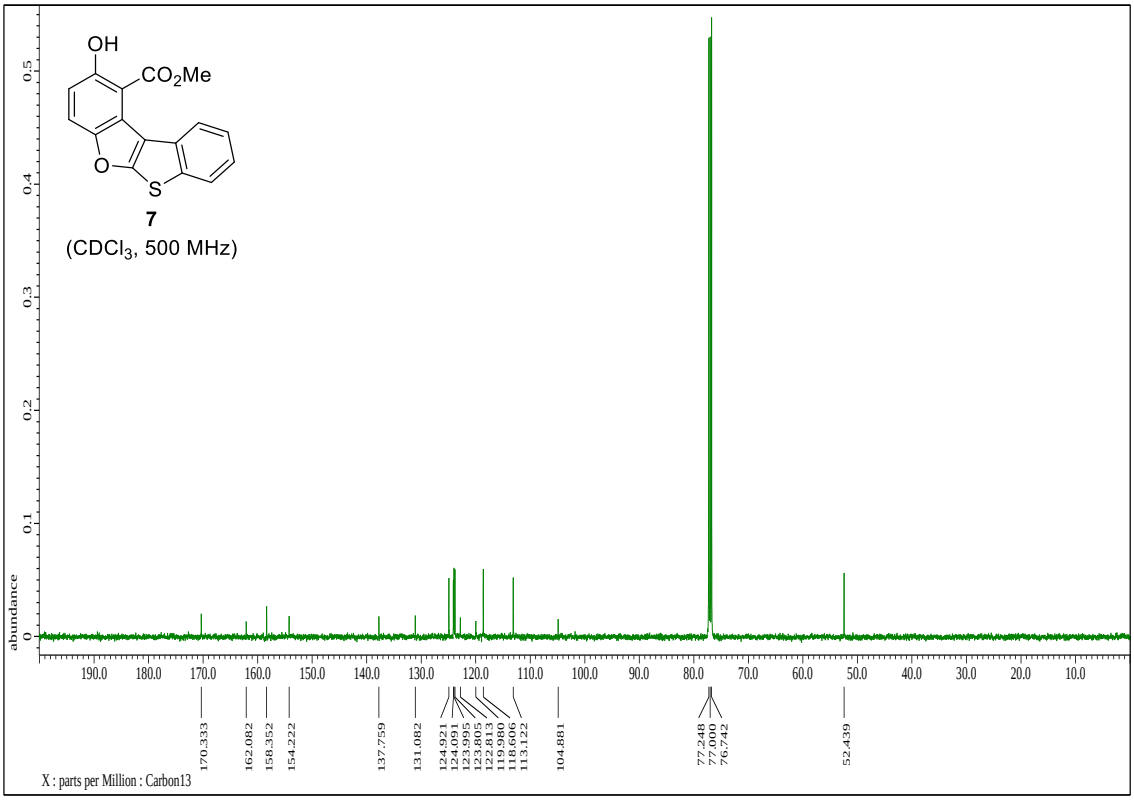

NOESY of methyl 2-hydroxybenzo[4,5]thieno[2,3-*b*]benzofuran-1-carboxylate (**7**)

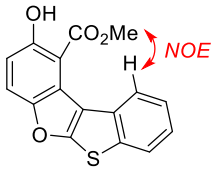

7

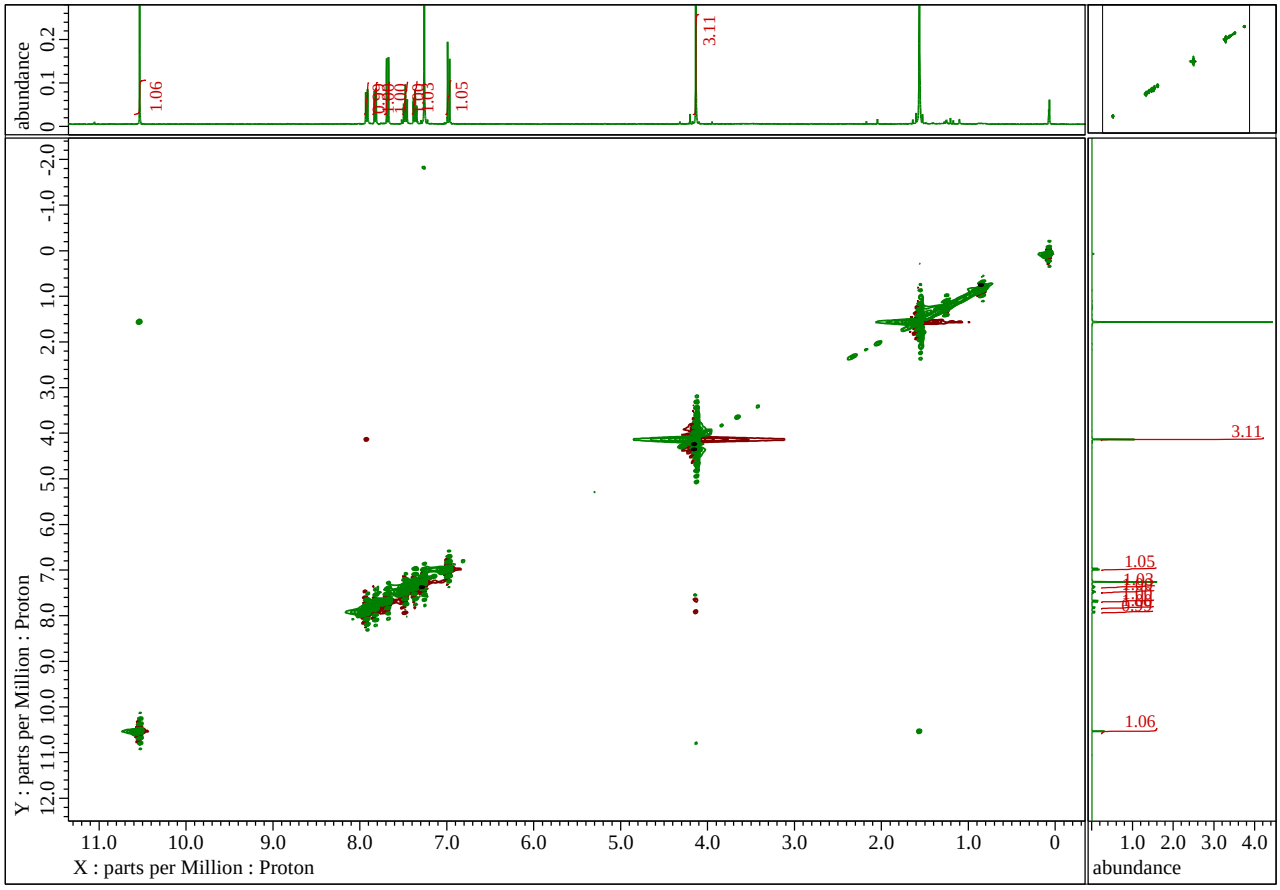

^{1}H NMR of thieno[3,2-*b*]thiophene (**authentic sample**)

^{1}H NMR (500 MHz, $CDCl_3$): δ 7.40 (d, J = 5.0 Hz, 2H-A), 7.28 (d, J = 5.0 Hz, 2H-B).

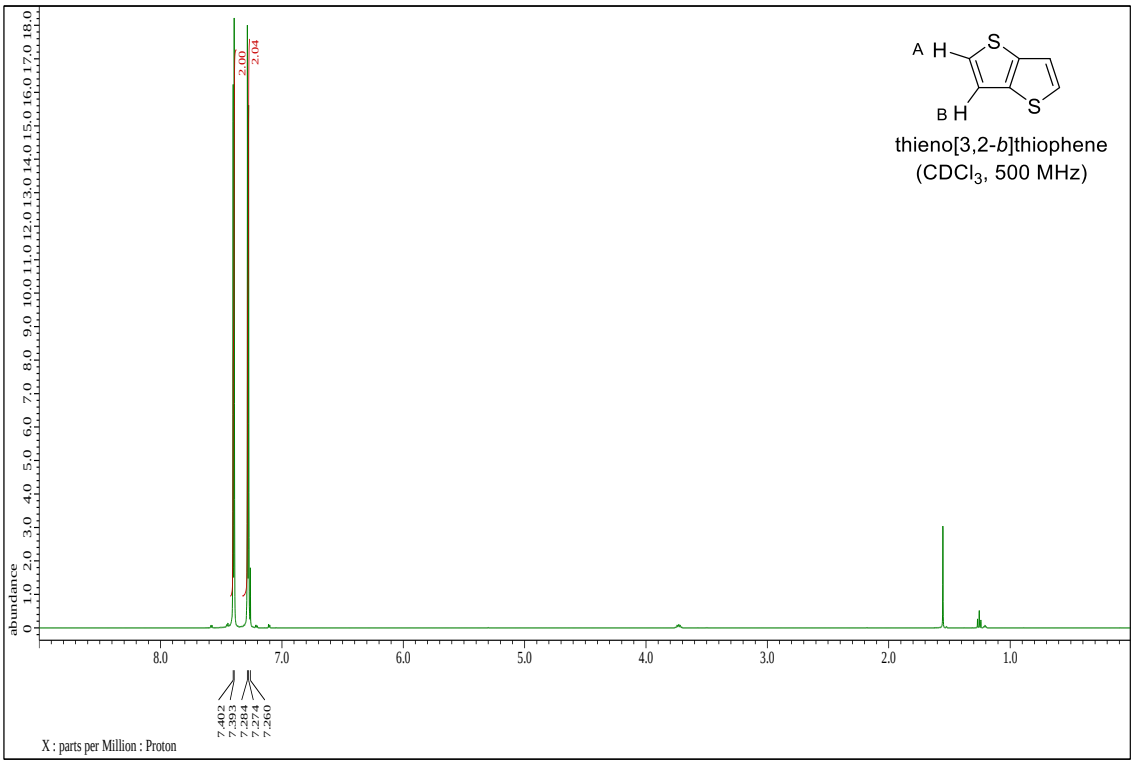

^{1}H NMR of thieno[3,2-*b*]thophene-2,5-d_2

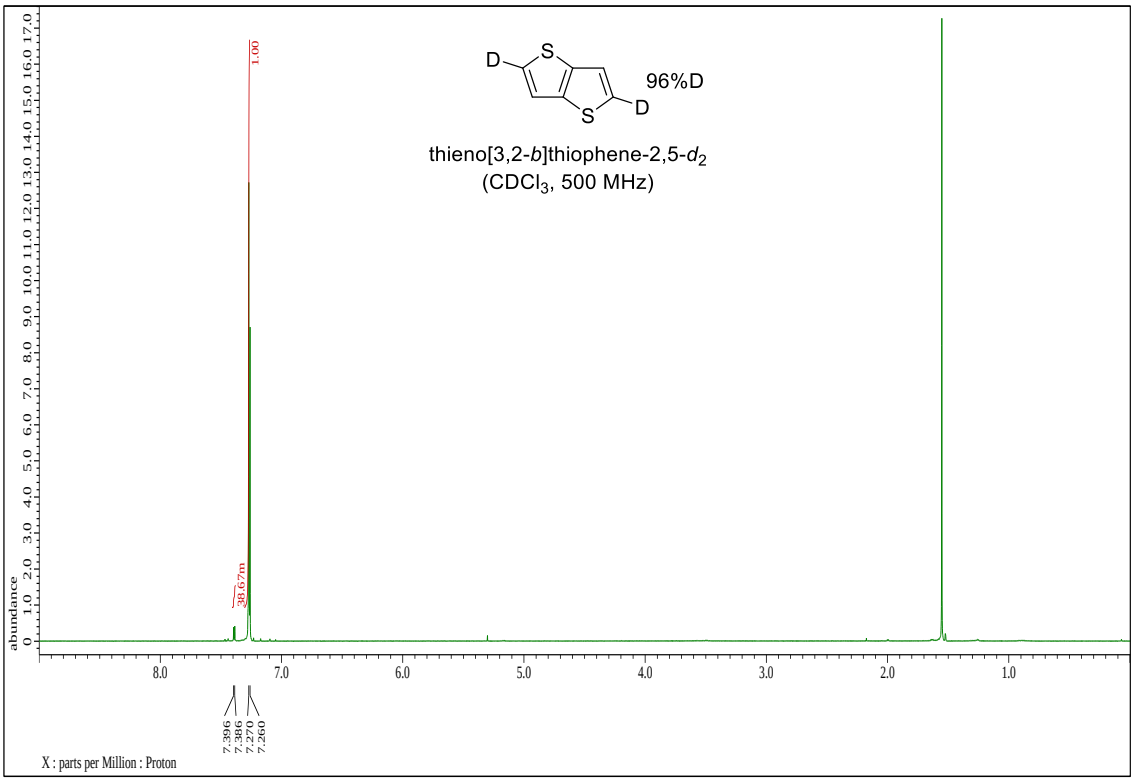

^{2}H NMR of thieno[3,2-*b*]thiophene-2,5-d_2

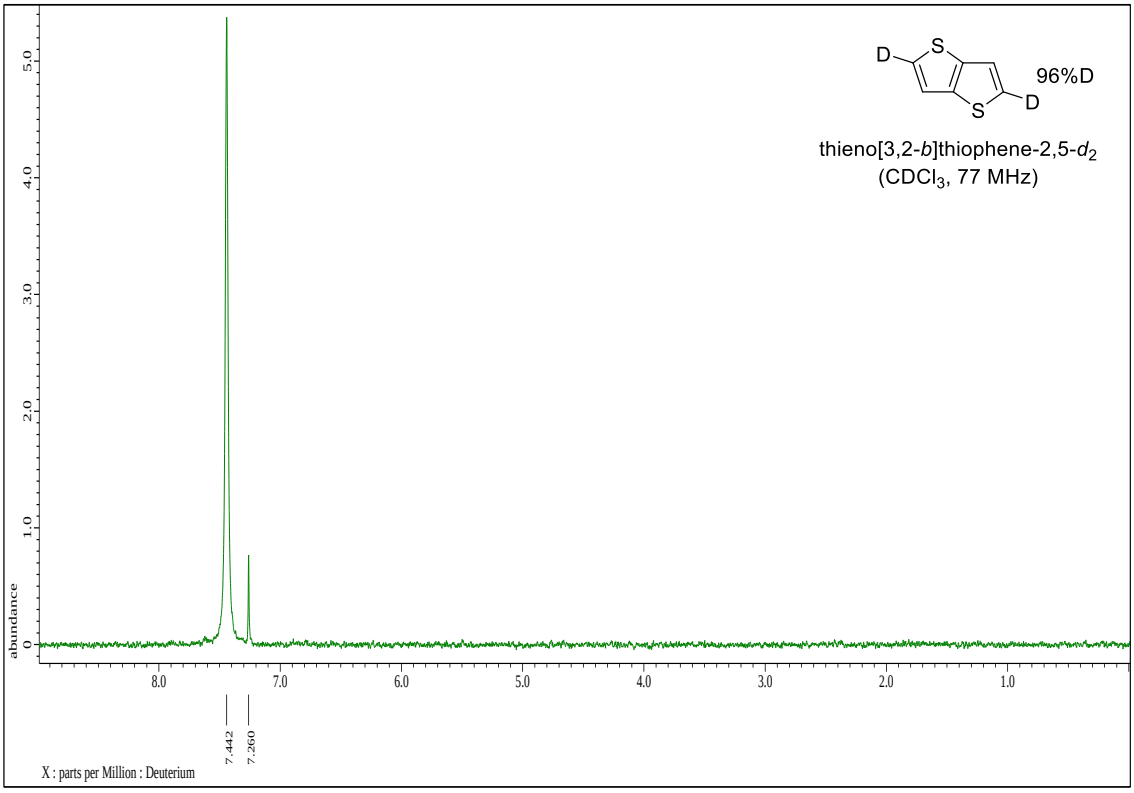

^{1}H NMR of **10-d_1**

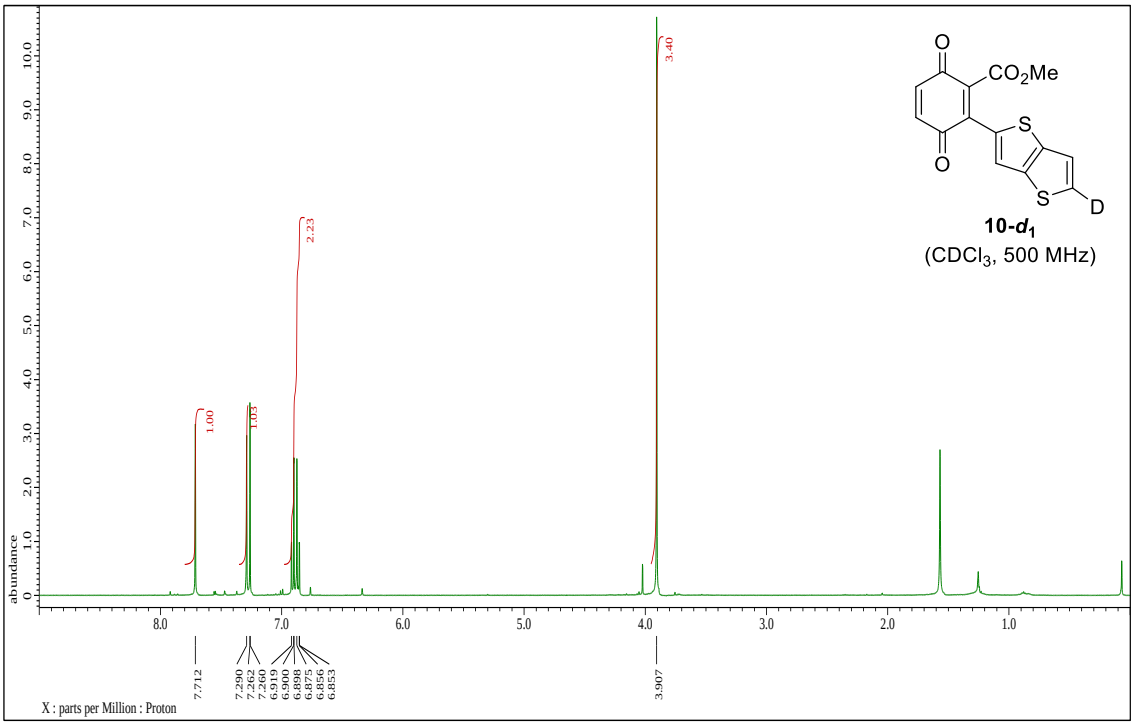

^{2}H NMR of **10-d_1**